External Nutrition Stimuli Induced Proteome and Phosphoproteome Responses of Maize Root Hairs and Arabidopsis Root Microsomal Fraction

Dissertation for Obtaining the Doctoral Degree

of Natural Sciences (Dr. rer. nat.)

Faculty of Natural Sciences

University of Hohenheim

Institute of Biology

Department of Plant Systems Biology

Submitted by

Zhi Li

From Jingzhou, Hubei, V.R. China

2021

Dean: Prof. Dr. Uwe Beifuß

1st reviewer: Prof. Dr. Waltraud Schulze

2ed reviewer: Prof. Dr. Uwe Ludewig

Submitted on: 19. 01. 2021

Oral examination on: 12. 04. 2021

This work was accepted by the Faculty of Natural Sciences at the University of Hohenheim on 18. 02. 2021 as “Dissertation for Obtaining the Doctoral Degree of Natural Sciences”.

Contents

List of Figures and Tables

Publication statement

Results of this thesis contributed to these publications;

Protein Dynamics in Young Maize Root Hairs in Response to Macro and Micronutrient Deprivation

Zhi Li,[†,§] Daniel Phillip,[‡,§] Benjamin Neuhäuser, [‡] Waltraud X. Schulze,[†] and Uwe Ludewig[*,‡]
†Department of Plant Systems Biology, University of Hohenheim, Garbenstraße 30, 70599 Stuttgart, Germany
‡Institute of Crop Science, Nutritional Crop Physiology, University of Hohenheim, Fruwirthstraße 20, 70599 Stuttgart, Germany

Original publication:

J. Proteome Res. 2015, 14, 8, 3362-3371

Publication Date: July 16, 2015

The authenticated version is available online at:

https://pubs.acs.org/doi/abs/10.1021/acs.jproteome.5b00399

https://doi.org/10.1021/acs.jproteome.5b00399

Own contributions:

I performed the experiment, the data analyses including figures and contributed to the writing of the manuscript.

ACKNOWLEDGMENTS
We thank Nadine Sommer for help with the establishment of the aeroponics system and Missael Romero for photographs of root hairs. This work was partially financed by a University of Hohenheim Faculty of Agriculture partnership grant to U.L. and W.X.S

Early nitrogen-deprivation responses in Arabidopsis roots reveal distinct differences on transcriptome and (phospho-)proteome levels between nitrate and ammonium nutrition

Jochen Menz[1], Zhi Li[2], Waltraud X. Schulze[2] and Uwe Ludewig[1,*]

[1] Institute of Crop Science, Nutritional Crop Physiology, University of Hohenheim, Fruwirthstr. 20, 70593 Stuttgart, Germany

[2] Institute for Physiology and Biotechnology of Plants, Plant Systems Biology, University of Hohenheim, Garbenstraße 30, 70593 Stuttgart, Germany

Original publication:

The Plant Journal (2016) 88, 717-734

Publication Date: September 15, 2016

The authenticated version is available online at:

https://onlinelibrary.wiley.com/doi/abs/10.1111/tpj.13272

https://doi.org/10.1111/tpj.13272

Own contributions:

I performed the experiment and data analyses for phosphoproteomic part.

ACKNOWLEDGMENTS

The authors thank H. Bremer for help with determination of nitrate and ammonium concentrations, and Anne Krapp from INRAAgroParisTech for the seeds of nlp7-mutants and Col-8.

Post-translational regulation of nitrogen transporters in plants and microorganisms

Aurore Jacquot[1], Zhi Li[2], Alain Gojon[1], Waltraud Schulze[2] and Laurence Lejay[1,*]

[1] Laboratoire de Biochimie et Physiologie Moléculaire des Plantes, Institut de Biologie Intégrative des Plantes 'Claude Grignon', UMR CNRS/INRA/SupAgro/UM2, Place Viala, 34060 Montpellier cedex, France

[2] Institute of Physiology and Biotechnology of plants, Plant Systems Biology, University of Hohenheim, Garbenstrasse 30, D-70593, Stuttgart, Germany

Original publication:

Journal of Experimental Botany, Vol. 68, No. 10 pp. 2567–2580, 2017

Publication Date: March 23, 2017

The authenticated version is available online at:

https://academic.oup.com/jxb/article/68/10/2567/3079360

https://doi.org/10.1093/jxb/erx073

Own contributions:

I contributed to the writing of the manuscript.

ACKNOWLEDGMENTS

The work in both laboratories is supported by a grant from the ANR in France and DFG in Germany (SIPHON ANR-13-ISV6-0002-01)

NRT2.1 C- terminus phosphorylation prevents root high affinity nitrate uptake activity in *Arabidopsis thaliana*

Aurore Jacquot[1], Valentin Chaput[1], Adeline Mauries[1], Zhi Li[2], Pascal Tillard[1], Cécile Fizames[1], Pauline Bonillo[1], Fanny Bellegarde[1], Edith Laugier[1], Véronique Santoni[1], Sonia Hem[1], Antoine Martin[1], Alain Gojon[1], Waltraud Schulze[2], Laurence Lejay[1*]

[1] BPMP, Univ Montpellier, CNRS, INRAE. Institut Agro, 34060 Montpellier, France

[2] Institute of Physiology and Biotechnology of plants, Plant System Biology, University of Hohenheim, Garbenstrasse 30, 70593, Stuttgart, Germany

Original publication:

New Phytologist

Publication Date: May 28, 2020

The authenticated version is available online at:

https://nph.onlinelibrary.wiley.com/doi/abs/10.1111/nph.16710

https://doi.org/10.1111/nph.16710

Own contributions:

I performed the rBIFC and mass spectrometry experiments including data analysis and designed the respective figures.

ACKNOWLEDGMENTS

This work was supported by an international grant from the ANR in France and DFG in Germany (SIPHON ANR-13-ISV6-0002-01), by a national grant from the ANR (TransN ANR-BLAN-NT09_477214) and by post-doctoral funding from the CNRS (E.L.).

A phospho-switch in the N-terminus of NRT2.1 affects nitrate uptake by controlling the interaction of NRT2.1 with NAR2.1

Zhi Li[1], Xu Na Wu[1], Aurore Jaquot[2], Larence Lejay[2], Waltraud X Schulze[1,*]

[1] Institute of Physiology and Biotechnology of plants, Plant Systems Biology, University of Hohenheim, Garbenstrasse 30, D-70593, Stuttgart, Germany

[2] Laboratoire de Biochimie et Physiologie Moléculaire des Plantes, Institut de Biologie Intégrative des Plantes 'Claude Grignon', UMR CNRS/INRA/SupAgro/UM2, Place Viala, 34060 Montpellier cedex, France

The authenticated version is available online at:

https://www.biorxiv.org/content/10.1101/2020.01.08.898254v1.abstract

https://doi.org/10.1101/2020.01.08.898254

Own contributions:

I performed the phosphoproteomics and rBIFC experiments, developed the PhosphoNetwork approach and performed all the data analyses. I designed the figures and made major contributions to the writing of the manuscript.

ACKNOWLEDGMENTS

We thank Zhaoxia Zhang for help with bioinformatics scripting and Sven Gombos for technical assistance in the lab. The work was supported by an international grant from the ANR in France (SIPHON ANR-13-ISV6-0002-01) and Deutsche Forschungsgemeinschaft (SCHU1533/8-1) in Germany.

Abbreviations

2-D DIGE	two dimensional gel electrophoresis
ABA	abscisic acid
ABC	ATP binding cassette
ABI1	abscisic acid-insensitive 1
ABI2	abscisic acid-insensitive 2
ACN	acetonitrile
AHA	proton-pumping ATPase
AKT1	Arabidopsis K^+ transporter 1
AMT	ammonium transporter
BL	brassinolide
BR	brassinosteroid
BRI1	brassinosteroid insensitive 1
BSK	BR-Signaling kinase
CBLs	calcineurin B-like proteins
CDPK	calcium-dependent protein kinase
CIPKs	CBL-interacting protein kinases
CLC	chloride channe l
CTR1	constitutive triple response 1
DSPTPs	dual specificity phosphatases
EIN2	ethylene-insensitive 2
ER	endoplasmic reticulum
FDR	false discovery rate
FWHM	full-width half-maximum
GOGAT	glutamine-2-oxoglutarate aminotransferase
GS	glutamine synthetase
HATS	high affinity transport system
HPCA1	hydrogen-peroxide-induced Ca^{2+} increases mutant 1
HPCAL1	hydrogen-peroxide-induced Ca^{2+} increases mutant like 1
IMAC	immobilized metal affinity chromatography
IPTG	isopropyl ß-D-thiogalactopyranoside
JA	jasmonic acid

LATS	low affinity transport system
LFQ	label free quantification
LRR	leucine-rich-repeat
MAPK	mitogen-activated protein kinase
MF	microsomal fraction
MFS	major facilitator superfamily
MS	mass spectrometry
NAR	nitrate assimilation related protein
NIA/NR	nitrate reductase
NIR	nitrite reductase
NRT	nitrate transporter
OPT	oligopeptide transporter
PIP	plasma membrane intrinsic protein
PMSF	phenylmethylsulfonyl fluoride
PNR	primary nitrate response
PP1	protein phosphatase types 1
PP2A	protein phosphatase types 2A
PP2B	protein phosphatase types 2B
PP2C	protein phosphatase types 2C
PTI	pattern-triggered immunity
PTMs	post-translational modifications
PTPs	protein tyrosine phosphatases
PTR	peptide transporter
rBiFC	ratiometric bimolecular fluorescence complementation
RLKs	receptor-like protein kinases
SIRK1	sucrose induced receptor kinase 1
SLAC1	slow anion channel associated 1
SLAH3	slow anion channel associated 1 homolog 3
SUS	sucrose synthase
TCA	tricarboxylic acid
TFA	trifluoroacetic acid
UBL	ubiquitin-like protein

Summary

Plant nutrients play diverse and vital roles in plant growth and development. Studying how plants uptake and respond to external nutrients has always been a concern of biologists. In my research, I firstly studied how the proteome of young maize root hair cells responded to different nutrient deficiencies. Then I carried out an investigation on the phosphoproteome responses of Arabidopsis root cell microsomal fraction to different external nitrogen stimuli.

Plants increase their root surface with root hairs to improve the acquisition of nutrients from the soil. The unicellular character of root hairs and their position at the root surface make them an attractive system to investigate adaptive processes of rhizodermal cells that are in direct contact with the soil solution. In young maize seedlings, roots are densely covered with root hairs, although nutrient reserves in the seed are sufficient to support seedling growth rates for a few days. We used a label-free quantitative proteomics approach to study protein abundance adjustments in 4 day old root hairs grown in aeroponic culture in the presence and absence of several macro- and micronutrients.

Compared to the proteome of root hairs developed under full nutrition, macronutrient deficiencies induced protein abundance changes in various cellular pathways. For example, lack of N in the medium repressed the primary N metabolism pathway, increased amino acid synthesis, but repressed their degradation, and affected the primary carbon metabolism, such as glycolysis. Glycolysis was similarly affected by K and P deprivation, but the glycolytic pathway was negatively regulated by the absence of the micronutrients Fe and Zn. In contrast, the deprivation of Mn had almost no effect on the root hair proteome. Our results indicate that the metabolism of very young root hairs adjusted to local nutrient deficiencies independently of total nutrient content in the seed and/or that root hairs sense the external lack of specific nutrients in the nutrient solution and adjust their metabolism accordingly.

Since nitrogen is a major and very important macronutrient, I focused on molecular mechanisms of nitrogen-related signaling in more detail. The activity of Arabidopsis dual-affinity nitrate transporter NRT1.1 can be regulated through phosphorylation mediated by CIPK23, and NRT1.1 is also a confirmed nitrate transceptor. There is evidence indicating that NRT2.1 could be another nitrate transceptor and its transport activity may be regulated through phosphorylation as well, but whether or how phosphorylation can regulate NRT2.1 activity is unknown. Besides these two, about one quarter of Arabidopsis nuclear genes are considered to be translated into membrane proteins which make plant membrane system vital for plants survival. Finding out whether these membrane located transceptor/predicted transceptor are involved in regulating root membrane phosphoproteome responses to external nitrogen is attractive. That is why answering these questions is the other part of my work. In order to do that, a label-free quantitative phosphoproteomics approach was performed to study the root membrane phosphoproteome from wild type, *nrt1.1* knock-out, and *nrt2.1* knock –out plants under different external nitrogen conditions.

Through over-representation analysis, several pathways were found up- and down-regulated under both nitrogen deprivation and nitrate resupply conditions. However there were still a few pathways found over-represented under specific conditions, such as glycolysis was only found over-represented in WT under ammonium deprivation. By analyzing the motifs of phopshopeptides, target motifs recognized

by MAPK and CDPK were found. After comparing the over-representation pathway analysis results and motif analysis results from wild type, *nrt1.1* knock-out, and *nrt2.1* knock –out plants, we speculate that NRT1.1 and NRT2.1 may function in regulating root membrane phosphoproteome responses to external nitrogen stimuli.

NRT2.1 is a major component of the high-affinity nitrate transporter in Arabidopsis. Five phosphosites were detected from NRT2.1 in this research, and through nitrate influx experiment, we know that all of these sites could affect NRT2.1 nitrate transport activity. Phosphorylation at Ser11 or Ser501 could inhibit NRT2.1 transport activity while phosphorylation at Ser28 or Thr521 activated its activity. The interaction of NRT2.1 with NAR2.1 is already known to be important for NRT2.1 transport activity. I showed by ratiometric bimolecular fluorescence complementation that this interaction could only be affected by phosphorylation of NRT2.1 at Ser28 or Ser21, but not by phosphorylation at other sites. We therefore propose, the interaction of NRT2.1 and NAR2.1 is regulated by phosphorylation of NRT2.1. In order to find out which kinase can phosphorylate those sites on NRT2.1, we created one in silico analysis method, the PhosphoNetwork. As a proof of principle in this PhosphoNetwork, we found several well-known kinases connected to their substrates. We were also successful in locating one kinase AT5G49770 (HPCAL1) which could interact with NRT2.1 *in vivo*, and phosphorylated NRT2.1 at Ser21 *in vitro*. At last, a phospho-switch model which requires a harmonious regulation of different phosphorylation events in HPCAL1 and NRT2.1 was built, and the regulatory mechanism of the nitrate transport activity could be explained through this model.

Besides helping to locate the kinase for the substrate, the PhosphoNetwork could also demonstrate kinases and their correlated proteins which may be involved in calcium and brassinosteroid signaling pathways. Furthermore, we found several proteins predicted to take part in communication between calcium and BR signaling pathways. NRT1.1 and NRT2.1 were further proposed possible roles in regulating root membrane phosphoproteome responses through the PhosphoNetwork. Moreover, this work showed that the PhosphoNetwork approach has a great potential to serve as a conventional tool used to verify signaling pathways mediated by phosphorylation, locate kinase/kinases or phosphatase/phosphatases for their substrate proteins.

Taken together, this work studied how the proteome from young maize root hair cells responds to different nutrition deprivation, and gives perspectives to the possible involvement of NRT1.1 and NRT2.1 in regulating root membrane phosphoproteome responses. This work also proposes a phospho-switch model that may explain how the NRT2.1 activity was regulated.

Zusammenfassung

Ohne Nährstoffe können Pflanzen sich nicht entwickeln und wachsen. Die Forschung an Nährstoffaufnahme und den den Mechanismen der Nährstoffwahrnehmung hat daher eine langer Tradition. Im Zuge meiner Promotion habe ich die Veränderung des Proteoms junger Maiswurzel-Haarzellen auf verschiedene Nährstoffmängel untersucht. Ein weiterer Schwerpunkt meiner Arbeit war die Erforschung von Veränderungen im Phosphoproteom von Arabidopsis Wurzelzell-Membranfraktion in Antwort auf verschiedene Stickstoffbedingungen.

Pflanzen erhöhen ihre Kontaktfläche zur Umwelt durch das Ausbilden von Wurzelhaaren, um die Aufnahme von Nährstoffen aus dem Boden zu maximieren. Aufgrund ihrer Position an der Wurzeloberfläche, ihres einzelligen Aufbaus und ihrer Bedeutung für den Nährstoffhaushalt sind Wurzelhaare ein attraktives System zur Erforschung der adaptiven Prozesse von rhizodermalen Zellen. Bei jungen Maiskeimlingen sind Wurzeln dicht mit Wurzelhaaren bedeckt, obwohl der Keimling ausreichende Nährstoffreserven bereitstellt, um eine hohe Wachstumsrate über einige Tage zu gewährleisten.

Wir verwendeten einen label-freien quantitativen proteomischen Ansatz, um Veränderungen der Proteinabundanz in vier Tage alten Wurzelhaaren in aeroponischen Wachstumskulturen in Gegenwart oder Abwesenheit verschiedener Makro- und Mikronährstoffen zu untersuchen.

Im Vergleich zu normalen Wachstumsbedingungen konnten unter dem Einfluss von Nährstoffmangel Veränderungen von Proteinabundanze beobachtet werden, die an verschiedenen zellulären Prozessen beteiligt sind. So wurden durch Stickstoffmangel beispielsweise der primäre Stickstoffmetabolismus und der Aminosäure Katabolismus gehemmt, während die Aminosäuresynthese verstärkt wurde. Auch ein Effekt auf den primären Kohlenstoffmetabolismus wie z.B. Glykolyse konnte beobachtet werden. Die Glykolyse wurde ebenfalls durch Kalium und Phosphatmangel beeinflusst, aber bei Eisen- oder Zinkmangel gehemmt. Im Gegensatz dazu hatte Manganmangel kaum Einfluss auf das Wurzelhaarproteom. Unsere Ergebnisse zeigen, dass sich der Metabolismus sehr junger Wurzelhaare unabhängig von dem Gesamtnährstoffstatus des Keimlings an sich verändernde Nährstoffverfügbarkeiten lokal anpassen kann.

Aufgrund der Bedeutung von Stickstoff als wichtiger Makronährstoff habe ich die Mechanismen der Stickstoff induzierten Signalantwort näher betrachtet. Die Aktivität des Arabidopsis-Dualaffinitäts-Nitrattransporter NRT1.1 kann durch die von CIPK23 vermittelte Phosphorylierung reguliert werden. NRT1.1 ist ebenfalls ein Nitrattranszeptor. Es gibt weitere Hinweise darauf, dass auch NRT2.1 ein weiterer Nitrattranszeptor sein könnte und seine Transportaktivität ebenfalls durch Phosphorylierung reguliert wird. Ob und wie diese Transportfunktion durch Phosphorylierung reguliert wird ist bislang unbekannt. Ein Teilaspekt meiner Arbeit beschäftigte sich daher mit der Frage, inwieweit die membranständigen Transzeptoren / Transporter an der Regulierung der Phosphoproteomantwort auf externe Stockstoffverbindung beteiligt sind. Um dieses Ziel zu erreichen, wurden wildtypische Pflanzen und nrt1.1 bzw. nrt2.1 knockout-Mutanten wechselnden Stickstoffbedingungen ausgesetzt und im Kontext eines quantitativ label-freien, phosphoproteomischen Versuchsansatzes untersucht.

Eine Überrepräsentationsanalyse zeigte die Beteiligung und Auf- und Ab- Regulierung verschiedener Signal-, oder Stoffwechselwege in Reaktion auf Stickstoff-Mangelbedingungen und das zur Verfügung stellen von Stickstoff. Für einige dieser überrepräsentierten Stoffwechselwege sind spezifische Bedingungen maßgeblich. So kann als Beispiel für die spezifische Reaktion des Wildtyps auf Ammoniummangel die Glykolyse angeführt werden.

Durch die Analyse der Phosphopeptide konnten die spezifischen Bindemotive der MAPK- und CDPK-Kinasen identifiziert werden. Durch den Vergleich der Ergebnisse dieser Motifanalyse mit den Ergebnissen der Überrepräsentationsanalyse stellen wir die Vermutung auf, dass NRT1.1 und NRT2.1 an der Regulierung der Reaktion des Wurzelmembran-Phosphoproteoms auf externe Stickstoffstimuli beteiligt sind.

NRT2.1 ist ein maßgeblicher Teil des hochaffinen Stickstofftransportsystems in Arabidopsis. Im Zuge dieser Arbeit konnten fünf Phosphorylierungsstellen identifiziert werden, für welche die Funktion der Regulierung der Transportaktivität über Nitrat-Einstrom-Experimente nachgewiesen werden konnte. So inhibiert die Phosphorylierung an Ser11 oder Ser501 die NRT2.1 transportrate, während Phosphorylierung an Ser28 oder Thr521 diese beförderte.

Der Einfluss der Interaktion von NAR2.1 mit NRT2.1 auf die Transportaktivität von NRT2.1 ist bereits bekannt. Durch ratiometrische bimoleculare Floureszenzkomplementation konnte ich zeigen, dass diese Interaktion von der Phosphorylierung von NRT2.1 an Ser28 oder Ser21, nicht aber von anderen Phosphorylierungsstellen abhängig ist. Aufgrund dieses Ergebnisses stellen wir fest, dass die Interaktion von NAR2.1 mit NRT2.1 durch die Phosphorylierung von NRT2.1 reguliert wird.

Um festzustellen, welche Kinase NRT2.1 an diesen Stellen phosphorylieren kann, haben wir eine in-silico Analysemethode – „PhosphoNetwork“ – entworfen. Da viele bekannte Kinase-Substrat Paare in diesem PhosphoNetwork gefunden werden konnten, ist die Methode grundsätzlich validiert. Als Interaktionspartner von NRT2.1 und als Kandidat für die Phosphorylierung von NRT2.1 konnte die Kinase AT5G49770 (HPCAL1) gefunden werden, welche in-vitro dazu in der Lage ist, NRT2.1 an Serin21 zu phosphorylieren. Mit diesen Informationen konnte letztlich ein Phospho-Schalter-Modell erdacht werden, welches die Nitrat-Transporter Aktivität von NRT2.1 über die harmonische Regulation der verschiedenen Phosphorylierungsstellen in HPCAL1 und NRT2.1 erklärt.

Über die Funktion der Zuordnung von Kinase und Substrat hinaus konnte das PhosphoNetwork auch Korrelationen zwischen Kinasen und Proteinen herstellen, welche am Kalzium- und Brassinosteroid-Signalweg beteiligt sein könnten. Ebenso konnten wir einige Proteine finden, für die eine Rolle in der Kommunikation zwischen Kalzium- und BR-Signalweg vorhergesagt wurde. Für NRT1.1 und NRT2.1 wurden im PhosphoNetwork weitere mögliche Rollen bei der Regulation des Wurzelmembran-phosphoproteoms vorhergesagt. Diese Arbeit hat gezeigt, dass der PhosphoNetzwerk-Ansatz einen vielversprechenden Ansatz zur Verifizierung von phosphorylierungs-regulierten Signalwegen darstellt, um Kinasen bzw. Phosphatasen ihren Substratproteinen zuzuordnen.

Insgesamt hat diese Arbeit einen Beitrag zur Erforschung des Proteoms von jungen Maiswurzel-Haarzellen und dessen Reaktion auf verschiedene Nährstoffmangelbedinungen geleistet. Dabei wurden verschiedene Perspektiven der Beteiligung von NRT1.1 und NRT2.1 an der Regulierung der Reaktion des Phosphoproteoms aufgezeigt und ein Phospho-Switch-Modell erarbeitet, welches die Forschungsergebnisse integriert und die NRT2.1-Aktivität erklärt.

(Translated by Max Gilbert)

1 Introduction

To support its survival, a plant requires certain nutrients just like other organisms on this planet. Depending on the amount of plant requirement, these nutrients are generally divided into macronutrient and micronutrient. The macronutrients are nitrogen (N), phosphorus (P), potassium (K), magnesium (Mg), calcium (Ca), and sulphur (S). Nutrients like iron (Fe), manganese (Mn), zinc (Zn), copper (Cu), boron (B), chlorine (Cl), molybdenum (Mo) and nickel (Ni) belong to the group of essential micronutrient, as the plant requires these in lower amounts. Plants uptake these nutrients from the soil through their root system which contains two major parts: the primary root and lateral roots. According to its activity, a plant root can be also classified into three different zones. In the meristematic zone, the cells undergo rapid mitosis to produce new cells for root growth, new cells close to the root apex will form the root cap, while those close to the root base will face a different fate. In the elongation zone, these new cells elongate rapidly providing the root with extra length. In the maturation zone also known as differentiation zone, well developed tissues appear including phloem, xylem, and root hairs. Due to its important role in the uptake variety of nutrients from the soil to support plant survival, biologists are always interested in finding out how the root system responds to different nutritional stimuli and how different nutrients are taken up by the root. Since a root grows underground, and this special environment makes it inaccessible. To cope with this problem, several nonsoil culture system were developed and widely used including agar plate, hydroponics, and aeroponics. Combining these non-soil culture systems with phenotyping, metabolomics, transcriptomics, and proteomics, it is becoming much easier for to interpret the relationship between plant root and nutrients systematically.

Knowing the nutrition stimuli related to biological processes from various differentiated cell types can help us with describing a more detailed story of plant biology. As a result, the single differentiated tricoblast cell forming a root hair has drawn biologist's attention to itself for its unique properties and functions. Besides, the acquisition of root hairs is relatively easy.

In order to deal with the heterogeneity and dynamic variations of natural nutrients in soil, plants have evolved various protein based nutrient uptake systems in their roots. Nitrogen, for instance, is one of the macronutrients. There are different forms of nitrogen in soil including ammonium, nitrate, urea, amino acids, and peptides. Plants have been found to possess corresponding transporters so the roots can uptake any nitrogen forms mentioned above. To cope with the fluctuation of certain nutrients in the soil, plants have also evolved transporters with different affinities for the same substrate, like high and low affinity nitrate transporters found in plant roots.

Most of nutrient uptake systems are found located at the plant cell's membrane systems, and phosphorylation has been found to regulate these proteins in diverse ways. So a better understanding of the membrane systems phosphoproteome would be a great help in unveiling the plant root's response to the availability of nutrients in the soil.

In my research, I chose MS-based proteomics as a method to firstly study how the proteome of maize root hair cells responds to the deprivation of different nutrients. I then used MS-based phosphoproteomics to study how the Arabidopsis root microsomal fraction (MF) responds to different

availability of the nitrogen nutrient. Thirdly, the regulatory mechanisms of nitrate uptake by NRT2.1 were explored.

1.1 Section 1: Root Hairs

1.1.1 Function of Root Hair

Root hairs are thin unicellular cell elongations of rhizodermal cells that grow into the rhizosphere to increase the root contact with soil and water and to acquire immobile nutrients from the soil (Datta et al., 2011). Their importance for model plants, such as the dicot model plant Arabidopsis, and for crops, such as the monocot barley, has been proven, especially when phosphorus availability is low (Bates and Lynch, 2001) (Gahoonia and Nielsen, 2003). However, root hairs have been implicated in the uptake of Ca^{2+}, K^{+}, NH_4^{+}, NO_3^{-}, Mn^{2+}, Zn^{2+}, Cl^{-}, and inorganic phosphate (Gilroy and Jones, 2000). Root hairs are also the entry site of rhizobial symbionts for nodule organogenesis, and they participate in root defense reactions against pathogens.

1.1.2 Formation of Root Hair

In maize, and most other crops with roots containing many cortical cell layers, the arrangement and spacing of root hairs do not follow a simple design and appear to be random (Clowes, 2000). Root hair development starts with asymmetric cell divisions from protodermal cells, and several proteins involved in root hair development were identified by genetic approaches (Nestler et al., 2014). In the model plant Arabidopsis, root hairs almost exclusively appear in trichoblast rhizodermal cell positions that have contact with two cortical cells, whereas nonhair cells have contact with only a single cortical cell and express the transcription factor GLABRA2 (Masucci et al., 1996). In trichoblasts, the leucin-rich-repeat receptor SCRAMBLED receives a position-dependent signal from the neighboring cell to regulate a quite complex network of position-dependent expression of transcription factors to regulate the fate of root hairs and their development (Datta et al., 2011) (Schiefelbein et al., 2014). Root hair formation in most monocots (e.g., rice) starts with asymmetric epidermal cell division that leads to a longitudinally shorter hair cell and a longer nonhair cell. However, in maize, the root hair cells are randomly mixed with nonhair cells. Maize root hair development shows parallels with that of dicots, and essential genes for root hair formation, such as *Roothairless 1*, a Sec3 encoding gene, is involved in vesicle trafficking for polar hair growth in dicots as well (Wen et al., 2005). However, there are also unique, essential proteins that are required for root hair formation in maize, such as the monocot-specific *Roothairless 3*, a glycosylphosphatidylinositol anchor protein (Hochholdinger et al., 2008), and the *Roothairless 5* NADPH oxidase (Nestler et al., 2014).

1.1.3 Different Nutrients Can Affect Root Hair Development

In many plant species, the low availability of phosphorus in the rhizosphere increases the length and density of root hairs. However, the deprivation of other elements, such as nitrogen, manganese, or iron can also result in an altered root hair density (Ma et al., 2001) (Foehse and Jungk, 1983). The plasticity of root hairs to specific nutrient deprivations also involves the phytohormones auxin and ethylene. Both hormones promote root hair growth at low nutrient concentrations, but they inhibit root hair development at higher nutrient levels (Pitts et al., 1998).

1.1.4 Root Hairs May Sense Environmental Nutrients at Maize Seedlings Early Stage

Although root hairs develop very early after germination in maize, they apparently do not contribute to the uptake of phosphate or nitrogen in the first 5 days after germination, as maize seedlings do not acquire phosphate and nitrogen from the nutrient medium at this early developmental stage (Nadeem et al., 2011). Instead, internal phosphate reserves from phytate degradation in the seed can support maximal growth until these stores are exhausted (after about 4 weeks) (Nadeem et al., 2011). The reserves of micronutrients (Fe, Zn, and Mn) in maize seeds are generally sufficient to support the maximal growth of seedlings for at least 2 to 4 weeks (White and Veneklaas, 2012), so uptake of these nutrients through roots and root hairs is initially not required. However, root hairs are in direct contact with the soil nutrient medium and may therefore already signal a lack of individual nutrients in the medium to the cellular metabolism and inner cell layers.

1.2 Section 2: Nitrogen as an Important Macronutrient

1.2.1 Nitrogen

Nitrogen (N) is a basic constituent of several biological macromolecules such as nucleotides, amino acids and proteins which are essential for all organisms. There are also different forms of N including organic N and inorganic N, among them the inorganic N forms ammonium and nitrate are the two major N sources for plants.

1.2.1.1 Inorganic Nitrogen

Plants can uptake nitrate through their roots. Some nitrate will be directly reduced to nitrite by nitrate reductase (NIA/NR) in the root cytoplasm, then nitrite reductase (NIR) reduces nitrite to ammonium in the plastids. Nitrate is also transported to the shoot where similar assimilation occurs. Ammonium derived from nitrate or taken up from the soil directly is further assimilated into glutamine via glutamine synthetase (GS)/glutamine-2-oxoglutarate aminotransferase (GOGAT) cycle (Oaks, 1994) (Lam et al., 1996). Plants can also store nitrate and ammonium in vacuoles, so they can use these sources under nitrogen limitation. Compared to ammonium, nitrate can be stored in larger quantities since ammonium is toxic to plants (Wang et al., 2018b). Plants do not uptake nitrate and ammonium only, but also can exclude them. Both nitrate and ammonium efflux can happen in plant roots and volatile nitrogen such as NH_3 may be released from aboveground parts of plants (Feng et al., 1994) (Segonzac et al., 2007) (Kumagai et al., 2011).

Besides serving as a nitrogen source, nitrate is found to be a signaling molecule as well. An exogenous supply of nitrate to *Arabidopsis thaliana* seeds could stimulate the germination of them (Alboresi et al., 2005). Root system architecture of *Arabidopsis thaliana* such as lateral root initiation, lateral root elongation, root hair growth, and primary root growth can be affected by nitrate as well (Zhang and Forde, 2000). Nitrate can cause a rapid transcriptional response in plants which induces gene expression within minutes and reaches a peak at approximately 30 min. This rapid transcriptional response named the primary nitrate response (PNR) (Deng et al., 1989) (Gowri et al., 1992), and no *de novo* protein synthesis is needed for the PNR (Gowri et al., 1992) (Wang et al., 2004). PNR includes gene expressions of nitrate transporter genes (from the nitrate transporter 1 and 2 families), nitrate assimilation genes

(NIA and NIR), and genes involved in the pentose phosphate pathway, glycolysis, and trehalose-6-P metabolism which provide the carbon scaffold and endow reducing power (Scheible et al., 1997) (Wang et al., 2003). Interestingly, applying different concentration of nitrate (less than 1 mM or higher than 1 mM) may induce corresponding levels of the PNR (Hu et al., 2009). One study also showed that nitrate may regulate tobacco leaf morphogenesis by maintaining biosynthesis and/or root to shoot transfer of cytokines (Walch‐Liu et al., 2000). Besides hormones, glutamine and small peptides were found to be involved in nitrate signaling as well (Muller and TOURAINE, 1992) (Miller et al., 2008a) (Gent and Forde, 2017) (Ohkubo et al., 2017). Calcium is now known as a key second messenger in plants (Dodd et al., 2010), some studies also showed that calcium may bridge the gap between nitrate signal and downstream regulators (Krouk, 2017) (Liu et al., 2017).

As another major inorganic nitrogen source, ammonium may function as a signaling molecule too (Bittsánszky et al., 2015) (Esteban et al., 2016) (Li et al., 2014).

1.2.1.2 Organic Nitrogen

There are several forms of organic nitrogen in nature such as urea, amino acids and peptides. Urea is an intermediate of plant arginine catabolism involved in nitrogen remobilization from source tissues, it can also be directly used as nitrogen fertilizer in agriculture. Two different mechanisms are involved in the usage of urea by plants, microbial in the soil can transform urea into ammonium and nitrate which can then be taken up and used by plants. The other mechanism is that plants can uptake urea directly from the soil and an internal hydrolysis will be applied to generate ammonium and nitrate which can be used by the plants (Witte, 2011). Amino acids can also be used as sources of nitrogen by plants in various ecosystems (Lipson and Näsholm, 2001) (Schimel and Bennett, 2004).

Previous studies have shown that exogenous L-glutamate applied at micromolar concentrations is able to inhibit primary root growth and stimulate root branching in the apical region of the primary root of Arabidopsis (Walch-Liu et al., 2006). This suggests that organic nitrogen may also have the potential to function as a molecular signal.

1.2.2 Transporters for Different Nitrogen Sources

Plant growth and productivity relies on nitrogen availability. Because of the heterogeneity and dynamic variations of natural nitrogen sources, plants have evolved a large variety of uptake systems for different nitrogen (Xu et al., 2012).

1.2.2.1 Nitrate Transporter

Proteins functioning as nitrate transporters have been found in higher plants, they can be classified into four families: nitrate transporter 1/peptide transporters (NRT1/PTR), NRT2s, chloride channels (CLC), and slow anion channel associated 1 homolog 3 (SLAC1/SLAH) (Wang et al., 2012).

As first cloned plant nitrate transporter gene in Arabidopsis, NRT1.1/CHL1 was found expressed in the root epidermal, cortical, and endodermal cells (Huang et al., 1996), and the expression of NRT1.1 could be induced by external nitrate (Tsay et al., 1993). Most of the nitrate transporters from the NRT1/PTR family exhibit a low affinity (LATS) for nitrate (K_M >1 mM), but NRT1.1/CHL1 displays both a high and low affinity for nitrate (Wang et al., 1998) (Liu et al., 1999) (Liu et al., 1999). Besides nitrate,

NRT1.1/CHL1 can transport auxin (Krouk et al., 2010b) which is important for stimulation of lateral root growth (Krouk et al., 2010b) (Bouguyon et al., 2015). NRT1.1/CHL1 also plays an important role in nitrate sensing (Ho and Tsay, 2010). Former research has provided evidence that a functional NRT1.1/CHL1 is required for primary nitrate responses in Arabidopsis (Gojon et al., 2011). Furthermore, it was shown that nitrate sensing and transport through NRT1.1/CHL1 is independent since nitrate does not need to be transported across the membrane when NRT1.1/CHL1 functions as a nitrate sensor to trigger the signal for the primary nitrate response (Ho et al., 2009). Besides the role in nitrate-responsive genes regulation, NRT1.1 was also found involved in regulation of cadmium uptake (Mao et al., 2014) and plant proton tolerance (Fang et al., 2016).

The NRT2 family belongs to the major facilitator superfamily (MFS) of transporters (Trueman et al., 1996), unlike dual-affinity transporter NRT1/PTR, all the characterized members from the Arabidopsis NRT2 family are high-affinity nitrate transporters (HATS) (Filleur et al., 2001). There are seven members of this gene family found in Arabidopsis (*At*NRT2.1-*At*NRT2.7), among them, NRT2.1 has been proven to be a major contributor to the HATS (Li et al., 2007). However, it has been shown that NRT2.1 alone cannot function as a high affinity nitrate transporter, it needs to interact with another nitrate assimilation related (NAR2.1) protein to form a functional complex (Orsel et al., 2006) (Li et al., 2007) (Yong et al., 2010). NRT2.1 was found located in the plasma membrane of epidermal and cortical cells in Arabidopsis roots (Chopin et al., 2007) (Wirth et al., 2007). The expression of NRT2.1 was firstly found induced under low nitrate condition and depressed under high nitrate status (Lejay et al., 1999) (Muños et al., 2004). But another study showed a more complex regulatory mechanism in NRT2.1 expression regulation. By using split-root and grafting experiments, people found a mobile peptide C-TERMINALLY ENCODED PEPTIDE (CEP) generated in N-starved roots could be translocated to shoot. Upon sensing of this peptide, two polypeptides CEP downstream1 (CEPD1) and CEPD2 were produced in shoot and translocated back to each root. And the expression of NRT2.1 could be then upregulated by these two polypeptides, especially in the roots exposed to high nitrate (Ohkubo et al., 2017).

*At*NRT2.1 may repress lateral root initiation in response to nutritional cues, and this role is independent of nitrate uptake (Little et al., 2005). Aquaporin water channels play very important roles in the water transport capacity (root hydraulic conductivity, L_{p_r}) of plant roots (Tournaire-Roux et al., 2003) (Sutka et al., 2011), the expression of some aquaporins (PIP1;1, PIP1;2, PIP2;1 and PIP2;3) seems to be regulated by *At*NRT2.1 which thus impacts on the L_{p_r} of Arabidopsis (Li et al., 2016). Another research on *At*NRT2.1 indicated its possible function in *Pseudomonas syringae*-induced plant defenses (Camanes et al., 2012). All these evidences suggest that *At*NRT2.1 is not only a high affinity nitrate transporter but also – in analogy to NRT1.1 – a possible nitrate sensor.

There are six members found in the Arabidopsis CLC family (*At*CLCa-*At*CLCf), among them *At*CLCa, *At*CLCb, *At*CLCc, and *At*CLCg are localized to tonoplasts (von der Fecht-Bartenbach et al., 2010). Existing evidences could only demonstrate *At*CLCa to be involved in vacuolar nitrate storage in plants (De Angeli et al., 2006), although *At*CLCb serves as a $2NO_3^-/H^+$ antiporter in Xenopus oocytes (von der Fecht-Bartenbach et al., 2010). Even less is known about the rest of this family.

The S-type anion channel (SLAC/SLAH) gene family is a small family which contains five genes, *SLAC1* and *SLAH1–SLAH4* (SLAC1 homologues). CO_2 and abscisic acid dependent plant stomatal closure is found to be controlled by these proteins (Negi et al., 2008). Interestingly, when being expressed in *Xenopus* oocytes, both SLAC1 and SLAH3 display nitrate transport activity (Negi et al., 2008) (Geiger et al., 2009). Another study on SLAH3 provided evidence that this protein may play a role in nitrate-dependent alleviation of ammonium toxicity in plants (Zheng et al., 2015).

1.2.2.2 Ammonium Transporter

Six ammonium transporters have been identified in Arabidopsis, and they can be classified into two groups, *At*AMT1 including *At*AMT1;1-*At*AMT1;5 and *At*AMT2;1 (Loqué and von Wirén, 2004). *At*AMT1;1, *At*AMT1;2, *At*AMT1;3, and most likely *At*AMT1;5 function as high-affinity ammonium transporters in the Arabidopsis root (Yuan et al., 2007). *At*AMT1;1 and *At*AMT1;3 also play roles in regulating Arabidopsis lateral root branching in response to ammonium, indicating that these two proteins may serve as transceptors as well (Lima et al., 2010). Transport activity of ammoniaby *At*AMT2;1 has been demonstrated by expressing this gene in a yeast ammonium transport mutant and in Xenopus oocytes (Sohlenkamp et al., 2000) (Neuhäuser et al., 2009).

1.2.2.3 Transporter for Organic Nitrogen

Some members from organic nitrogen transporters have been characterized to date. By performing a heterologous complementation experiment of a urea uptake-defective yeast (*Saccharomyces cerevisiae*) mutant, several proteins *At*TIP1;1, *At*TIP1;2, *At*TIP2;1, *At*TIP4;1, and *At*DUR3 involved in urea uptake were isolated. Among them, *At*TIP1;1, *At*TIP1;2, *At*TIP2;1, *At*TIP4;1 can serve as water channels and may be involved in equilibrating urea concentrations between different cellular compartments of Arabidopsis (Liu et al., 2003b), while *At*DUR3 functions as a high-affinity urea/H^+ Symporter (Liu et al., 2003a). Besides these proteins, *At*TIP1;3 and *At*TIP5;1 were also found as water and urea channels, and both of them are Arabidopsis pollen-specific (Soto et al., 2008).

Four Arabidopsis amino acid transporters (*At*LHT1, *At*AAP1, *At*AAP5, and *At*ProT2) have been well characterized, and they differ in substrate selectivity and affinity. *At*AAP1 plays a role in neutral and acidic amino acids uptake when soil concentrations are higher than 50 µm (Lee et al., 2007b) (Svennerstam et al., 2011), while *At*LHT1 and *At*AAP5 are involved in uptake neutral and acidic amino acids, and basic amino acids at lower concentrations (Svennerstam et al., 2008) (Svennerstam et al., 2011). *At*ProT2 functions in proline uptake in root (Lehmann et al., 2010) (Grallath et al., 2005).

Based on the length of their substrates, plant peptide transporters can be generally classified into three different gene families: PTR family is responsible for transporting di- and tripeptides; OPT (oligopeptide transporter) family play a role in transporting peptides containing 4-5 amino acids; transport of peptides with more than 6 amino acids is mediated by members of ABC (ATP binding cassette) gene family, one subfamily from of ABC transportes in animals - TAP (transport associated with antigen processings) was found to transport peptides of 8-12 amino acids (Stacey et al., 2002) (Wolters et al., 2005), in Arabidopsis three TAP proteins have been identified, but the function of them still needs further investigation (Rentsch et al., 2007).

1.2.3 Post-translational Modification

A lot of studies have shown that many proteins undergo post-translational modifications (PTMs), which play important roles in regulating the activity and function of proteins. In general, PTMs are covalent processes that include the reversible addition and removal of functional groups by phosphorylation, acylation, glycosylation, nitration, methylation, sumoylation, oxidation, and ubiquitination (Mann and Jensen, 2003) (Seo and Lee, 2004). These PTMs can only happen in the organism and amino acid-specific way, and there is no doubt that with the development of new technology more PTMs will be discovered and characterized.

To date, many PTMs have been well studied. In higher plants, methylation was found on histone lysine or arginine, it is very important in regulating diverse developmental processes and silencing repetitive sequences in order to maintain genome stability (Liu et al., 2010). Proteins can be degraded by the proteasome after being targeted by ubiquitin, this Ub-proteasome pathway in plants plays an important role in the regulation of diverse cellular processes (Glickman and Ciechanover, 2002) (Welchman et al., 2005). Sumoylation is an ubiquitin-like protein (UBL) conjugation process, but unlike ubiquitin, sumoylation may attenuate target protein degradation (Kerscher et al., 2006). In plants, sumoylation is involved in responses to the environment, hormonal responses, phytopathogen infection and pathogen defense, and in controlling of flowering (Miura et al., 2007).

Among PTMs, protein phosphorylation might be the most important and best characterized one with a well-established role in regulation transport proteins. Phosphorylation can be found mainly on serine, threonine, and tyrosine residues of plant proteins, it can regulate protein function through different mechanisms. Arabidopsis K^+ transporter 1 (AKT1), responsible for K^+ uptake in roots, was found to be activated by phosphorylation (Lee et al., 2007a). The activity of aquaporin water channel PIP2;1 in Arabidopsis can be regulated by phosphorylation at Ser280 and Ser283 (Prado et al., 2013). The dual affinity of *At*NRT1.1 is regulated by phosphorylation of the Thr101 residue, *At*NRT1.1 serves as a high-affinity nitrate transporter when Thr101 is phosphorylated, while dephosphorylation at this residue can turn NRT1.1 into a low-affinity transporter (Liu and Tsay, 2003). Another study of yeast *Hansenula polymorpha* showed that under nitrogen limitation condition, phosphorylation could prevent a high affinity nitrate transporter YNT1 delivery from the secretion to the vacuole, in this case YNT1 could accumulate at the plasma membrane to cope with nitrogen depletion (Mart ń et al., 2011). This research demonstrates that phosphorylation can regulate protein localization as well. Besides its role in modulating protein activity, protein-protein interaction and protein-RNA interaction can also be affected by phosphorylation (Xiao and Manley, 1997).

Interestingly, more and more evidence has shown that PTMs can function in orchestrated manners. The activity of plant NR can be decreased by phosphorylation (Huber et al., 1992) (Hey et al., 2009), but sumoylation can increase its activity (Park et al., 2011). Unlike the antagonistic effects caused by sumoylation and phosphorylation on NR activity, both modifications of phytochrome B inhibit light-induced signaling in Arabidopsis (Medzihradszky et al., 2013) (Sadanandom et al., 2015). Crosstalk between phosphorylation and ubiquitination is also well demonstrated (Dai Vu et al., 2018).

1.2.4 Kinase and Phosphatase

Signal transduction in plants can be achieved through reversible protein phosphorylation mediated by protein kinases and protein phosphatases, and many biological processes can be regulated in this way.

Protein kinases are known to be involved in cellular signal transduction. The model plant Arabidopsis genome encodes more than 1000 protein kinases, they can be classified into different families, but only some of these families have been well studied. Leucine-rich-repeat (LRR) receptor kinase is a large protein kinase family which harbors an N-terminal LRR domain predicted to recognize and bind a ligand (Zhao et al., 2018). Mitogen-activated protein kinase (MAPK) is another well-known protein kinase family which was firstly revealed to be involved in immunity and stress responses. Recent studies have shown that plant growth and development also require functional MAPKs, other investigation have demonstrated that MAPKs are downstream of receptor-like protein kinases (RLKs) from which multiple functional pathways are initiated. Interestingly, some of these pathways often share the same MAPK components and some use a complete MAPK cascade (Xu and Zhang, 2015). Ca^{2+} concentration in plants can be affected by abiotic and biotic stimuli coming from the environment or from physiological processes happening within the organism (Webb et al., 1996) (Hetherington and Brownlee, 2004). These findings have made Ca^{2+} a well-known intracellular messenger (Dodd et al., 2010). Calcium-dependent protein kinase (CDPK) family, which contains a calcium-activation domain, is considered as a Ca^{2+} sensor that can translate the change of intracellular Ca^{2+} concentration into downstream signaling events (Harmon et al., 2000). Besides CDPKs, Calcineurin B-like proteins (CBLs) are a Ca^{2+} sensor protein family, CBLs can interact with certain protein kinases termed CBL-interacting protein kinases (CIPKs) to form complexes which are important in plant responses to environmental stimuli (Hashimoto et al., 2012).

In the past decades, with the help of knowledge from classic forward and reverse genetics, people were able to identify several kinases and their substrates. For example, through studying mutant Arabidopsis plants, one CDPK-CPK6 was found as a positive regulator of the plant hormone ABA control of S-type anion channels in guard cells (Mori et al., 2006), from a further study, the activity of one central guard cell S-type anion channel SLAC1 was found regulated through phosphorylation mediated by CPK6 (Brandt et al., 2012). In another approach, after applying genetic screen to over 50 kinase mutant lines, CIPK23 showed an ammonium hypersensitivity phenotype which was correlated with the phenotype of an AMT quadruple knock out mutant, further investigation demonstrated that the ammonium transport activity of AMT1.1 and AMT1.2 can be inhibited through phosphorylation mediated by CIPK23 (Straub et al., 2017). Besides its role in regulating the activity of AMTs, CIPK23 was also found down-regulated in a NRT1.1 knock out line from a microarray analysis. More evidence has further proven that CIPK23 can phosphorylate NRT1.1 at threonine 101 which turns NRT1.1 into a high affinity nitrate transporter (Ho et al., 2009). Further examples to study kinases involved in transporter regulation come from the brassinosteroid (BR) signaling pathway. Brassinolide (BL) is one kind of steroid hormones which plays a very important role in developmental and physiological processes of plants. This hormone can bind to the extracellular domain of a receptor kinase brassinosteroid insensitive 1 (BRI1). By combining two dimensional gel electrophoresis (2-D DIGE) and mass spectrometry (MS) analysis, BL-induced phosphorylation could be detected from two receptor-like cytoplasmic kinases in Arabidopsis, which were named BR-Signaling kinase 1 and 2 (BSK1 and BSK2), and the results from an *in vitro*

kinase assay and *in vivo* protein-protein interaction investigation indicated that BR could activate the BL-receptor BRI1. BRI1 could then phosphorylate BSK1 so the BR signal can be transduced from extracellular into intracellular (Tang et al., 2008). The experimental strategies used in these studies have greatly improved our understanding of kinases and their associated substrates, however classic forward or reverse genetic methods require a lot of labor and sometimes a long time period.

A lot less is known about protein phosphatases involved in plant membrane transporter regulation. Protein phosphatases can be generally divided into following families: protein tyrosine phosphatases (PTPs), dual specificity phosphatases (DSPTPs), protein phosphatase types 1 (PP1), protein phosphatase types 2A (PP2A), protein phosphatase types 2B (PP2B), protein phosphatase types 2C (PP2C) (Schweighofer et al., 2004). Compared to protein kinases in plants, less is known about plant protein phosphatases, the most well studied protein phosphatases in plants should be abscisic acid-insensitive1 and 2 (ABI1 and ABI2) both of which play a role in abscisic acid (ABA) signal transduction, and belong to the PP2Cs.

1.3 MS-based Proteomics and Phosphoproteomics

The continuous development of protein mass spectrometry makes it possible to analyze thousands of phosphoproteins in vivo within a short time, therefore MS-based proteomics and phosphoproteomics have become valuable tools in investigating regulatory changes over time and/or between conditions.

Previous analyses by a shotgun proteomics approach gave the first view of the maize root hair proteome (Nestler et al., 2011). In the inbred B73 line, almost 2600 proteins were identified in root hairs, a similar number of proteins as was identified in the dicot *Arabidopsis thaliana* (Lan et al., 2013). In contrast, in soybean root hairs, more than the double number of proteins was identified (Brechenmacher et al., 2012). Several development- associated proteins, metabolic proteins and, noteworthy, many nutrient transporters were identified.

Through phosphoproteomic analysis, Stecker was able to reveal that osmotic stress not only stimulated phosphorylation of MAPKs in Arabidopsis but also stimulated phosphorylation of proteins involved in 5’ messenger RNA decapping and phosphatidylinositol 3,5-bisphosphate synthesis (Stecker et al., 2014). MAPKs are important for plant defense, a phosphoproteomic study showed that MPK3, MPK4, and MPK6 have both specific and shared substrate, this work also revealed the interplay between MAPKs and CDPKs (Rayapuram et al., 2018). Phosphoproteomic analysis was also applied to investigate regulatory mechanisms of plant innate immune responses (Kadota et al., 2019), iron-deficient signaling in Arabidopsis root (Lan et al., 2012), mechanism of maize salt-stress tolerance (Zhao et al., 2019), responses to ABA (Umezawa et al., 2013) and BR (Lin et al., 2015) signaling pathway in Arabidopsis. Besides these, phosphoproteomics analysis was used to study the global dynamic phosphorylation patterns of Arabidopsis resupplied with nitrate or ammonium as well. (Engelsberger and Schulze, 2012). The knowledge learned from phosphoproteomic analysis has greatly facilitated our research in plant biology.

1.4 Aim of the Research

1.4.1 The Role of Root Hairs in Nutrient Uptake and Sensing

The complex mechanisms of root hair development and adjustments to nutrient stress are of great importance for the plant. Growth adjustments ensure that limited nutrient resources can be used more efficiently. Previous studies identified gene modules involved in response to nutrient deprivation in the roots of model plants (Scheible et al., 2004) (Krouk et al., 2010a) (Morcuende et al., 2007) (Osuna et al., 2007) (Lin et al., 2011). However, these analyses mostly focused on gene expression differences within complex tissue preparations. Gene expression may not match the protein abundance changes, and there is strong evidence for cell-type specific responses to nutrient deprivation, such as nitrogen deprivation (Gifford et al., 2008). These subtle changes may be masked when complex tissue mixtures are analyzed. Taking advantage of the root hair cell as a single, well-defined cell type, we will quantify the relative protein expression under full nutrition and in situations where a single nutrient is omitted from the nutrient solution. **We hypothesize that individual responses to macro- and micronutrient deprivations will be detectable in root hairs as early as a few days after germination, and we aim at identifying key pathways regulated upon the lack of a single macro- or micronutrient**.

1.4.2 In-depth Arabidopsis Root MF Phosphoproteomic Study of Nitrogen-induced Signaling

All living cells are enclosed in the plasma membrane serving as a boundary to separate the cytoplasm from the external environment and to protect contents within cells. Besides plasma membrane, higher plant cells also contain intracellular membrane-enclosed organelles such as endoplasmic reticulum (ER), nucleus, Golgi apparatus, chloroplast, mitochondria, and vacuole. These membrane systems do not only work as boundaries, with the help of different proteins (transporters, kinases, receptors, and channels) associated with these membranes, these systems also play an important role in communication between the extracellular environment and the cell and in coordination between different cellular organelles. For this reason, more and more studies are focused on discovering how the proteome and phosphoproteome from the microsomal fraction respond to external stimuli. One of these studies has demonstrated that applying different nitrogen (nitrate or ammonium) to nitrogen starved Arabidopsis seedlings could result in different phosphorylation patterns of microsomal proteins (Engelsberger and Schulze, 2012). From this investigation, phosphosites from several nitrogen transporters were found as well, such as nitrate transporter NRT2.1, ammonium transporters AMT1.1 and AMT1.3. How phosphorylation can regulate NRT1.1 transport activity has been well demonstrated, however, whether or how NRT2.1 can be regulated through phosphorylation is still unknown. Furthermore, as a nitrate transceptor and a potential nitrate transceptor, NRT1.1 and NRT2.1 have raised a lot of attention. However previous research was almost exclusively focused on their nitrate transport activity, their role in regulating plant development, and immune response or their function in transcriptional regulation (Bouguyon et al., 2015) (Camanes et al., 2012) (Cerezo et al., 2001) (Filleur et al., 2001) (Ho et al., 2009). But there is another interesting question, as whether these two membrane located proteins function in regulating root MF phosphoproteome responses. **I want to find out how NRT2.1 is precisely regulated by phosphorylation. I also would like to study whether NRT1.1 or NRT2.1 plays a role in regulating microsomal phosphoproteome responses to external nitrogen stimuli.**

2 Materials and Methods

2.1 Materials and Methods Used in Section 1: The Role of Root Hairs in Nutrient Uptake and Sensing

2.1.1 Plant Material and Aeroponic Growth System

Zea mays hybrid seeds (var. surprise, KWS, Germany) were surface-sterilized for 10 min in 10% H_2O_2 and subsequently rinsed several times with sterile double-distilled water. Seeds were placed on small holders on top of an aeroponic box system (22 L volume; Supporting Information Figure S1), which was kept in a climate chamber with 24/20 °C day/night temperature regime. The day length was set to 16 h, and the relative humidity was around 70−72%. Every nutrient deprivation experiment was carried out in three biological replicates. For every treatment and control replicate, 28 seeds were placed on sterilized 2.5 × 5 cm^2 moist filter paper rolled in 5 × 10 cm^2 foam. The aeroponic box system contained a nebulizer (Fogstar 100, Seliger, Germany) and a ventilation unit (IP68, Elektrosil, Germany). Germination rates were between 85 and 95%. The box was filled with 7 L of nutrient medium, and the seeds were covered for 2 days with sterilized transparent plastic foil and subsequently with black foil. Root hairs were harvested after 2 additional days.

2.1.2 Nutrient Deprivation Conditions

The nutrient solution was a modified 1/4 Hoagland solution (1 mM NH_4NO_3, 1 mM KH_2PO_4, 1 mM $CaCl_2$, 0.5 mM $MgSO_4$, 100 μM Na_2Fe(II)-EDTA, 9 μM $MnCl_2$, 0.77 μM $ZnSO_4$, 0.32 μM $CuSO_4$, 0.46 μM H_3BO_3, 0.02 μM Na_2MoO_4, pH 6, adjusted with KOH or NaOH). Nutrient deprivation media were identical to the control medium, except that a single nutrient was omitted (N, Fe, Mn, Zn). For P deprivation, KH_2PO_4 was replaced by KCl; for K deprivation, KH_2PO_4 was replaced by NaH_2PO_4. Supporting Information Table S1 gives an overview of the composition of the individual nutrient solutions.

2.1.3 Root Hair Harvest

Roots from each seedling were harvested separately, and root hairs belonging to the same nutrient treatment were combined within one biological replicate. Thereby, one aeroponic box was considered to be one replicate. Before harvesting the root hairs, the root tip of all seminal roots was removed, and the roots were submerged into liquid nitrogen. The frozen root hairs were then gently scraped off with a thin nylon line directly into a 1.5 mL tube filled with liquid nitrogen (Supporting Information Figure S1). Samples were stored at −80 °C after evaporation of the liquid nitrogen.

2.1.4 Protein Preparation for Mass Spectrometry

Root hairs were directly extracted with 6 M urea, 2 M thiourea, pH 8, and cell debris was pelleted by centrifugation at 20800g. Extracted proteins were predigested for 3 h with endoprotei- nase Lys-C (0.5 μg/μL; Wako Chemicals, Neuss) at room temperature. After 4-fold dilution with 10 mM Tris-HCl, pH 8, samples were digested with 4 μL of sequencing grade modified trypsin (0.5 μg/μL; Promega) overnight at 37 °C. After overnight digestion, trifluoroacetic acid (TFA) was added until the pH was less than 3 to stop digestion. Digested peptides were desalted over a C18 tip (PepMan, ThermoScientific)

(Gifford et al., 2008) and dissolved in 5% acetonitrile (ACN) and 0.1% TFA before mass spectrometric analysis.

2.1.5 LC−MS/MS Analysis of Peptides

Tryptic peptide mixtures were analyzed by LC−MS/MS using a nanoflow Easy-nLC1000 (Thermo Scientific) HPLC system and a quadrupole Orbitrap hybrid mass spectrometer (Q-Exactive Plus, Thermo Scientific) as a mass analyzer. Peptides were eluted from a 75 μm × 50 cm C18 analytical column (PepMan, Thermo Scientific) on a linear gradient running from 4 to 64% acetonitrile in 240 min and sprayed directly into the Q-Exactive mass spectrometer. Proteins were identified by MS/ MS using information-dependent acquisition of fragmentation spectra of multiple charged peptides. Up to 12 data-dependent fragment spectra were acquired at a resolution of 35,000 and with an isolation width of 1.2 *m/z*. The normalized collision energy was set to 25%. Full-scan spectra were acquired at 70,000 full-width at half-maximum resolution. Singly charged ions were excluded, and ions were dynamically excluded for 30 s within a 5 ppm mass window.

Protein identification and ion intensity quantitation was carried out by MaxQuant, version 1.4.1.2 (Cox and Mann, 2008). Spectra were matched against the maize proteome (Zmays_284_6a from Phytozome with 88,760 entries) using Andromeda (Cox et al., 2011). Thereby, carbamidomethylation of cysteine was set as a fixed modification; oxidation of methionine and protein N-terminal acetylation were set as variable modifications. Mass tolerance for the database search was set to 20 ppm on full scans and 0.5 Da for fragment ions. Multiplicity was set to 1. For label-free quantitation, retention time matching between runs was chosen within a time window of 1 min over a 20 min section. Peptide false discovery rate (FDR) and protein FDR cutoffs were set to 0.01. Hits to contaminants (e.g., keratins) and reverse hits identified by MaxQuant were excluded from further analysis. A full list of all identified peptides is found in Supporting Information Table S2.

2.1.6 Mass Spectrometric Data Analysis and Statistics

Reported ion intensity values were used for quantitative data analysis. cRacker (Zauber and Schulze, 2012) was used for label-free data analysis based on the MaxQuant output (evidence.txt). All proteotypic peptides were used for quantitation. Briefly, within each sample, ion intensities of each peptide ions species (each *m/z*) were normalized against the total ion intensities in that sample (peptide ion intensity/total sum of ion intensities). Subsequently, each peptide ion species (i.e., each m/z value) was scaled against the average normalized intensities of that ion across all treatments. For each peptide, values from at least three biological replicates then were averaged after normalization and scaling.

For quantitation of the nutrient deprivation responses, pairwise *t*-tests between deprived and control conditions were carried out and Benjamini−Hochberg multiple-testing correction was applied (Benjamini and Hochberg, 1995). Protein functions were assigned by Mapman (Thimm et al., 2004), and subcellular locations were derived from SUBA (Tanz et al., 2012) by matching maize proteins to their closest Arabidopsis orthologue. Over-representation and network analyses were done using Fisher's exact test.

2.2 Materials and Methods Used in Section 2: In-depth Arabidopsis Root MF Phosphoproteomic Study of Nitrogen-induced Signaling

Arabidopsis thaliana plants of the ecotype Columbia-0 (Col-0), *nrt2.1* knock-out mutant (Cerezo et al., 2001) were used for nitrogen deprivation experiment. Besides these two, *nrt1.1* knock-out mutant (salk_097431) was used for nitrate resupply experiment.

2.2.1 Sample Preparation for LC-MS/MS Analysis

2.2.1.1 Microsomal Fraction Isolation

Microsomal fraction was isolated according to a former research (Pertl et al., 2001) with minor modifications. In general, approximate 1 g frozen root tissue was firstly broken into small pieces with a hammer, then these pieces were homogenized in a glass potter tissue grinder (10 mL glass vessel, Cat.: 89026-382 and 10 mL plain plunger, Cat.: 89026-394, VWR LLC, Radnor, PA) with 10 mL homogenisation buffer (330 mM sucrose, 100 mM KCl, 1 mM EDTA and 50 mM Tris-MES, pH 7.5) and freshly added 5 µL mL^{-1} Protease Inhibitor Cocktail, 5 mM DTT, 1 mM Phenylmethylsulfonyl Fluoride (PMSF) and phosphatase inhibitors (25 mM NaF, 1 mM Na_3VO_4, 1 mM Benzamidine, 3 µM Leupeptin). After passing through four layers of Miracloth (Cat.: 475855-1R, Merck KGaA, Darmstadt) the homogenate was collected with a 50 ml tube and centrifuged at 7,500 × g for 15 min, then the supernatant was transferred to a fresh tube and spined again at 48,000 × g for another 80 min. The MF pellet was resuspended with 100 µL UTU buffer (6 M urea and 2 M thiourea dissolved in 10 mM Tris-HCl pH8.0) and stored at -80 ℃ until further processing (Figure 1A).

2.2.1.2 In-solution Trypsin Digestion

150 µg microsomal faction was needed for in-solution trypsin digestion. Microsomal fraction was firstly spined for 10 min at 10000 rpm to pellet any insoluble material, then supernatant was transferred to a fresh 1.5 ml tube, 3 µL reduction buffer (1 µg/µL DTT in water; 6.5 mM) was added, after 30 min incubation at room temperature, 3 µL alkylation buffer (5 µg/µL iodoacetamide in water; 27 mM) was applied and incubated for another 20 min at room temperature. 1.5 µL LysC (0.5 µg/µL) was added and incubated at room temperature for 3 h. Sample was then diluted with 4 volumes 10 mM Tris-HCl (pH 8), after that, 3 µL trypsin (0.4 µg/µL, Promega) was added and incubated overnight at room temperature (Figure 1A).

2.2.1.3 Desalting Digested Peptide with C_{18}-Stage Tip

C_{18}-Stage tip was used for peptide desalting (Rappsilber et al., 2003). In order to prepare C_{18}-Stage tip, place an Empore Disk C18 (product number: 12145004, Varian) on a plastic petri dish which has a flat and clean surface, then punch out a small disk using a blunt-tipped hypodermic needle, after that, the disk in the needle can be transferred into a 200 ul pipette tip, this C_{18}-Stage tip can be used for further steps. Before loading samples, C_{18}-Stage tip was conditioned by adding 50 µL Solution B (80% v/v ACN, 0.5% v/v acetic acid), after centrifugation at 2000 × g, 100 µL Solution A (0.5% v/v acetic acid) was added to equilibrate the tip, and then the tip was spined at 2000 × g till all solution was out, this equilibration step should be repeat once. Overnight trypsin digested sample was acidified by adding approximate 1/50 volume of 10% v/v TFA to reach pH 2. This sample should be spined at 14000 rpm

for 10 min to pellet any insoluble debris. The clarified sample then could be loaded into the equilibrated stage tip through centrifugation at 2000 × g for 10 min. Then the tip was washed through being filled with 100 µL Solution A and spined at 2000 × g for 6 min, this wash step was repeated for once. Sample was eluted by adding twice 20 µL Solution B (Figure 1A).

2.2.1.4 Phosphopeptide Enrichment for Nitrogen Deprivation Samples

Before loading digested peptides, stage tips was firstly made according to 2.2.1.3, while C_{18} was replaced by C_8. Then suspend 1.5 mg of 10 µm TiO_2 beads (GL-Science 5020-7510) with methanol (sigma) and transfer them into prepared C_8 stage tip. After 5 min centrifugation at 2000 × g, TiO_2 filled C_8 stage tip was equilibrated by adding 100 µL solution A (0.1% v/v TFA, 5% v/v ACN), after another 2000 × g centrifugation for 5 min, TiO_2 filled C_8 stage tip was ready for loading digested peptides. Desalting digested peptides from 2.2.3 was mixed with 100 µL solution A and then loaded into equilibrated TiO_2 C_8 stage tip followed by centrifugation for 5 min at 1000 × g. TiO_2 C_8 stage tip was washed by adding 100 µL solution A and spinning at 2000 × g for 5 min, repeat this wash step once. Enriched phosphopeptides can be first eluted by adding 50 µL 5% ammonia (WAKO, 010-03166) and centrifugation at 2000 × g for 5 min, and then eluted again by adding 50 µL 5% v/v piperidine (WAKO, 166-02773) and centrifugation at 2000 × g for 5 min, both eluates should be acidified through adding 50 µL 20% phosphoric acid (sigma). After being mixed, the mixture of both acidified eluates should be desalted following 2.2.1.3 (Figure 1A).

2.2.1.5 Phosphopeptide Enrichment for Nitrate Resupply Samples

An improved phosphopeptide enrichment method (Wu et al., 2017) was used to enrich phosphopeptide from nitrate resupply samples. In general, 1.5 mg TiO_2 beads were firstly washed with 100 µL elution buffer (1% v/v ammonia solution) for 10 min with continuous vortex and then centrifuged at 2,500 × g at room temperature for 2 min to discard elution buffer. After that, TiO_2 beads were further equilibrated with 50 µL binding buffer (1 M glycolic acid, 80% v/v ACN, 5% v/v TFA) for 60 s and centrifuged at 2,500 × g at room temperature for 2 min to discard solution, repeat this equilibration step for twice. Dried digested peptides from 2.2.1.3 were resuspended with 100 µL binding buffer and mixed with equilibrated TiO_2 beads, after 20 min continuous vortex, centrifuged at 2,500 × g at room temperature for 2 min to discard solution. The mixture was washed once with 100 µL binding buffer for 30 s and centrifuged at 2,500 × g at room temperature for 2 min to discard solution, repeat this step for two times. This mixture was then washed again with 100 µL wash buffer (80% v/v ACN, 1% v/v TFA) and centrifuged at 2,500 × g at room temperature for 2 min to discard wash buffer, repeat this wash step twice. Enriched peptides were eluted from TiO_2 beads with 1% v/v ammonia solution and 15 min incubation, repeated this elution step for two times, and collected all 240 µL eluate. The eluate was immediately acidified with 60 µL of 10% v/v formic acid. This acidified mixture was then desalted following 2.2.1.3 (Figure 1A).

2.2.2 RNA Extraction and Reverse Transcription

Total RNA isolation was performed by using peqGOLD total RNA kit (12-6627-02). Minor modification was applied to the instruction manual. In general, approximate 40 mg root tissue was ground in liquid nitrogen, after the liquid nitrogen has completely evaporated, added 400 µL RNA lysis

buffer T. The lysate was directly transferred into a DNA removing column placed in a 2.0 mL collection tube. After 1 min centrifugation at 12.000 × g at room temperature, collected the flow-through lysate into a new 1.5 mL tube. 400 µL 70 % Ethanol was added to the lysate and mix thoroughly by vortexing. Well mixed lysate was added into a PerfectBind RNA Column which had been placed in a new 2.0 mL collection tube. After centrifugation at 10.000 × g for 1 min, discarded the collection tube containing flow through liquid. Placed the PerfectBind RNA Column in a fresh 2 mL collection tube, 500 µL RNA Wash Buffer I to the PerfectBind RNA Column and centrifuged for 15 sec at 10.000 × g. Discarded the flow-throw liquid and reuse the collection tube for next step. Added 600 µL RNA Wash Buffer II to the PerfectBind RNA Column and centrifuged for 15 sec at 10.000 × g. Discarded the flow-through liquid. Repeat this wash step and discard the flow-through liquid. Placed the PerfectBind RNA Column containing RNA in the collection tube and centrifuged for 2 min at 10.000 × g to completely dry the column matrix. Placed the PerfectBind RNA Column into a fresh 1.5 mL tube and added 50 µL RNAse-free ddH_2O on to the binding matrix in the PerfectBind RNA Column and eluted RNA by centrifugation at 5.000 × g for 1 min.

cDNA-Synthesis Kit H Plus (03-2040) from peqlab was used for reverse transcription. A total volume of 20 µL reaction mixture was prepared on ice containing approximate 2.5 µg total RNA, 0.5 µg Oligo$(dT)_{18}$ 4 µL 5 x reaction buffer, 20 u RNase inhibitor, 2 µL dNTP mix, 1 µL peqGOLD M-MuLV H Plus Reverse Transcriptase. This mixture was incubated for 1 hour at 42 °C, then terminated by heating at 70 °C for 10 min.

2.2.3 Creation of Site-Directed Mutagenesis

Site-directed mutagenesis was carried out according to the instruction manual of quickchange II site-directed mutagenesis kit (Agilent Technologies, United States).

Preparation of the mutant strand synthesis reaction was shown in Supplementary Table S2, cycling parameters were described in Supplementary Table S3, oligonucleotide primers used in the synthesis were in Supplementary Table S4.

2.2.4 Recombinant Protein Expression

All those coding sequences of phosphopeptides found from NRT2.1 were synthesized and ligated to expression vector pET21a(+) by company POLYQUANT. The coding sequence of kinase cytoplasmic domain was amplified from cDNA and ligated to expression vector pET21a(+). The *E. coli* BL21 (DE3) strain (Novagen) was used for the transformation of the expression vector construct. All the primers used in this experiment were shown in Supplementary Table S5.

Recombinant kinase cytoplasmic domain expression and purification was performed as described previously (Pratt et al., 2006) with minor modification. Inoculated 10 mL LB medium (10 g/L Tryptone, 5 g/L yeast extract and 10 g/L NaCl) with 50 µg/mL ampicillin with a single colony BL21 carrying relevant expression construct, incubated overnight at 37 °C with continuous shaking at 180 rpm, transferred 1 mL of this overnight culture to prewarmed medium (37 °C) and incubated with shaking at 180 rpm 37 °C. 50 µL 1 M IPTG (isopropyl ß-D-thiogalactopyranoside) was added when the OD_{600} reached between 0.6 and 0.8 to start induction. Collected all the cells with a 50 mL tube by centrifugation at 4000 rpm for 15 min after 6 hours induction. Added 2.5 mL 1 × BugBuster protein

extraction reagent (Novagen), resuspended cells by placing the 50 mL tube on a rocker platform for 15 min at room temperature. Centrifuged at 16000 × g at 4 °C for 20 min, supernatant was collected for Immobilized Metal Affinity Chromatography (IMAC). Recombinant kinase intracellular domain was enriched through IMAC, Ni^{2+}-NTA (Sepharose, 1 mL, IBA) column was firstly equilibrated by adding 5 column volume (CV) binding buffer (20 mM phosphate buffer pH7.4, 0.5 M NaCl, 20 mM imidazole), collected supernatant was then applied into the column in 1 mL steps, discarded the flow-through. The column then was washed with 10 CV binding buffer in 1 mL steps. The bound material was eluted with 5 CV (5 mL) elution buffer (20 mM phosphate buffer pH7.4, 0.5 M NaCl, 500 mM imidazole) in 1 mL steps. All the 5 mL eluates were dialyzed against 2 L 20 mM phosphate buffer (pH 7.4) overnight at 4 °C (Figure 1B).

For expression and purification of construct carrying coding sequences of phosphopeptides from NRT2.1, after resuspending cells by placing the 50 mL tube on a rocker platform for 15 min at room temperature and then centrifugation at 16000 × g at 4 °C for 20 min, the pellet was resuspended with 2.5 mL 1 × BugBuster containing 50 µL lysozyme (10 mg/mL), 15 mL 1:10 dilution of BugBuster was added and mixed by vortexing for 1 minute. Discarded supernatant after 15000 × g centrifugation for 15 min at 4 °C. Then the pellet was resuspended and washed with 15 mL 1:10 dilution of BugBuster and mixed by vortexing for 1 minute, centrifuged at 15000 × g for 15 min at 4 °C, discarded the supernatant. Repeat this wash step for one time. The pellet can be used for IMAC and dialysis following steps as described above (Figure 1B).

2.2.5 in Vitro Kinase Assay

In vitro kinase assay was performed as described in ADP-GloTM Kinase assay kit (Promega, Germany) with minor modifications. 1nM recombinant kinase cytoplasmic domain was incubated with 5ug substrate (desalted trypsin digested recombinant protein containing peptides found phosphorylated from NRT2.1) in kinase reaction buffer (40 mM Tris-HCl, pH 7.5, 1 mM $MgCl_2$, 0.01%BSA, 50 uM NaF, 1 uM Na_3VO_3, 1 mM $CaCl_2$, 100 uM ATP, 1 mM DTT). After incubation at room temperature for 1 hour, reaction was terminated by heating at 90 °C for 10 minutes. Then phosphopeptide enrichment and desalting as described in 2.2.5 and 2.2.3 was performed to collect phosphopeptides for MS analysis (Figure 1B).

2.2.6 in Vitro Kinase Activity Assay

A luciferase-based in vitro kinase activity assay was performed according to the manufacturer's instructions of ADP-Glo™ kinase assay kit (Promega, Germany). 1nM recombinant kinase cytoplasmic domain was incubated with generic kinase substrate myelin basic protein (MBP) in kinase reaction buffer. After incubation for one hour, 30 µL ADP-GLO reagents (Promega, Germany) was added and incubated for 40 minutes. Then kinase detection reagents were added and incubated for another hour. Luminescence as a measure of ATP conversion from ADP was recorded with a luminometer (Tecan M200 Pro).

2.2.7 Protein-Protein Interaction Analysis

Transient expression of ratiometric bimolecular fluorescence complementation (rBiFC) construct in *Nicotiana benthamiana* was applied for protein-protein interaction analysis. The investigation was performed as described previously (Grefen and Blatt, 2012), gateway-compatible cloning vector pBiFCt-2in1-CC was kindly provided by Dr. Christopher Grefen (ZMBP, Tübingen, Germany). All the primers used in this experiment were shown in Supplementary Table S6. Inoculated 15 mL LB medium with 50 μg/mL rifampicin and 50 μg/mL spectinomycin with a single colony of *Agrobacterium tumefaciens* (strain GV3101) carrying certain expression construct, incubated overnight at 28 °C with continuous shaking at 150 rpm, *Agrobacterium* (strain C58C1) carrying the pBinG1 vector with the P19 gene was also incubated overnight at 28 °C with continuous shaking at 150 rpm in 15 mL LB medium with 50 μg/mL kanamycin (Kapila et al., 1997). Cells were collected through centrifugation at 2,000 × g for 15 min and then resuspended with resuspension buffer (10 mM Tris-MES pH 7.5, 10 mM $MgCl_2$ and 150 μM acetosyringone). The infiltration solution was prepared by mixing *Agrobacteria* carrying the pBiFCt-2in1-CC vector and *Agrobacteria* carrying the pBinG1 vector at a final OD600 0.5 and 0.25 respectively, incubated the solution for 1 h at room temperature. Leaves of three weeks old *Nicotiana benthamiana* were then infiltrated.

Two days after infiltration, fluorescence from infiltrated *Nicotiana benthamiana* leaves were observed and recorded by a Zeiss LSM700 confocal microscope (20X/0.75-NA objectives). The YFP and RFP fluorochromes were excited with 488 nm and 561 nm, respectively. Emitted light was collected at a range of 500-550 nm for YFP and 575-625 nm for RFP. All images throughout all experiments were collected using exactly the same settings. From each image, three to four regions were chosen and the YFP/RFP ratio was calculated by a software Zen 2.3 (blue edition). To calibrate YFP/RFP ratios, the known interaction of NRT2.1 with NAR2.1 was used as reference (Laugier et al., 2012).

2.2.8 Nitrate Influx Assay

Root NO_3^- influx assay was performed by Aurore Jaquot (BPMP, INRA, CNRS, Université Montpellier, France), all the steps were as described previously (Laugier et al., 2012). Briefly, the plants were sequentially transferred to 0.1 mM $CaSO_4$ for 1 min, to a complete nutrient solution, pH 5.8, containing 0.2mM $^{15}NO_3$ (99 atom % excess ^{15}N) for 5 min, and finally to 0.1mM $CaSO_4$ for 1 min. Roots were then separated from shoots, and the organs dried at 70 ℃ for 48 h. After determination of their dry weight, the samples were analyzed for total nitrogen and atom % ^{15}N using a continuous flow isotope ratio mass spectrometer coupled with a C/N elemental analyzer (model ANCA-MS; PDZ Europa, Crewe, UK). Each influx value is the mean of 6 to 12 replicates.

2.2.9 Data Analysis and Visualization

Peptides mixtures were analyzed by nanoflow Easy-nLC (Thermo Scientific) and Orbitrap hybrid mass spectrometer (Q-exactive, Thermo Scientific). Peptides were eluted from a 75 μm x 50 cm analytical C18 column (PepMan, Thermo Scientific) on a linear gradient running from 4% to 64% acetonitrile over 135 min. Proteins were identified based on the information-dependent acquisition of fragmentation spectra of multiple charged peptides. Up to twelve data-dependent MS/MS spectra were acquired in the

linear ion trap for each full-scan spectrum acquired at 70,000 full-width half-maximum (FWHM) resolution.

MaxQuant version 1.5.3.8 (Cox and Mann, 2008) was used for raw file peak extraction and protein identification against the Arabidopsis database TAIR10 (35,386 entries). Protein quantification was performed in MaxQuant using the label free quantification (LFQ) algorithm (Cox et al., 2014). The following parameters were applied: trypsin as cleaving enzyme; minimum peptide length of seven amino acids; maximal two missed cleavages; carbamidomethylation of cysteine as a fixed modification; N-terminal protein acetylation, oxidation of methionine as variable modifications. For phosphopeptide identification also the phosphorylation of serine, threonine, and tyrosine was included as variable modifications. Peptide mass tolerance was set to 20 ppm and 0.5 Da was used as MS/MS tolerance. Further settings were: "label-free quantification" marked, multiplicity set to 1; "match between runs" marked with time window 2 min; peptide and protein FDR set to 0.01; common contaminants (trypsin, keratin, etc.) excluded. Phosphorylation sites were determined by the site-scanning algorithm search engine Andromeda (Cox et al., 2011).

The phosphpoproteomic data (evidence.txt) derived from MaxQuant was normalized and quantified by the R based script cRacker (Zauber and Schulze, 2012) (version 1.496). Within each sample, all peptide intensities were normalized to fraction of total ion-intensity sums. Subsequently, peptide intensities were scaled across samples or treatments. For each peptide, values from three or four biological replicates were averaged after normalization and mean scaling. Protein group averages were calculated from proteotypic peptides.

Other statistical analyses were carried out with Sigma Plot (version 11.0) and Excel (Microsoft, 2013). Over-representation analysis was done via Fisher's exact test, p values were adjusted using Bonferroni correction.

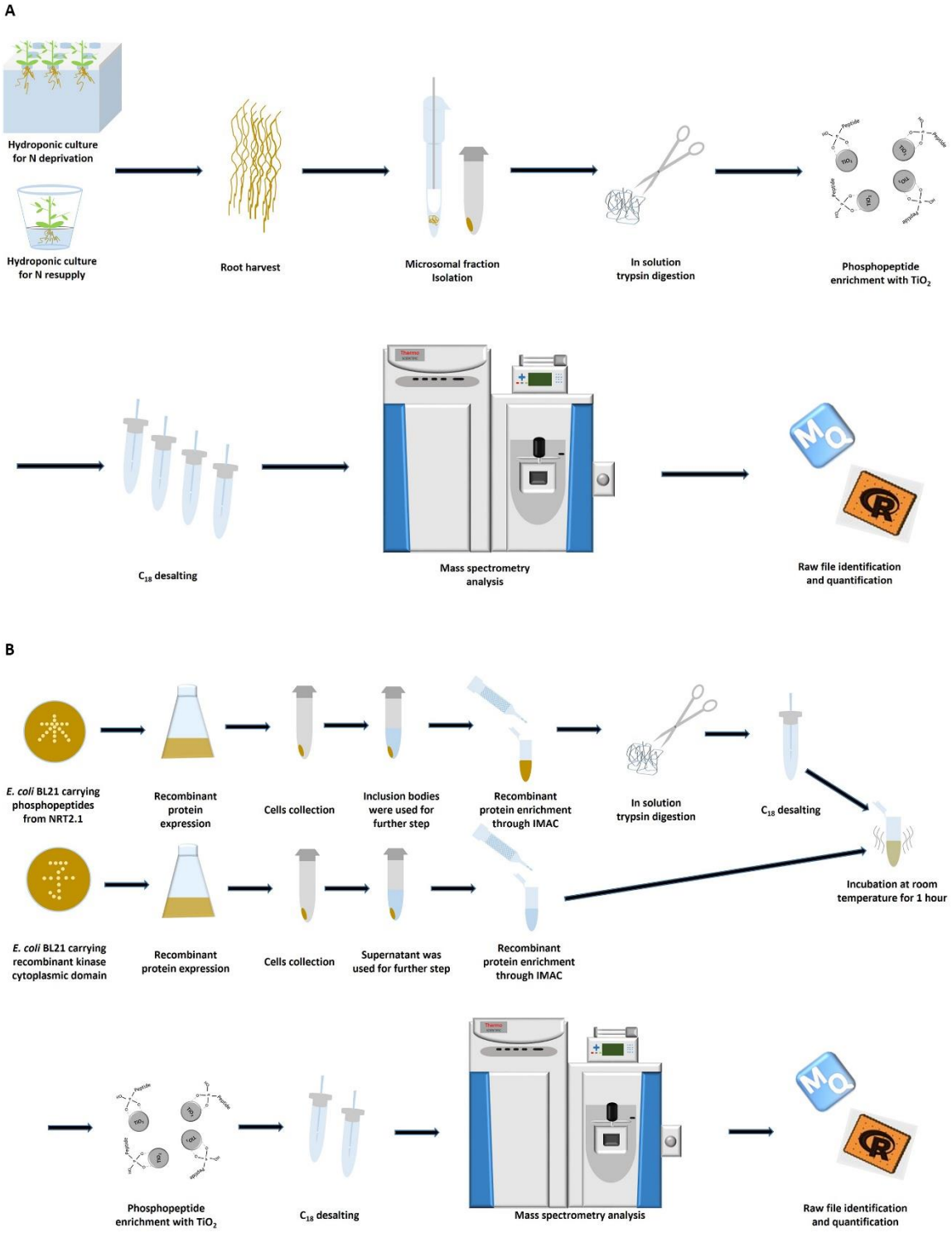

Figure 1: Experiment workflow. (A) Workflow for sample prepar ation and data analysis; (B) Workflow for in vitro kinase assay.

3 Results

3.1 Section 1: The Role of Root Hairs in Nutrient Uptake and Sensing

3.1.1 The Root Hair Nutrient-Dependent Data Set

In the aeroponic system used in this study, the maize seedlings established a dense array of root hairs on primary and seminal roots, which were covered with droplets of nutrient solution (Figure 2A). Although these droplets prevented high-resolution analysis of the root hair length and density under the different nutrient deprivation conditions, there was no obvious visible phenotype under the different conditions. In all nutrient deprivation conditions, a similar maximal growth of seedlings was observed within the 4 days of growth until harvest. However, after 11 days of growth on agar plates, the root hairs under phosphorus deprivation were longer and denser than those in the control (Supporting Information Figure S2), similar to observations in other species.

The proteome of these young maize root hairs across all replicates and conditions consisted of a total of 4,574 identified proteins. This exceeded the previously published root hair proteome by about 2,000 proteins (Nestler et al., 2011). The majority of previously identified proteins (2,161 proteins; 85%) overlapped with our new data set. However, a total of 366 proteins (15%) were identified only in the previous study (Figure 2B). On average, 2,923 proteins were quantified in comparisons of nutrient deprived conditions and full nutrition control conditions. Most of the proteins identified were cytosolic, followed by nuclear proteins, mitochondrial proteins, plastidial proteins, and plasma membrane proteins (Figure 2C). The distribution of functional categories based on Mapman (Figure 2D) revealed that the largest fraction of proteins with assigned functions was “protein-related” (bin 29), containing proteins involved in proteins synthesis and targeting as well as regulatory proteins and the protein degradation pathway. Within bin 29, most proteins were indeed ribosomal proteins, followed by proteins involved in post-translational modifications, proteins involved in vesicle trafficking, and the proteins of the proteasome and ubiquitination pathway.

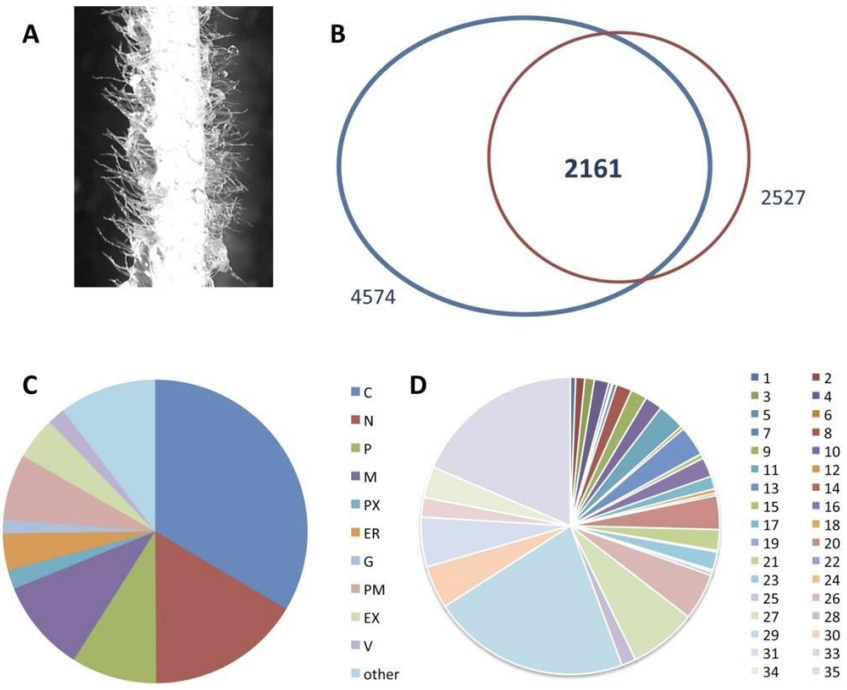

Figure 2: Root hair in the aeroponic system and an overview of the proteomic result. (A) Root hairs under control conditions in the aeroponic system. (B) Venn diagram of proteins identified in this study compared to that in the published work of Nestler et al (Nestler et al., 2011). (C) Distribution of identified proteins to different subcellular compart- ments. (D) Distribution of identified proteins to functional categories according to Mapman. Abbreviations: C, cytosol; N, nucleus; P, plastid; M, mitochondrion; PX, peroxisome; ER, endoplasmic reticulum; G, golgi; PM, plasma membrane; EX, extracellular; V, vacuole

The proteins identified under the deprivation of different nutrients and under full nutrition control conditions showed a large overlap (Figure 3). Less than 150 proteins were identified as being nutrient-deprivation-specific. For both macro- (Figure 3A) and micronutrients (Figure 3B), a minor set of proteins (4 to 144) was exclusively associated with a single nutrient deprivation. This indicates that the root hair proteome remained largely constant regarding its general composition but that the abundance distribution of individual proteins changed in response to deprivation of different nutrients (Table 1).

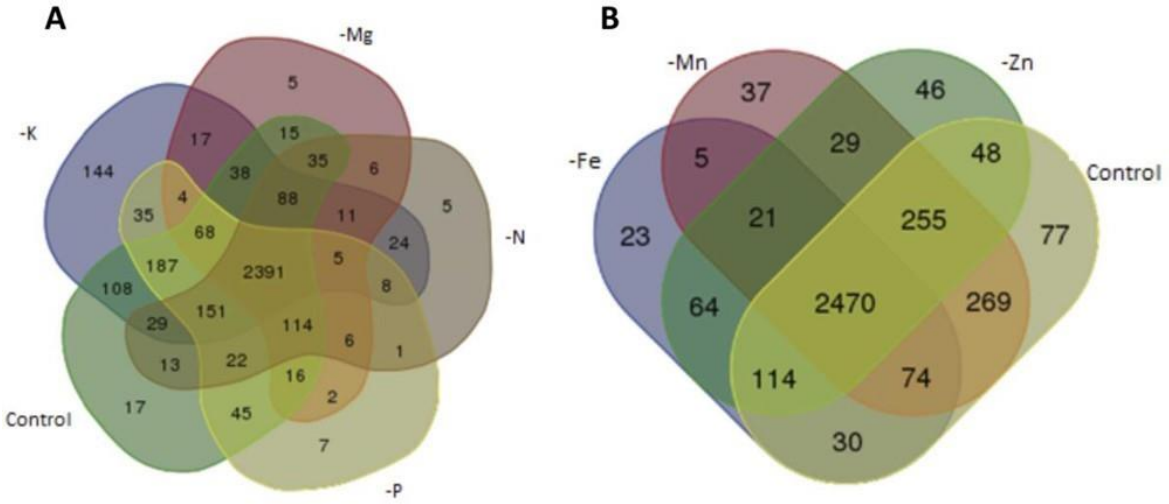

Figure 3: Overlap of identified proteins under different nutrient- deprived conditions and the full nutrition control for macronutrients (A) and micronutrients (B).

Table 1: Overview of the number of proteins down- or upregulated under deprivation of different nutrients (left) and pearson correlation matrix of responses under nutrient deficiencies (right)[a]

	down	up
N	38	58
P	71	52
K	553	72
Mg	94	65
Mn	29	34
Fe	573	74
Zn	440	62

	N	P	K	Mg	Mn	Fe	Zn
N	1	0.41	0.42	0.5	0.33	0.25	0.23
P	0.41	1	0.43	0.24	0.31	0.24	0.32
K	0.42	0.43	1	0.3	0.2	0.49	0.47
Mg	0.5	0.24	0.3	1	0.29	0.15	0.11
Mn	0.33	0.31	0.2	0.29	1	0.07	0.09
Fe	0.25	0.24	0.49	0.15	0.07	1	0.71
Zn	0.23	0.32	0.47	0.11	0.09	0.71	1

[a]Proteins were counted only if the *p*-value of a pairwise *t*-test between nutrient deprivation and control conditions was lower than 0.05 after multiple testing correction according to Benjamini–Hochberg (Benjamini and Hochberg, 1995).

For quantitation of protein abundance, a label-free strategy with peak matching between runs was applied. This strategy allows comparisons to be easily made between several (here, 7) conditions and provides broad proteome coverage (Schulze and Usadel, 2010). However, a drawback of the label-free comparison is its lower quantitative precision. Here, the average relative standard deviation was 0.35 (Supporting Information Figure S3). Nevertheless, comparisons between the nutrient deprivation conditions and full nutrition controls resulted in a normal distribution of protein abundance ratios (Figure 4) and large, significant differences between nutrient conditions. In comparisons for iron (Fe), zinc (Zn), and potassium (K) deprivation, the distribution of abundance ratios was slightly skewed, with more proteins being downregulated than upregulated. The protein abundance ratios for manganese (Mn) deprivation showed a particularly narrow distribution, with very few regulated proteins found at all. For example, in Mn-deprived conditions, only 29 proteins were found to be downregulated, whereas 34

proteins were upregulated. In contrast, under iron, zinc, and potassium deprivations, 573, 440, and 553 proteins were downregulated, whereas only 74, 62, and 72 proteins were upregulated (Table 1). Interestingly, the responses to iron and zinc deprivations were highly similar (r = 0.71, Table 1). Similar and overlapping protein abundance changes were also observed for iron and potassium deprivations (r = 0.49), zinc and potassium deprivations (r = 0.47), and potassium and phosphate deprivations (r = 0.43). Almost no overlap in the protein abundance changes was identified for iron and manganese deprivations (r = 0.07) as well as for zinc and manganese deprivations (r = 0.09, Table 1).

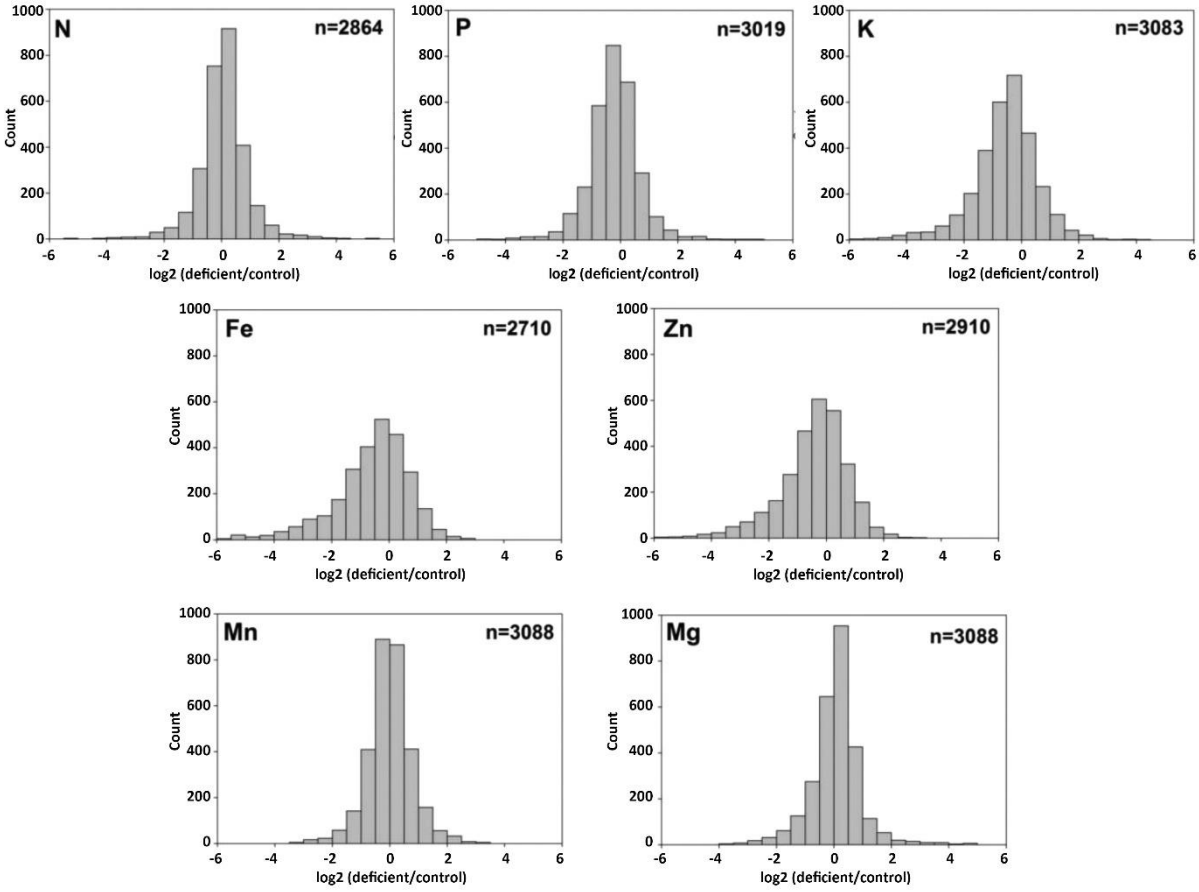

Figure 4: Histograms of log_2 values of protein abundance ratios between nutrient-deprived conditions compared to full nutrition controls.

The aim of this study was to identify processes and pathways regulated upon deprivation of different kinds nutrients during early root hair development. These processes are shown as a network in which each nutrient deprivation condition is represented as a network hub (Figure 5). Affected processes according to Mapman (Thimm et al., 2004) are indicated as nodes. The line style of the edges indicates downregulated (dotted lines) or upregulated (solid lines) processes. The network analysis confirms the strong similarity of responses between iron and zinc deprivations. A large number of processes are coregulated under deprivation of either nutrient. Potassium deprivation resulted in the largest number of over-represented regulated responses (n = 23), whereas for manganese, the number of responses with only 4 over-represented pathways was lowest. This resembles the high number of total regulated proteins under potassium deprivation and the low total number of regulated proteins under manganese deprivation (Table 1).

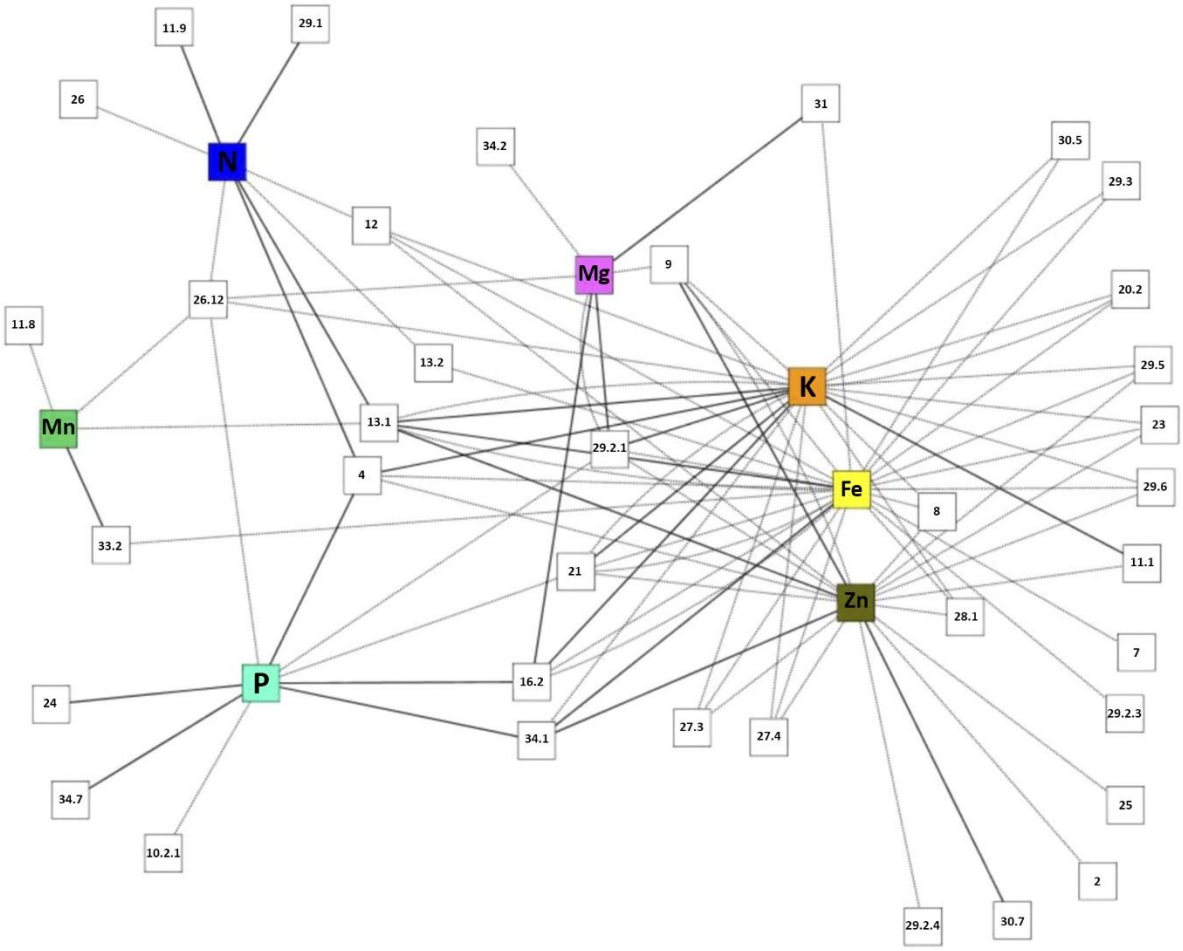

Figure 5: Network of Mapman pathways affected by different nutrient deficiencies. Hubs are represented as different nutrient-deprived conditions, nodes are Mapman processes, and edge style indicates downregulation (dotted) or upregulation (solid). Only processes significantly enriched after over-representation analysis are shown. The Mapman bins are encoded as follows: 2, major CHO metabolism; 4, glycolysis; 7, oxidative pentose phosphate pathway; 8, TCA cycle; 9, mitochondrial electron transport; 10, cell wall; 11, lipid metabolism; 12, nitrogen metabolism; 13.1, amino acid synthesis; 13.2, amino acid degradation; 20, stress; 21, redox; 23, nucleotide metabolism; 24, biodegradation of xenobiotics; 25, C1-metabolism; 26, peroxidases; 27.3, transcription factors; 28.1, DNA synthesis/chromatin structure; 29.1, amino acid activation; 29.2.1, ribosomal proteins; 29.2.3, protein synthesis initiation; 29.2.4, protein synthesis enlongation; 29.3, protein targeting; 29.5, protein degradation; 29.6, protein folding; 30.5, signaling G-proteins; 30.7, signaling 14-3-3; 31, cell cytoskeleton; 33.2, development; 34.1, transport ATPases; 34.7, transport phosphate; 34.2, transport porins.

3.1.2 Processes Affected by Nutrient Deprivations

The common responses among iron, zinc, and potassium deprivations included a downregulation of protein degradation (bin 29.5), regulation of proteins involved in the tricarboxylic acid (TCA) cycle (bin 8), and particular proteins involved in RNA−RNA binding (bin 27.4) as well as redox processes (bin 21). Furthermore, transcription factors (bin 27.3) were particularly downregulated under iron and zinc deprivations (Table 2). Peroxidases (bin 26.12) were downregulated under magnesium deprivation as well as under deprivations of manganese, nitrogen, and phosphorus. Proteins of the mitochondrial electron transport chain (bin 9) were downregulated under magnesium, iron, and potassium deprivations, whereas zinc deprivation resulted in an up- or downregulation of specific members of this process.

Central primary metabolism, such as glycolysis (bin 4), was affected by iron, zinc, potassium, nitrogen, and phosphorus deprivations. Nitrogen, phosphorus, and potassium deprivations led to an upregulation of glycolytic proteins, whereas iron and zinc deprivations resulted in its depression. Nitrogen assimilation (bin 12) was downregulated under nitrogen deprivation as well as under iron, zinc, and potassium deprivations. In contrast, amino acid synthesis (13.1) was upregulated under nitrogen deprivation, whereas amino acid degradation (13.2) was downregulated. Amino acid synthesis was also upregulated under zinc deprivation, and specific amino acid synthesis pathways were up- and downregulated under iron and potassium deprivations.

Secondary metabolism (bin 16.2) was upregulated under phosphorus deprivation as well as under magnesium and potassium deprivations, whereas the phenylpropanoid pathway was downregulated under iron deprivation. Lipid metabolism was affected in multiple ways: Fatty acid synthesis (bin 11.1) was downregulated under zinc deprivation and upregulated under potassium deprivation. Metabolism of sterols (bin 11.8) was downregulated under manganese deprivation. Lipid degradation (bin 11.9) was upregulated under nitrogen deprivation. Cell wall cellulose biosynthesis (bin 10.2.1) was downregulated under phosphorus deprivation.

Ribosomal proteins (bin 29.2.1) were downregulated under iron, zinc, and phosphorus deprivation, up- and downregulated under magnesium deprivation, and upregulated under potassium deprivation. Cellular organization, such as cytoskeleton and vesicle trafficking (bin 31), was downregulated under iron deprivation and upregulated under manganese deprivation. Transport processes were affected, notably, phosphate transporters were upregulated under phosphate deprivation (bin 34.7). Proton-pumping ATPases (bin 34.1) were upregulated under iron, zinc, and potassium deprivations (Table 2).

Table 2: Over-representation analysis of pathways under deprivation of different nutrients[a]

BIN	Binname	N	*p*-value	P	*p*-value	K	*p*-value	Mg	*p*-value	Fe	*p*-value	Mn	*p*-value	Zn	*p*-value
2	major CHO metabolism													down	1.6×10^{-4}
4	Glycolysis	up	1.3×10^{-7}	up	7.5×10^{-8}	up	8.7×10^{-6}							down	1.6×10^{-4}
8	TCA/org. transformation					down	2.2×10^{-9}							down	1.6×10^{-9}
9	mitochondrial electron transp./ATP synth.					down	2.3×10^{-5}	down	3.9×10^{-10}					u/d	4.2×10^{-4}
11.1	lipid metab..FA synth. & FA elongation													down	1.1×10^{-4}
12	N-metabolism	down	4.4×10^{-4}			down	3.5×10^{-5}							down	2.9×10^{-4}
13.1	amino acid metabolism.synthesis	up	2.1×10^{-4}			u/d	3.0×10^{-6}							up	2.1×10^{-4}
13.2	amino acid metabolism.degradation	down	1.6×10^{-4}												
16.2	Secondary metabolism.phenylpropanoids					up	4.8×10^{-4}	up	4.6×10^{-4}	down	1.2×10^{-6}				
20.2	stress.abiotic					down	1.0×10^{-4}								
21	Redox			down	9.1×10^{-4}	down	1.4×10^{-5}			down	4.9×10^{-10}			down	4.5×10^{-6}
21.2	redox.ascorbate and glutathione									down	3.8×10^{-6}				
23	nucleotide metabolism					down	3.4×10^{-4}			down	9.8×10^{-5}			down	6.5×10^{-6}
24	biodegradation of xenobiotics			up	7.7×10^{-4}										
26	Misc	down	4.6×10^{-4}												
26.12	misc.peroxidases	down	1.8×10^{-6}	down	5.0×10^{-4}	down	7.9×10^{-4}	down	4.6×10^{-5}						
27.3	RNA.regulation of transcription									down	3.4×10^{-4}			down	1.3×10^{-4}
27.4	RNA.RNA binding					down	9.3×10^{-7}			down	5.5×10^{-9}			down	2.6×10^{-7}
28.1	DNA.synthesis/chromatin structure					down	3.4×10^{-12}			down	1.1×10^{-12}			down	1.0×10^{-7}
29.1	protein.aa activation	up	4.7×10^{-4}												
29.2.1	protein.synthesis.ribosomal protein			down	7.1×10^{-4}	up	1.3×10^{-4}	u/d	4.3×10^{-22}	down	1.1×10^{-11}			down	3.9×10^{-8}
29.2.3	protein.synthesis.initiation									down	4.8×10^{-4}				
29.2.4	protein.synthesis.elongation													down	5.6×10^{-4}
29.3	protein.targeting					down	1.9×10^{-4}								
29.5	protein.degradation					down	2.8×10^{-4}			down	1.3×10^{-5}			down	6.4×10^{-5}
29.6	protein.folding					down	3.9×10^{-4}			down	4.5×10^{-4}			down	9.2×10^{-5}
30.5	signaling.G-proteins					down	1.0×10^{-4}								
30.7	signaling.14-3-3 proteins													up	3.4×10^{-4}
31	Cell							up	7.1×10^{-4}	down	2.0×10^{-4}				
33.2	developm. late embryogenesis abundant									down	8.0×10^{-4}	up	3.2×10^{-4}		
34.1	transport.P- and v-ATPases			up	1.4×10^{-5}	down	1.6×10^{-6}			up	2.1×10^{-5}			up	4.2×10^{-4}
34.2	transport.porins							down	6.9×10^{-5}						
34.7	transport.phosphate			up											

[a]Pathways and protein categories are given as Mapman

3.1.3 Root Hair Development

Three genes in maize of different molecular functions are essential for root hair formation, and mutations in these genes result in hairless roots (Rth) (Nestler et al., 2014) (Wen et al., 2005) (Hochholdinger et al., 2008). The proteins encoded by the genes *Rth1*, *Rth3*, and *Rth5* were identified in our data set. In particular, RTH5 was significantly upregulated under phosphate, zinc, iron, and manganese deprivations. Interestingly, the increase in root hair length and density upon P deprivation is a general feature found throughout the plant kingdom, and an increase in root hair density upon removal of Zn, Mn, Fe, and P, but not other elements, has been observed in ref 11. Indeed, there was a positive correlation of the expression level of RTH5 with the root hair surface of maize at later stages of older seedlings. The other RTH proteins showed only nonsignificant fluctuations or were not detected under some conditions.

Within these presented pathways and processes, a selection of individual proteins significantly regulated under specific macro- and micronutrient deprivations is worth discussing specifically.

3.1.4 Nitrogen

The downregulation of glutamine synthase, nitrite reductase, and glutamate dehydrogenase, all primary enzymes involved in nitrogen assimilation, was observed. Furthermore, the plasma membrane proton pumps AHA2 and AHA11 were downregulated, as were several peroxidases. The amino acid synthesis for methionine and aromatics and some glycolytic enzymes (fructose-1,6-bisphosphatase, phos- phoglyerate kinase, glceraldehyde-3-phosphate dehydrogenase, pyrophosphate−fructose-6-phosphate 1-phosphotransferase, enolase) were upregulated. Unfortunately, the expected increase of nitrate uptake transporters could not be confirmed due to a lack of these proteins being identified under nitrogen- deprived conditions.

3.1.5 Phosphorus

With phosphate deprivation, the plasma membrane proton pump AHA2 and the high-affinity phosphate transporter PHT1;4 were upregulated, consistent with the typical phosphate mobilization and uptake strategy of plants. Interestingly, phenylammonia lyase and other enzymes of the phenylpropanoid pathway were also upregulated, and the glycolytic pathway (phosphoglucomutase, pyrophosphate− fructose-6-phosphate 1-phosphotransferase, phosphoglycerate/bisphosphoglycerate mutase) was stimulated.

3.1.6 Potassium

Several proteins with unknown functions were repressed under potassium deprivation, whereas cell wall precursor synthesis was stimulated.

3.1.7 Magnesium

The central enzyme in controlling sugar metabolism, hexokinase, and the vacuolar sugar transporter TMT2 were downregulated. By contrast, many ribosomal proteins and cytoskeleton proteins (tubulins) were upregulated.

3.1.8 Iron

Several transcription factors and diverse metabolic processes, such as mitochondrial electron transport (NADH-ubiquinone reductase, cytochrome c, ATP synthase), glycolysis (enolase, glucose-6-phosphate isomerase, glyceralde-hyde-3-phosphate dehydrogenase), and nitrogen metabolism (glutamate dehydrogenase, nitrite reductase) were repressed, potentially indicating that iron is a cofactor in these processes. Redox proteins were also suppressed by iron deprivation. However, citrate (a chelator for Fe transport in the xylem) synthesis and AHA2 were upregulated. Sucrose degradation (sucrose synthase) was repressed, and hexokinase, an enzyme producing glucose-6-phosphate (also for sucrose synthesis), was upregulated.

3.1.9 Zinc

The TCA cycle (several isoenzymes of malate dehydrogenase, pyruvate dehydrogenase), glycolysis, carbohydrate metabolism (glyceraldehyde-3-phosphate dehydrogenase, enolase, sucrose-phosphatase, sucrase, fructase, invertase), and nitrogen metabolism (glutamate synthase, glutamate-ammonia ligase) were downregulated under zinc deprivation, potentially reflecting that zinc acts as a cofactor for several enzymes in primary carbon metabolism. Redox proteins were also down-regulated, as these may not be required with lower internal zinc concentrations. Proton-pumping ATPase (AHA2) and enzymes for the synthesis of aromatic amino acids (shikimate kinase) were upregulated (Table 2).

3.1.10 Manganese

Only a few proteins were detected with significant abundance changes. One of them was sucrose synthase (SUS4), which was upregulated.

Finally, coregulation within specific processes is shown for selected pathways (Figure 6). Hierarchical cluster analysis identified a similar coregulation of the glycolytic pathway (Figure 6A, bin 4) as well as N and amino acid metabolism (Figure 6C, bins 12 and 13) between Zn and Fe deprivations, whereas the macronutrients N, P, and K showed responses that were more similar and clustered together. Repression of TCA cycle metabolism (Figure 6B) and ribosomes (Figure 6D) by Zn and Fe deprivation was also apparent, confirming a significant overlap of their deprivation responses. Transport processes (Figure 6E) were coregulated between Fe and Zn deficiencies as well as between Mg and N deficiencies. Regarding redox proteins, the responses between P and Zn deficiencies clustered together, as did responses of Mg and N deficiencies (Figure 6F).

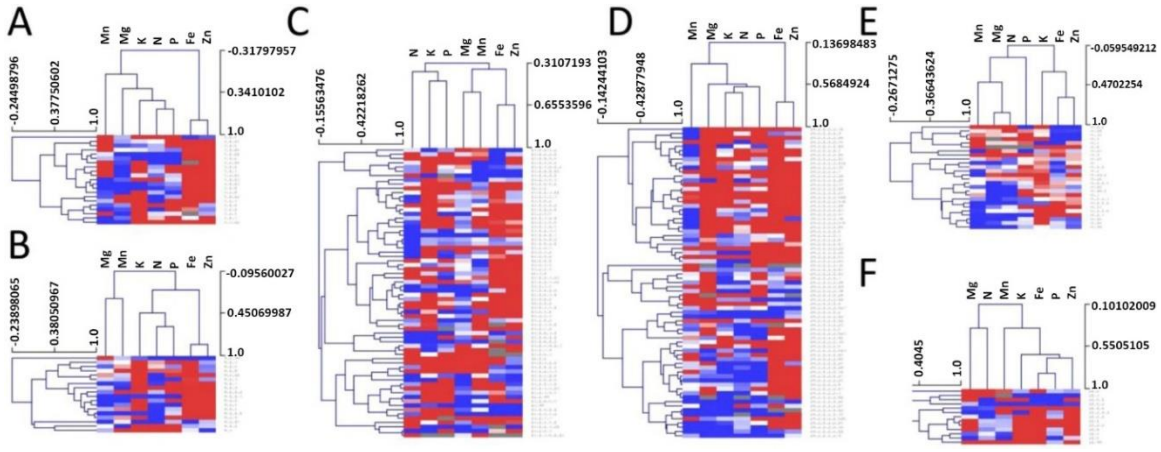

Figure 6: Hierarchical clustering of consolidated proteins within selected Mapman pathways with respect to deprivation of different nutrients using a Pearson correlation distance matrix (red, downregulation; blue, upregulation). (A) Glycolysis (bin 4), (B) TCA-cycle (bin 8), (C) N and amino acid metabolism (bins 12, 13), (D) ribosomes (bin 29.2.1.2), (E) transport (bin 34), and (F) redox (bin 24). Rows represent individual proteins involved in the respective processes

3.2 Section 2: In-depth Arabidopsis Root MF Phosphoproteomic Study of Nitrogen-induced Signaling

3.2.1 Experiment Design

To explore more on the early response of root microsomal fraction phosphoproteome to depletion or resupply of each nitrogen compound from the nutrient solution, phosphoproteomic analysis was used in this research.

For nitrogen deprivation experiment, one hydroponic culture system (Conn et al., 2013) with minor modifications was used. In general, seeds were transferred into a climate room and grown under short-day condition (10 h light with 22 ℃ and 14 h darkness with 18 ℃, light intensity was set to 200 µmol m^{-2} sec^{-1}) after being stratified for 3 days at 4 ℃. Modified ¼ Hoagland nutrient solution (1 mM KH_2PO_4; 0.5 mM $MgSO_4$; 0.1 mM Na_2EDTA-Fe; 1 mM $CaCl_2$; 9 µM $MnSO_4$; 0.765 µM $ZnSO_4$; 0.32 µM $CuSO_4$; 0.016 µM Na_2MoO_4; 46 µM H_3BO_3) was used as hydroponic culture medium (pH was adjusted to 6). Three independent plant growth experiments were carried out for each condition. The total growth period lasted for 35 days, 10 days after germination, the medium was replaced by fresh one, and then was renewed once a week. Plants first grew for 30 days in the medium with 1.5 mM NH_4NO_3 as nitrogen source, and then they were separated into two groups, one group was transferred to the medium with 1.5 mM $(NH_4)_2SO_4$ as nitrogen source, the other group was transferred to the medium with 3 mM KNO_3 as the only nitrogen source, this adaption period lasted for 5 days before nitrogen deprivation. For N-depleted medium, nitrogen was replaced by 1.5 mM K_2SO_4. For induction of N-depletion medium, roots were first quickly rinsed in N-free for twice and then placed into a pot filled with N-depleted medium for 15 min or 3 h. Roots were harvested and frozen in liquid nitrogen at time point 0 in the respective N-solution (NH_4^+ or NO_3^-), and 15 min and 3 h after transfer to N-free medium (Figure 7A) (Menz et al., 2016).

For nitrate resupply experiment, a different hydroponic culture system was used (Schlesier et al., 2003). Sterilized seeds were transferred into a growth chamber and grown under long-day condition (16 h light with 22 ℃ and 8 h darkness with 20 ℃, light intensity was set to 200 µmol m^{-2} sec^{-1}) after being stratified for 3 days at 4 °. Medium to grow the plants in hydroponics contained 0.5 mM KNO_3; 0.25 mM $Ca(NO_3)_2$; 1 mM KH_2PO_4; 1 mM $MgSO_4$; 0.1 mM Na_2EDTA-Fe; 50 µM KCl; 30 µM H_3BO_3; 5 µM $MnSO_4$; 1 µM $ZnSO_4$; 1 µM $CuSO_4$; 0.1 µM Na_2MoO_4; 1% m/v sucrose. For starvation medium, 0.5 mM KNO_3 and 0.25 mM $Ca(NO_3)_2$ were replaced with 0.25 mM K_2SO_4, pH for both grow and starvation medium was adjusted to 5.8. The total growth period lasted for 21 days, growth medium was renewed once a week. On day 19, growth medium was replaced with starvation medium, on day 21, KNO_3 was added to the starvation medium to a final concentration of 0.2mM or 3mM. Roots were harvested and frozen in liquid nitrogen at time point 0, 5 min, and 10 min (Figure 7B).

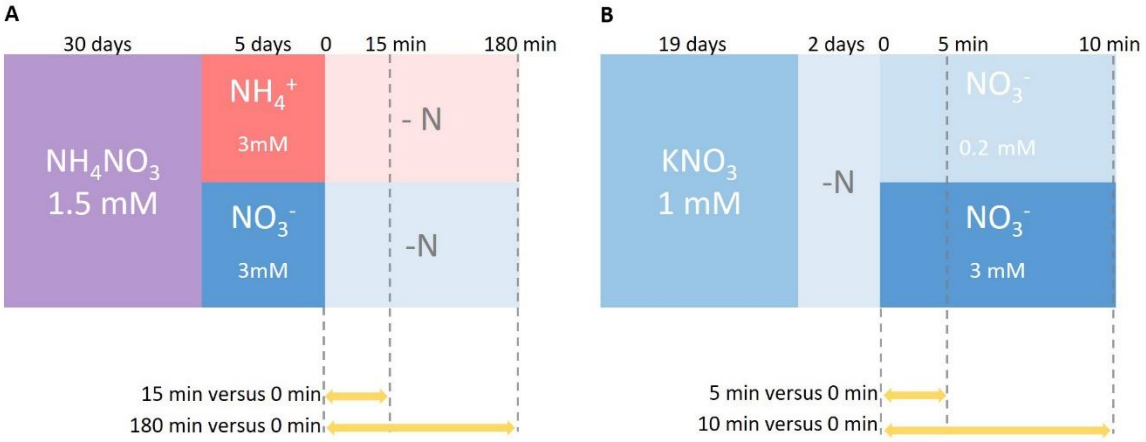

Figure 7: Experiment design. (A) Experiment design for nitrogen deprivation; (B) Experiment design for nitrate resupply

3.2.2 Phosphoproteomic Analysis

In the nitrate deprivation experiment, 774 phosphopeptides from 479 proteins were found in *nrt2.1* knock-out line, 826 phosphopeptides from 501 proteins were found in WT. In the ammonium deprivation experiment, 796 phosphopeptides from 485 proteins were identified in *nrt2.1* knock-out line and 827 phosphopeptides corresponding to 499 proteins were found (Figure 8A). In the low (0.2 mM) amount nitrate resupply group, 2887 phosphopeptides from 1308 proteins were found in *nrt1.1* knock-out line, 2936 phosphopeptides from 1320 proteins were found in *nrt2.1* knock-out line, 2812 phosphopeptides from 1283 proteins were detected in WT (Figure 8B). In the high (3 mM) nitrate resupply group, 2527 phosphopeptides from 1196 proteins were identified in *nrt1.1* knock-out line, 2704 phosphopeptides from 1264 proteins were identified in *nrt2.1* knock-out line, 2618 phosphopeptides corresponding to 1238 proteins were found in WT (Figure 8C).

A total of 833 serines (Ser/S), 170 threonines (Thr/T), 30 tyrosines (Tyr/Y) were identified as phosphorylation sites from nitrogen deprivation experiment (Figure 8D). A total of 4749 serines, 701 threonines, 17 tyrosines were identified as phosphorylation sites from nitrate resupply experiment (Figure 8E).

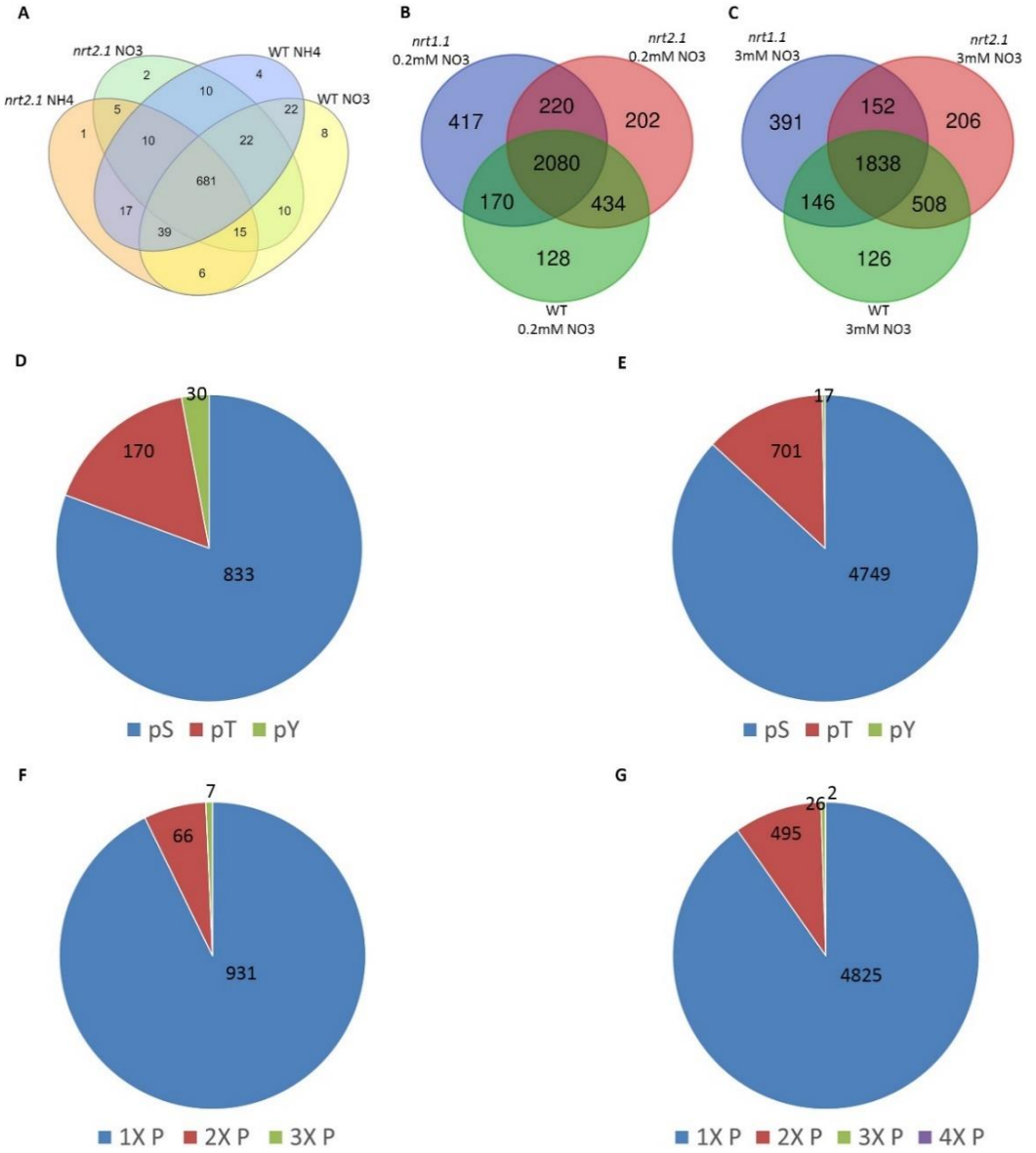

Figure 8: An overview of the phosphoproteomic analysis. (A) Venn diagram showing the number of phosphopeptides detected in *nrt2.1* under ammonium deprivation condition (*nrt2.1* NH4), in *nrt2.1* under nitrate deprivation condition (*nrt2.1* NO3), in Col wild-type under ammonium deprivation condition (WT NH4), in Col wild-type under nitrate deprivation condition (WT NO3); (B) Venn diagram showing the number of phosphopeptides detected in *nrt1.1* under 0.2mM nitrate resupply condition (*nrt1.1* 0.2mM NO3), in *nrt2.1* under 0.2mM nitrate resupply condition (*nrt2.1* 0.2mM NO3), in Col wild-type under 0.2mM nitrate resupply condition (WT 0.2mM NO3); (C) Venn diagram showing the number of phosphopeptides detected in *nrt1.1* under 3mM nitrate resupply condition (*nrt1.1* 3mM NO3), in *nrt2.1* under 3mM nitrate resupply condition (*nrt2.1* 3mM NO3), in Col wild-type under 3mM nitrate resupply condition (WT 3mM NO3); (D) Distribution of phosphorylated residues in each peptide detected in nitrogen deprivation experiment; (E) Distribution of phosphorylated residues in each peptide detected in nitrate resupply experiment; (F) Distribution of the number of phosphosites per peptide detected in nitrogen deprivation experiment; (G) Distribution of the number of phosphosites per peptide detected in nitrate resupply experiment.

3.2.2.1 Over-representation Analysis of Phosphoprotein

To obtain functional insights into the biological processes, mapman pathway over-representation analysis was conducted (Thimm et al., 2004). I decided to use one standard deviation of $\log_2$(fold change) of phosphopeptides as the threshold for both deprivation and resupply data so both data sets could include the same percentage of phosphopeptides for analysis. As a result, in the nitrogen deprivation experiment, those proteins with phosphopeptides $\log_2$ (fold change) higher than 0.4 or lower than -0.4 were considered as significantly over- or under-represented analysis. For the nitrate resupply experiment, these thresholds were set to 0.6 and -0.6.

Most over-represented pathways were found under both nitrogen deprivation and nitrate resupply conditions including regulation of transcription (bin 27), biotic stress (bin 20.1.1), DNA synthesis (bin 28.1), sugar transporter (bin 34.2), ammonium transporter (bin 30.5), calcium signaling (30.3) and receptor kinase (bin 30.2). But there were several over-represented pathways that could only be found under certain treatment, glycolysis (bin 4.1) and cell wall precursor synthesis (10.1.4) could only be found over-represented under nitrogen deprivation while G-proteins (bin 30.5), miscellaneous enzyme groups (bin 26), nitrate metabolism (bin 12.1.1) and protein degradation (bin 29.5) found over-represented under nitrate resupply (Figure 9).

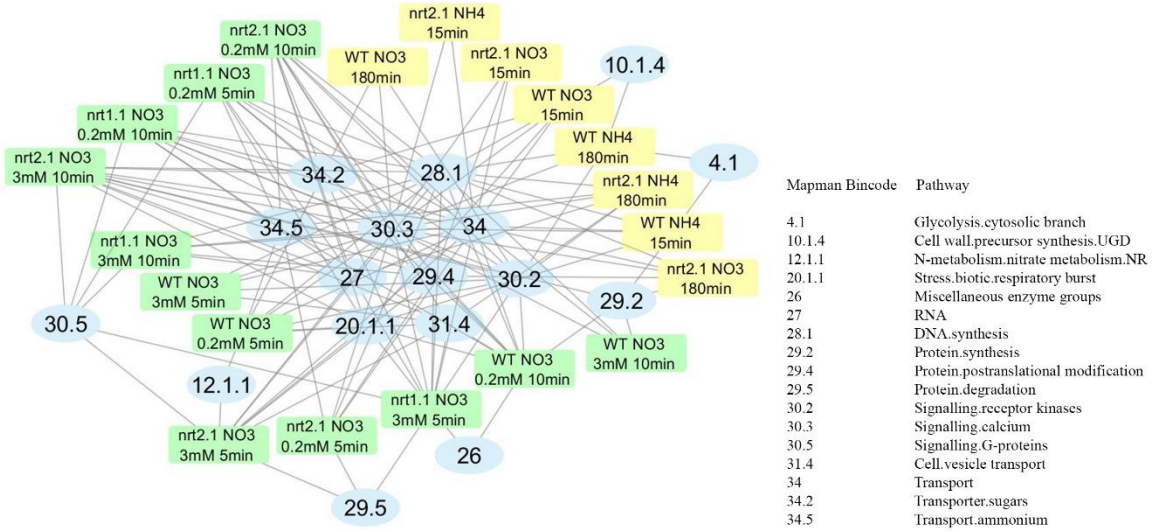

Figure 9: Mapman pathway over representation analysis for phosphoprotein. In the nitrogen deprivation experiment, those proteins with phosphopeptides $\log_2$(fold change) higher than 0.4 or lower than -0.4 were chosen for over-representation analysis, for the nitrate resupply experiment, these thresholds were set to 0.6 and -0.6. The *P*-value is obtained from Fisher's exact test with Benjamini-Hochberg correction, those pathways with P-value less than 0.001 were chosen.Yellow square means nitrogen deprivation experiment, green square means nitrate resupply experiment, blue circle means mapman bicode for different pathways. (WT NO3 15min: Col wild-type under nitrate deprivation condition for 15 minutes; nrt2.1 NH4 15min: nrt2.1 knock-out line under ammonium deprivation condition for 15 minutes)

3.2.2.2 Detection of Phosphosite-Motifs

In order to gain insights into the possible numbers and variety of kinases involved in the responses motifs, online server MoMo (Bailey et al., 2009) was used to identify significant phosphorylation motifs. Those phosphopeptides from proteins used in pathway over-representation analysis were chosen and submitted to the server, Motif-X was chosen as algorithm, width was set to 15, minimum number of occurrences was 5, *P*-value threshold was set to 0.000001.

Nine different kind of motifs ([-R-X-X-pS-], [-pS-P-], [-pS-F-], [-K-X-X-X-X-X-pS], [-R-S-X-pS], [-pS-P-X-X-S-], [-R-X-X-pS-P-], [-L-X-R-X-X-pS-], and [-pS-P-P-]) were detected from both deprivation and resupply experiments (Figure 4). Based on some kinases and their known substrate proteins, these motifs were further consolidated into 4 groups, the most frequently detected motif [-pS-P-] was the minimal target motif of MAPK (Amanchy et al., 2007) (Miller et al., 2008b), there were two more motifs [-pS-P-P-] and [-pS-P-X-X-S-] containing this target motif suggesting they may be recognized by certain MAPK as well, so these three motifs were assorted into group A. [-R-X-X-pS-], [-R-S-X-pS], and [-L-X-R-X-X-pS-] could be assigned to the more general motif [-R-X-X-pS-], which is a known recognition motif for SnRK2 or CDPK (Kobayashi et al., 2005) (Furihata et al., 2006) (Choi et al., 2005) (Zhu et al., 2007), and these belonged to group B. [-pS-F-] and [-K-X-X-X-X-X-pS] were assigned to group C which have not been found to be recognized by any kinase family. Interestingly, in both experiments, [-pS-F-] could only be detected in down-regulated group. There was a special motif [-R-X-X-pS-P-], it carried both motifs which can be assigned to group A and group B, suggesting proteins carrying this motif could be phosphorylated by kinases from MAPK family, SnRK2, and CDPK, this motif belonged to group D (Figure 10).

Except group C, other groups (A, B, and D) could be detected in both up-regulated and down-regulated groups.

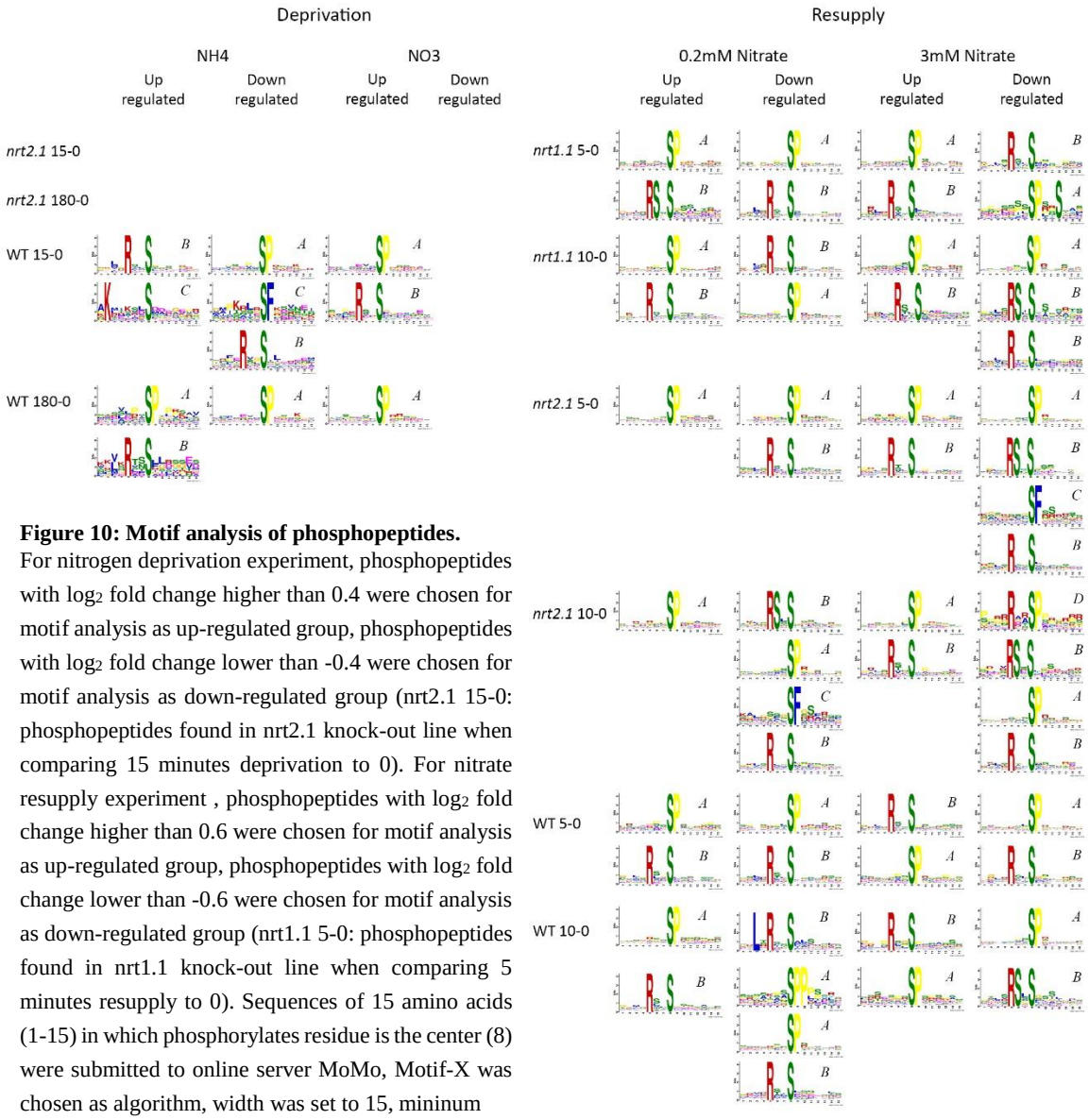

Figure 10: Motif analysis of phosphopeptides.
For nitrogen deprivation experiment, phosphopeptides with log_2 fold change higher than 0.4 were chosen for motif analysis as up-regulated group, phosphopeptides with log_2 fold change lower than -0.4 were chosen for motif analysis as down-regulated group (nrt2.1 15-0: phosphopeptides found in nrt2.1 knock-out line when comparing 15 minutes deprivation to 0). For nitrate resupply experiment , phosphopeptides with log_2 fold change higher than 0.6 were chosen for motif analysis as up-regulated group, phosphopeptides with log_2 fold change lower than -0.6 were chosen for motif analysis as down-regulated group (nrt1.1 5-0: phosphopeptides found in nrt1.1 knock-out line when comparing 5 minutes resupply to 0). Sequences of 15 amino acids (1-15) in which phosphorylates residue is the center (8) were submitted to online server MoMo, Motif-X was chosen as algorithm, width was set to 15, mininum number of occurrences was 5, P-value threshold was set to 0.000001. Motifs with adjusted p-value less than 0.05 were presented. Detected motifs could be classified into four groups labeled with *italic bold letters A, B, C,* and *D.*

3.2.2.3 Predicted Secondary Structure of NRT2.1 and Phosphosites Detected from NRT2.1

Online web tool PROTTER (Omasits et al., 2013) was used to predict the secondary structure of NRT2.1, it contains 12 transmembrane domains (Figure 11A).

Five different phosphosites S11, S21, S28, S501, and T521 from NRT2.1 were identified from nitrogen deprivation experiment (Figure 11B). Phosphorylated T521 could only be detected from nitrate deprivation root samples. As except S28, the phosphorylation trends of S11, S21, and S501 from nitrate deprivation samples were opposite to those from ammonium deprivation samples. (Figure 11B). However phosphorylated S21 could not be detected in low nitrate resupply experiment (Figure 11C). Resupplying low amount nitrate (0.2 mM) WT plants after 5 minute resulted in an increased phosphorylation at S11 and S28, but after 10 minute, phosphorylation at S11 and S28 decreased. In *nrt1.1* knock-out plant, when being resupplied with 0.2 mM nitrate, the abundance of phosphorylated S11 decreased at 5 minute and became even less at 10 minute, but when being resupplied with 3 mM nitrate, the amount of phosphorylated S11 did not change at 5 minute or 10 minute. When being resupplied with 0.2 mM nitrate, phosphorylated S28 in *nrt1.1* mutant increased at 5 minute but decreased at 10 minute. When being resupplied with 3 mM nitrate, phosphorylated S28 in *nrt1.1* mutant became lower at 5 minute and even lower at 10 minute. For WT and *nrt1.1* mutant, the amount of phosphorylated S501 decreased at 5 minute under 0.2 mM nitrate or 3 mM nitrate, at 10 minute the amount of phosphorylated S501 from WT resupplied with 3 mM nitrate became even less, but increased in *nrt1.1* mutant. When 0.2 mM nitrate was resupplied to WT, the amount of phosphorylated S501 increased after 10 minute, and the abundance of phosphorylated S501 was as similar as it at 5 minute in *nrt1.1* mutant. In *nrt1.1* mutant when resupplied with either 0.2 mM or 3 mM nitrate the amount of phosphorylated T521 decreased at 5 minute and stayed at similar low lever after 10 minute. When 0.2 mM nitrate was resupplied to WT, the amount of phosphorylated T521 kept increasing at 5 minute and 10 minute. When 3 mM nitrate was resupplied to WT, the amount of phosphorylated T521 increased at 5 minute and decreased at 10 minute.

The phosphorylation responses of S11, S21, S28, S501, and T521 from NRT2.1 could not only be affected differently by either ammonium or nitrate deprivation but also affected differently by low amount (0.2 mM) nitrate or high amount (3 mM) nitrate resupply. Besides this, NRT1.1 seemed to be also involved in the NRT2.1 phosphorylation response to nitrogen. All these results indicated that the regulation mechanism of NRT2.1 phosphorylation could be very complex.

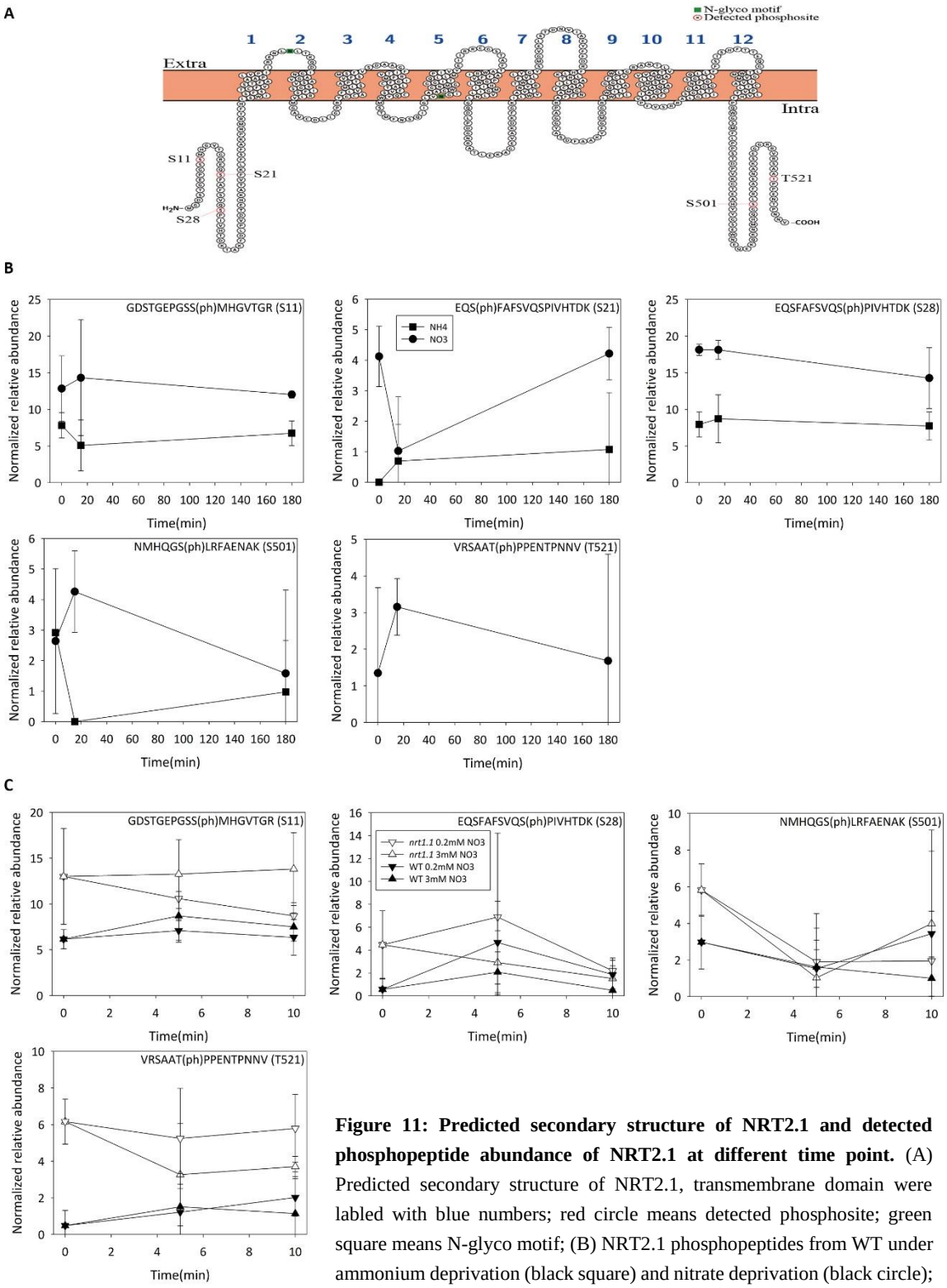

Figure 11: Predicted secondary structure of NRT2.1 and detected phosphopeptide abundance of NRT2.1 at different time point. (A) Predicted secondary structure of NRT2.1, transmembrane domain were labled with blue numbers; red circle means detected phosphosite; green square means N-glyco motif; (B) NRT2.1 phosphopeptides from WT under ammonium deprivation (black square) and nitrate deprivation (black circle); (C) NRT2.1 phosphopeptides from nrt1.1 knockout mutant under 0.2mM nitrate resupply (white down triangle), NRT2.1 phosphopeptides from nrt1.1 knockout mutant under 3mM nitrate resupply (white up triangle), NRT2.1 phosphopeptides from WT under 0.2mM nitrate resupply (black down triangle), NRT2.1 phosphopeptides from WT under 3mM nitrate resupply (black up triangle)

3.2.3 NRT2.1 Activity Regulation by Phosphorylation

3.2.3.1 Phosphorylation on Different Sites of NRT2.1 May Affect Its Nitrate Transport Activity

In order to investigate whether the phosphorylation sites identified for NRT2.1 can affect the nitrate-uptake activity, site-directed mutants of NRT2.1 were created. These phosphosites were mutated to phosphomimicking Aspartate (D) or phosphodead Alanine (A). Then these mutated NRT2.1 versions were transformed and expressed in the *nrt2.1* knock-out line, nitrate influx assay was then applied to test transgenic seedlings carrying different NRT2.1 versions. Unfortunately, for Serine 21 (S21), only S21A version was successfully got and tested.

Interestingly, different phosphosites mutations resulted in different effection on nitrate influx. After 4 hours induction, in the phosphodead S11A mutant a higher nitrate influx was observed compare to phosphomimicking S11D and S11A mutant even had a higher influx than wild type (Figure 12A). Only phosphodead S21A was tested, and a lower nitrate influx was observed compare to wild type. S21A showed a slightly higher nitrate influx compare to *nrt2.1* knock-out mutant, but this difference was not statistically significant (Figure 12B). In the phosphodead S28A mutant, nitrate influx was lower than phosphomimicking S28D mutants (Figure 12C). S501A mutant showed a higher nitrate influx than S501D mutant (Figure 12D). While T521A mutant showed a lower nitrate influx than T521D mutant (Figure 12E).

3.2.3.2 Phosphorylation on Different Sites of NRT2.1 May Affect Its Interaction with NAR2.1

Former research demonstrated that the interaction between NRT2.1 and NAR2.1 (AT5G50200) plays a very important role in regulating nitrate transport activity of NRT2.1 (Okamoto et al., 2006) (Kotur et al., 2012) (Laugier et al., 2012). In order to find out whether the change of nitrate influx caused by phosphorylation at different sites is mediated by affected interaction between NRT2.1 and NAR2.1, rBIFC (Grefen and Blatt, 2012) was applied to investigate the interaction between NAR2.1 and different NRT2.1 mutants. The known interaction of NRT2.1 with NAR2.1 was used as a reference. Phophodead S11A mutant and phosphomimicking S11D mutant did not affect the interaction of NRT2.1 with NAR2.1, both mutants showed higher interaction with NAR2.1 compare to wild type NRT2.1. Similar results were observed from phophodead S501A mutant and phosphomimicking S501D mutant, as well as phophodead T521A mutant and phosphomimicking T521D mutant. Interestingly, NRT2.1 with phophodead S21A mutant showed higher interaction with NAR2.1 compare to wild type NRT2.1 and NRT2.1 with phosphomimicking S21D mutant. However, the interaction between NRT2.1 with phosphodead S28A mutant and NAR2.1 was much weaker than for NRT2.1 with phosphomimicking S28D (Figure 13).

Phosphorylation/dephosphorylation at S21 or S28 of NRT2.1 may be involved in regulation of NRT2.1 through affecting the interaction with NAR2.1, however the interaction and nitrate influx assay results from S11A/D, S501A/D, and T521A/D indicated that the interaction between NRT2.1

and NAR2.1 may be the necessary but not the only condition to regulate its nitrate uptake activity. Combining these results we can see regulation of nitrate uptake activity of NRT2.1 through phosphorylation could be very complicated.

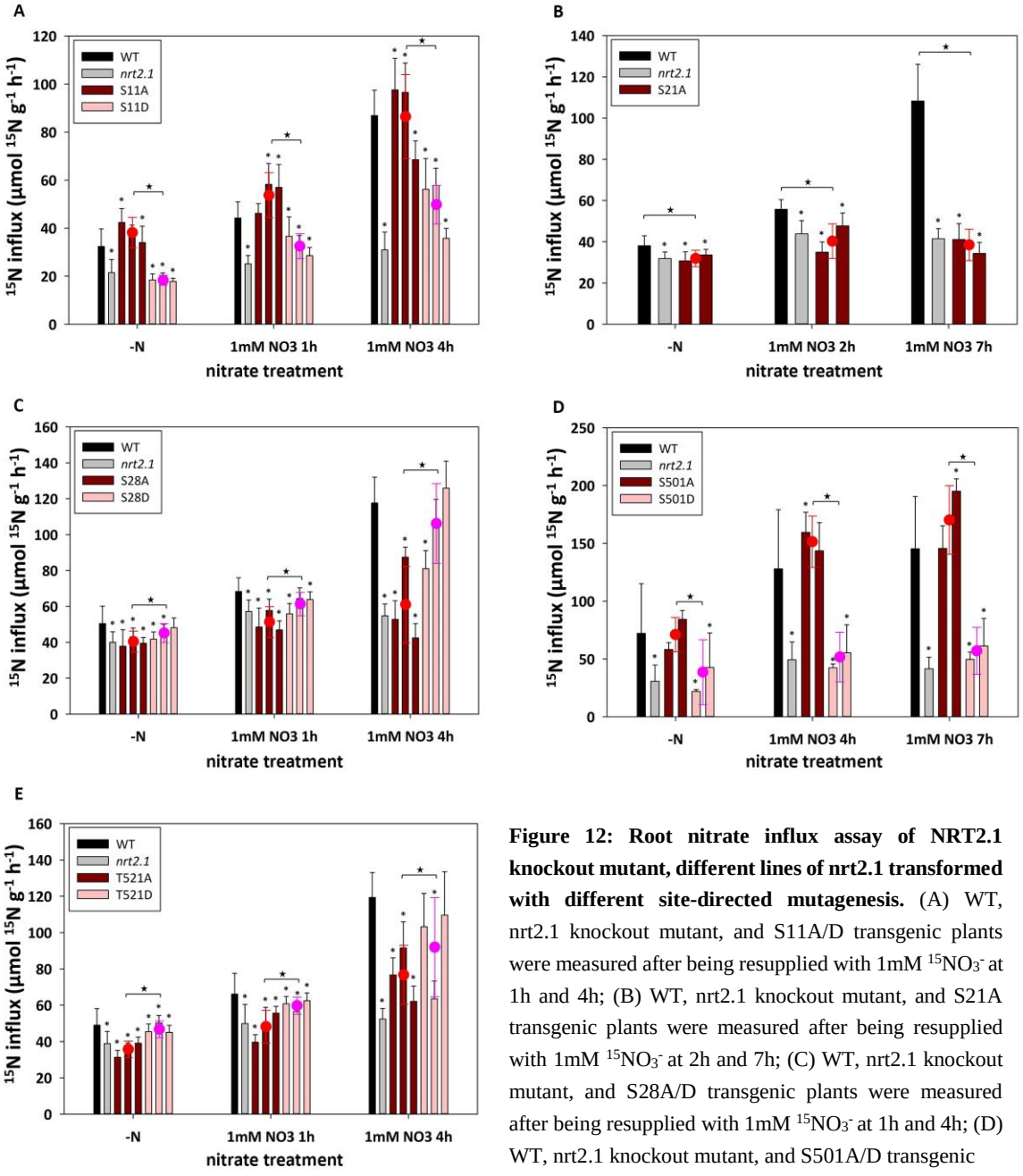

Figure 12: Root nitrate influx assay of NRT2.1 knockout mutant, different lines of nrt2.1 transformed with different site-directed mutagenesis. (A) WT, nrt2.1 knockout mutant, and S11A/D transgenic plants were measured after being resupplied with 1mM $^{15}NO_3^-$ at 1h and 4h; (B) WT, nrt2.1 knockout mutant, and S21A transgenic plants were measured after being resupplied with 1mM $^{15}NO_3^-$ at 2h and 7h; (C) WT, nrt2.1 knockout mutant, and S28A/D transgenic plants were measured after being resupplied with 1mM $^{15}NO_3^-$ at 1h and 4h; (D) WT, nrt2.1 knockout mutant, and S501A/D transgenic plants were measured after being resupplied with 1mM $^{15}NO_3^-$ at 4h and 7h; (E) WT, nrt2.1 knockout mutant, and T521A/D transgenic plants were measured after being resupplied with 1mM $^{15}NO_3^-$ at 1h and 4h. Red circle means the average of phosphodead lines, purple circle means the average of phosphomimic lines. Asterisks indicate significant differences to the wild type with p-value < 0.05, five point star indicate significant differences (p-value < 0.05) between different mutants (S-A/S-D. T-A/T-D) on the same site. Student test and Benjamini-Hochberg Procedure were chosen to calculate the p-value

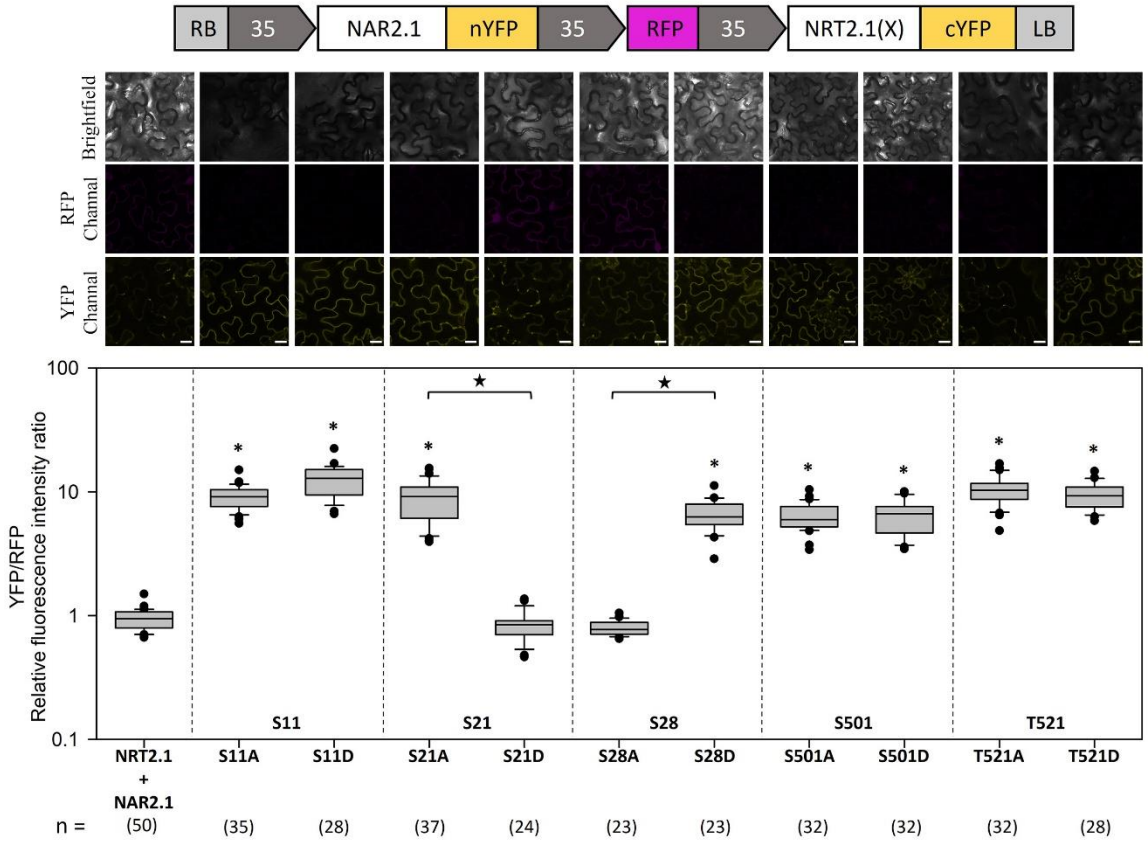

Figure 13: rBiFC results of NAR2.1 and NRT2.1 (different site mutants). The interaction of NRT2.1 and NAR2.1 was used as positive control. Numbers in the parentheses indicate the number of cells quantified. Asterisks indicate significant differences to the positive control with *p*-value < 0.05, five point star indicate significant differences between different mutants (S-A/S-D. T-A/T-D) on the same site (Dunn's pairwise multiple comparison was used to calculate the *p*-value). Representative images are shown above the boxplot graphs (scale bars: 10 µm)

3.2.4 PhosphoNetwork

Interaction and activity of proteins can be regulated through phosphorylation/dephosphorylation. Based on this mechanism I built a PhosphoNetwork assuming activity of the kinases which can phosphorylate NRT2.1 is also regulated by phosphorylation or dephosphorylation.

Figure 14 demonstrates the PhosphoNetwork. In general, the network was constructed in 4 steps as follow:

Step1. Phosphorylation profiles of phosphorylation sites from different proteins were correlated with the phosphorylation profiles of sites in identified kinases or phosphatases using pearson correlation analysis. Since either phosphorylation or dephosphorylation may regulate the activity of kinase or phosphatase, this means the phosphorylation trend of kinase or phosphatase can be

either positive or negative correlated with the phosphorylation of their target proteins. So phosphopeptides with pearson correlation's r value higher than 0.9 and lower than -0.9 were assigned to target phosphopeptides with strong correlation.

Step2. Phosphopeptides with strong correlation were considered as regulatory protein pairs and were chosen to build NetWork Database 1

Step3. Because kinase or phosphatase must directly interact with their target proteins to phosphorylate or dephosphorylate them. To further narrow down my candidates, protein-protein interaction database STRING (protein.links.v10.5) was used, and those interactions with score higher than 400 were chosen to build NetWork Database 2.

Step4. Those proteins which can be found in both NetWork Database 1 and NetWork Database 2 were then used to build the bona-fide PhosphoNetwork.

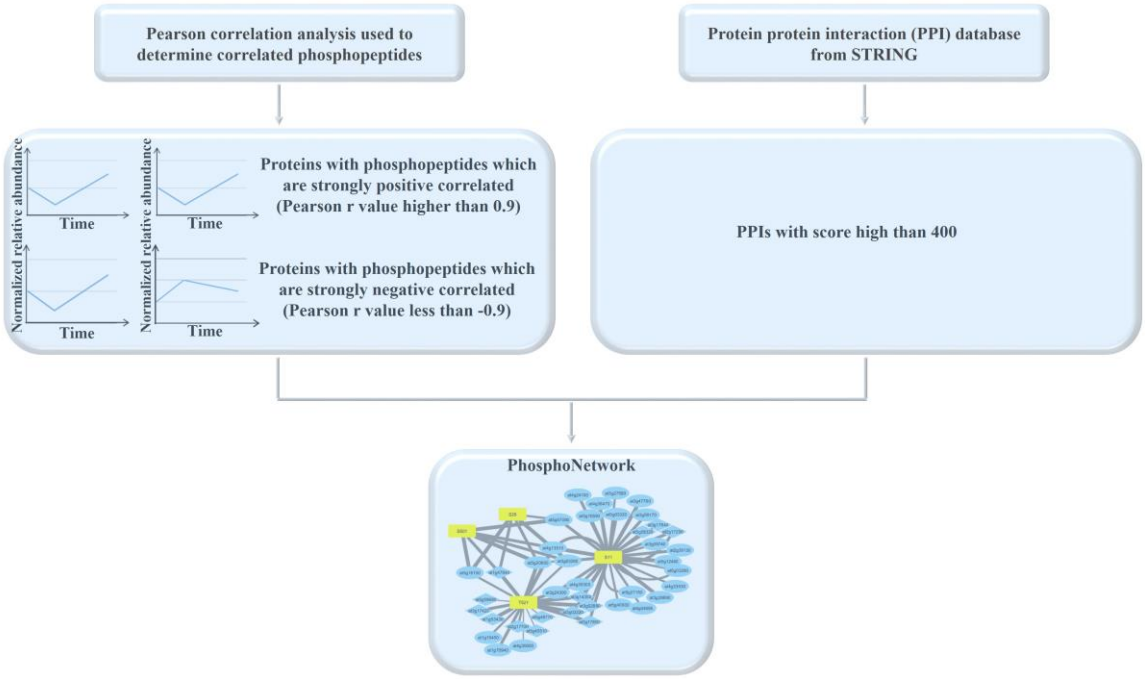

Figure 14: Demonstration of how to build the PhosphoNetwork.

PhosphoNetwork can be further be divided into two major groups, group 1-kinase PhosphoNetwork contains kinases and their highly correlated proteins, in group 2-phosphatase PhosphoNetwork there are only phosphatases and their highly correlated proteins.

3.2.4.1 Kinase PhosphoNetwork Found in Deprivation Experiment

Kinase PhosphoNetwork contains 53 kinases and 122 other proteins as putative substrates, which displayed phosphorylation profiles highly correlated with those kinases phosphorylation.

One very recent research just revealed a leucine-rich repeat transmembrane protein kinase AT3G02880 (QSK1) may act as a coreceptor which can enhance Sucrose Induced Receptor Kinase 1 (SIRK1) activity and help recruiting substrate proteins, such as aquaporins (Wu et al., 2019). In the kinase PhosphoNetwork, phosphosites serine 319 and serine 621 of QSK1 were correlated with two aquaporins PIP2.4 (AT5G60660) and PIP2.8 (AT2G16850) as well. Besides these two aquaporins, one purine transmembrane transporter ATPUP18 (AT1G57990) and a calcium-binding EF hand family protein AT1G05150 were also found correlated with phosphorylation of QSK1 (Figure 15).

Phosphorylation of CBL3 (AT4G26570) was correlated with several kinases which are known to be involved in calcium signaling including CPK1 (AT5G04870), CPK6 (AT2G17290), CPK7 (AT5G12480), CPK8 (AT5G19450), CPK13 (AT3G51850), CPK29 (AT1G76040) (Figure 15).

NRT2.1 had more correlated kinases than other proteins in the network. A total of 28 kinases showed high correlation with NRT2.1. This may further indicate a very complicated regulation mechanism of NRT2.1 phosphorylation, or NRT2.1 may serve like a hub playing a very important role in phosphorylation dependent signal transduction (Figure 15).

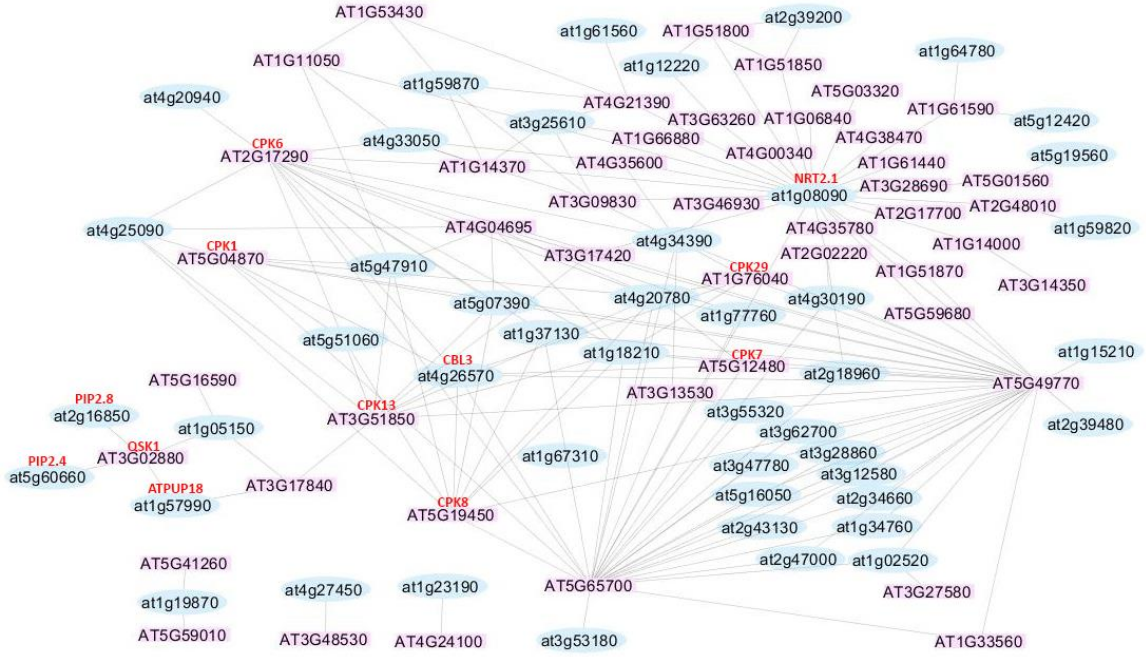

Figure 15: Kinase PhosphoNetwork built from nitrogen deprivation experiment. Purple square node means kinase, blue circle node means kinase related protein.

However these correlations could not always be detected under every condition, for instance, correlation between QSK1 and PIP2.8 could only be found under ammonium deprivation condition, neither ATPUP18 nor AT1G05150 was found correlated with QSK1 under nitrate deprivation condition in WT. CBL3 which belongs to the Ca^{2+} sensor protein family was only found correlated with CPK1 under ammonium deprivation in WT, and with CPK6 under every conditions (Table 3).

Table 3: Part of correlations found in nitrogen deprivation experiment. This table shows correlations (part of all correlations found in nitrogen deprivation experiment) could not always be detected under every conditions. C means found correlated, NC means not found correlated.

Protein A	Protein A Correlated Protein	WT		*nrt2.1*	
		NH_4 deprivation	NO_3 deprivation	NH_4 deprivation	NO_3 deprivation
AT3G02880 QSK1	AT1G05150 calcium-binding EF hand family protein	C	NC	C	C
	AT1G57990 purine transmembrane transporter ATPUP18	C	NC	C	C
	AT2G16850 PIP2.8	C	NC	C	NC
	AT5G60660 PIP2.4	C	C	C	C
AT4G26570 CBL3	AT1G76040 CPK29	C	NC	C	C
	AT2G17290 CPK6	C	C	C	C
	AT3G51850 CPK13	NC	NC	C	NC
	AT5G04870 CPK1	C	NC	NC	NC
	AT5G12480 CPK7	C	C	C	NC
	AT5G19450 CPK8	C	NC	C	NC
	AT5G49770	C	NC	C	C
	AT5G65700	C	C	NC	C

3.2.4.2 Kinase PhosphoNetwork Found in Resupply Experiment

Since a new and optimized phosphopeptide enrichment method (Wu et al., 2017) was used in nitrate resupply experiment, more phosphopeptides could be identified, as a result the size of both kinase and phosphatase PhosphoNetwork increased. In order to focus on certain interesting information from kinase PhosphoNetwork, only proved kinase-substrates and NRT2.1 correlated kinases were shown in Figure 16.

Previous research has demonstrated phosphatases from group A PP2Cs could interact and inactivate ABA-activated kinases (SnRK2s) through dephosphorylation (Umezawa et al., 2009), interestingly, in the resupply kinase PhosphoNetwork (Figure 16), one kinase from SnRK2s, SnRK2.2 (AT3G50500) was found correlated with several phosphatases from PP2Cs including AT1G22280, AT1G34750 (CIPP1), and AT2G33700 indicating the activity of SnRK2.2 may be also regulated by one or more phosphatases from these PP2Cs through dephosphorylation. An ER membrane-localized protein ethylene-insensitive 2 (EIN2 AT5G03280) can positively regulate

ethylene responses, and its activity is regulated through phosohorylation which is mediated by a Raf-like protein constitutive triple response 1 (CTR1 AT5G03730) (Ju et al., 2012), the correlation between these two proteins was confirmed by the kinase PhosphoNetwork Figure 16. In 2014, Haruta et al. demonstrated that H^+–ATPase 2 (AHA2 AT4G30190) mediated proton transport can be inhibited by phosphorylation at Ser899, which is caused by the interaction of a secreted peptide RALF (rapid alkalinization factor) and its receptor kinase FERONIA (AT3G51550) (Haruta et al., 2014), and this correlation can also be found in the PhosphoNetwork (Figure 16).

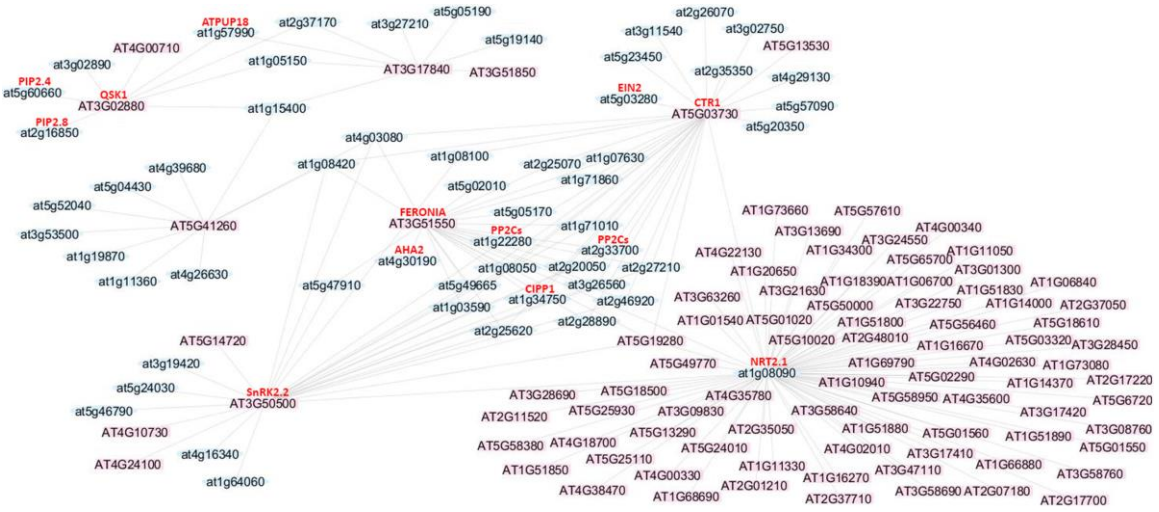

Figure 16: Kinase-substrates proved by other research and NRT2.1 correlated kinases. Purple square node is kinase, blue circle node is kinase highly correlated protein.

All those calcium dependent kinases, BR related kinases, and MAP kinases as well as their correlated proteins were chosen to build a sub kinase PhosphoNetwork. In order to gain a clear view. Proteins in the sub kinase PhosphoNetwork were further consolidated into 6 groups, MAPK module, BR module, calcium signaling module, Hub1, Hub2, and Hub3 (Figure 17).

Some MAPK cascades have been well studied, jasmonic acid (JA) can regulate root growth of *Arabidopsis thaliana* through activating MAPK kinase 3 (MKK3)-MAPK 6 (MPK6) cascade (Takahashi et al., 2007), meristem quiescence or active growth in Arabidopsis can be regulated through the MKK7-MPK6 kinase cascade (Dóczi et al., 2019). In the MAPK module (Figure 15B), MKK4 (AT1G51660) was correlated with MAPKKK3 (AT1G53570), MKKK4 (AT1G63700), and MAPKKK7 (AT3G13530), indicating more novel MKKK-MKK kinase cascades may exist, and MKK4 could be a key regulator of them. MAP kinase substrate 1 (MKS1 AT3G18690) was also correlated with MKK4, suggesting MKS1 may be phosphorylated by one or more substrates MAPK of MKK4. There are also some MAPKs (AT1G18160 AT1G67890) which have not been

studied found correlated with MAPKKK3, these two MAPKs may be involved in MAPKKK3 mediated MAPK cascade.

In the calcium signaling module, there are two Ca^{2+}-dependent protein kinases, CPK6 (AT2G17290) and CPK1 (AT5G04870) (Figure 17). CPK6 can interact with CBL5 to form a complexes which can further phosphorylate and activate the guard cell anion channel SLAC1 (AT1G12480) (Saito et al., 2018), CPK1 mediated phosphorylation of the calmodulin-regulated Ca^{2+}-pump ACA2 can inhibit its Ca^{2+}-transport activity (Hwang et al., 2000). SLAH3 (AT5G24030), one homologue of SLAC1, is correlated with CPK6, besides SLAH3, ACA1 (AT1G27770), ACA11 (AT3G57330), and ACA10 (AT4G29900) are also correlated with CPK6, suggesting these ACAs and SLAH3 may be substrates of CPK6. Unlike CPK6, CPK1 only found correlated with ACA1 (Figure 17).

In the BR module, BAK1-interacting receptor-like kinase 2 (BIR2 AT3G28450) were correlated with three BRI1 suppressor (BSU1)-like proteins, BSL1 (AT4G03080), BSL2 (AT1G08420), and BSL3 (AT2G27210). BR-signaling kinase 8 (BSK8 AT5G41260) was correlated with BSK3, BSL1 and 2. BSK1 was found correlated with BSL1 (Figure 17).

Interestingly, in the sub kinase PhosphoNetwork, some proteins were found correlated with proteins from different modules. These proteins were then grouped into three Hubs, Hub1 containing one LRR kinase AT5G25930 which only correlated with kinases from calcium signaling module and BR module. Hub2 only correlated with proteins from calcium signaling module and MAPK module, containing a pattern-triggered immunity (PTI) compromised receptor-like cytoplasmic kinase 1 (PCRK1 AT3G09830), a barely any meristem 1 (BAM1 AT5G65700), two LRR kinases AT5G49770 and AT4G36180, and two proteins (AT1G64060, AT5G47910) belong to respiratory burst oxidase homolog f. Hub 3 was correlated with proteins from MAPK module and BR module, there are 20 proteins in this Hub, surprisingly, 11 of them are phosphatases including AT1G34750, AT1G22280, AT2G25070, AT2G25620, AT2G33700 from PP2Cs, AT2G35350, AT2G28890, AT1G07630 from poltergeist like proteins, kinase associated protein phosphatase (KAPP AT5G19280), one protein tyrosine phosphatase (PTP1 AT1G71860), and AT2G46920. Besides these phosphatases, there are BSL1-3, NRT2.1, NRT2.2 as well (Figure 17)

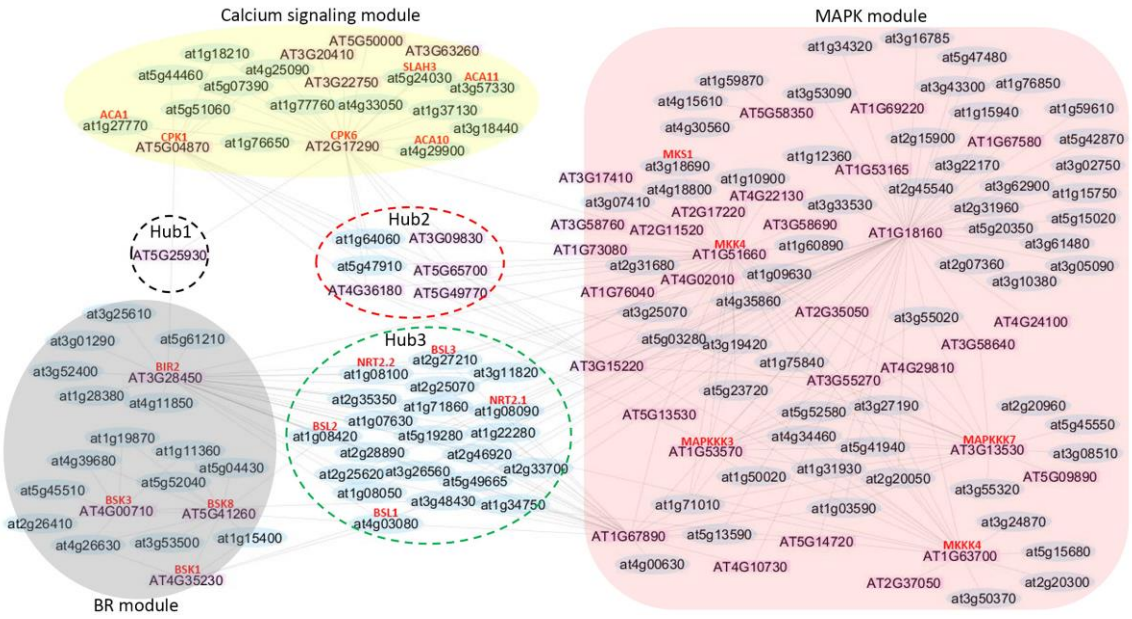

Figure 17: Sub kinase PhosphoNetwork containing BR, MAPK, and calcium signaling related kinases and their correlated proteins. Purple square node is kinase, blue circle node is kinase highly correlated protein. Proteins covered by red area belong to MAPK module, Proteins covered by gray area belong to BR module, proteins covered by yellow area belong to calcium signaling module. Protein in black dot line circle is predicted cross-talk hub1 between BR module and calcium signaling module, proteins in red dot line circle is predicted cross-talk hub2 between calcium signaling module and MAPK module, proteins in green dot line circle is predicted cross-talk hub3 between BR module and MAPK module.

Like PhosphoNetwork from nitrogen deprivation data, not all correlations could be detected from every conditions. Table4 shows some correlations that could be found under certain conditions only.

Table 4: Part of correlations found in nitrate resupply experiment. This table shows correlations (part of all correlations found in nitrate resupply experiment) could not always be detected under every conditions. C means found correlated, NC means not found correlated.

Protein A	Protein A Correlated Protein	WT		*nrt2.1*		*nrt1.1*	
		0.2 mM	3 mM	0.2 mM	3 mM	0.2 mM	3 mM
AT3G50500 SnRK2.2	AT1G22280 phosphatase from PP2Cs	NC	C	NC	C	C	NC
	AT1G34750 phosphatase from PP2Cs	C	NC	NC	NC	NC	NC
	AT2G25620 phosphatase from PP2Cs	C	C	NC	NC	C	NC
	AT2G33700 phosphatase from PP2Cs	C	C	NC	NC	NC	NC
AT5G03730 CTR1	AT5G03280 EIN2	C	C	C	C	C	C
AT3G51550 FERONIA	AT4G30190 AHA2	C	C	C	C	C	C

AT1G51660 MKK4	AT1G53570 MAPKKK3	NC	NC	C	NC	NC	NC
	AT1G63700 MKKK4	NC	NC	C	NC	NC	NC
	AT3G13530 MAPKKK7	C	NC	NC	NC	NC	NC
	AT3G18690 MKS1	C	NC	C	NC	NC	NC
AT2G17290 CPK6	AT5G24030 SLAH3	C	C	C	C	C	C
	AT1G27770 ACA1	C	C	C	C	C	C
	AT3G57330 ACA11	C	NC	C	NC	C	NC
	AT4G29900 ACA10	C	C	C	C	C	C
AT5G04870 CPK1	AT1G27770 ACA1	C	C	C	C	C	C
AT3G28450 BIR2	AT1G08420 BSL2	C	C	C	C	C	C
	AT2G27210 BSL3	NC	C	NC	NC	C	NC
	AT4G03080 BSL1	NC	NC	NC	C	C	C
AT5G41260 BSK8	AT1G08420 BSL2	NC	C	NC	C	NC	C
	AT4G03080 BSL1	NC	C	NC	C	NC	C
	AT4G00710	NC	C	C	C	C	NC
AT4G35230 BSK1	AT4G03080 BSL1	C	C	C	C	C	C

3.2.4.3 Phosphatase PhosphoNetwork

Phosphatase PhosphoNetwork found in nitrogen deprivation experiment contains 3 phosphatases, AT1G34750 and AT1G22280 from PP2C family, and one mitogen-activated protein kinase phosphatase MKP1 (AT3G55270). There were two proteins, phytosulfokin receptor 1 (PSKR1 AT2G02220) and a LRR kinase AT5G49770 showing correlation with all three phosphatases. Both, AT1G22280 and AT1G34750 (CERK-1 INTERACTING PROTEIN PHOSPHATASE 1, CIPP1) have correlation with NRT2.1 (Figure 18A).

In the nitrate resupply Phosphatase PhosphoNetwork, there were phosphatases from PP2Cs, such as AT1G22280, AT1G71860, AT2G46920, AT1G03590, AT1G07630, and AT5G19280 which had more correlated proteins compare to others, indicating these phosphatases may be involved in more phosphorylation mediated regulation (Figure 18B).

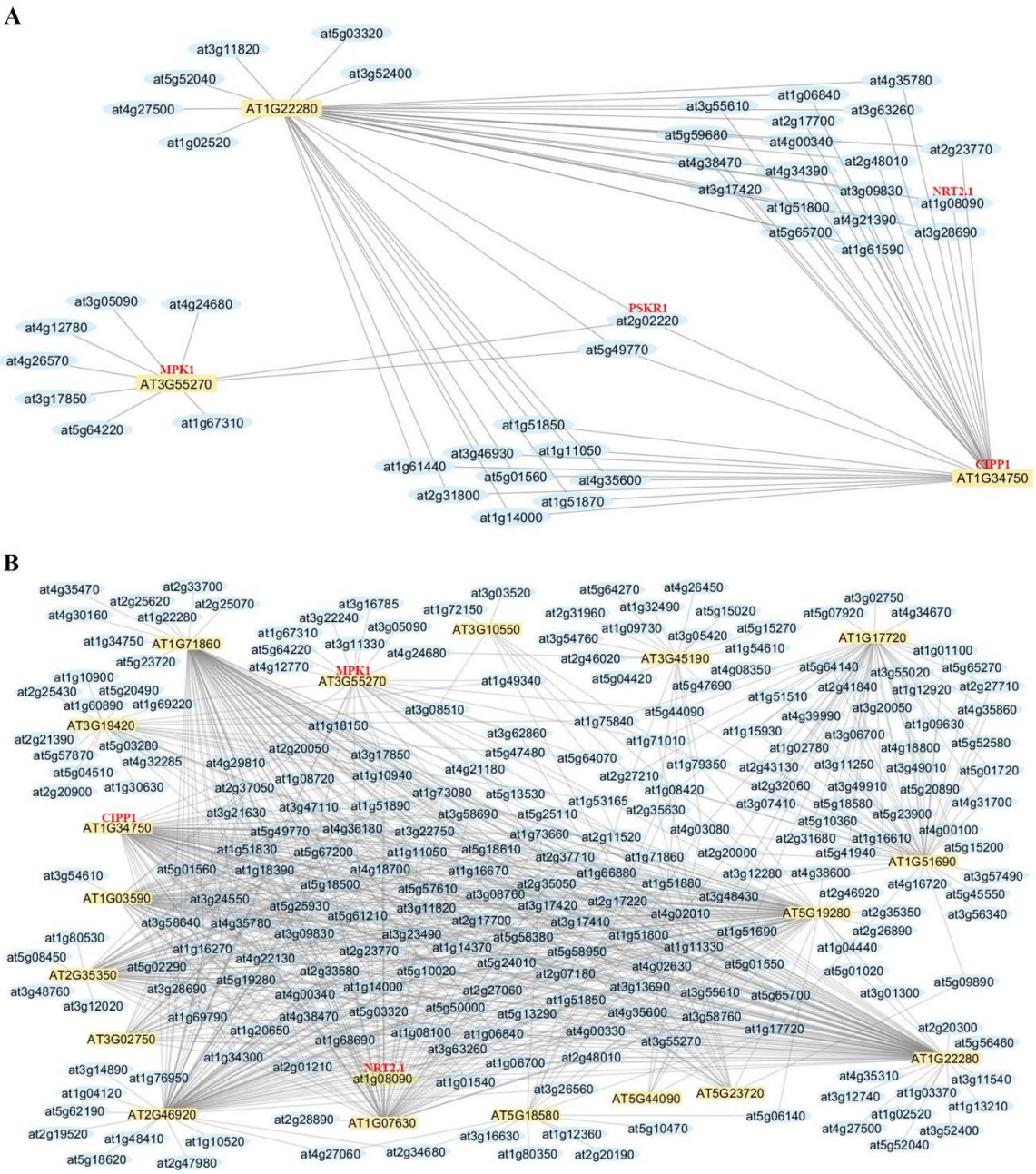

Figure 18: Phosphatase PhosphoNetwork. (A) Phosphatase PhosphoNetwork built from nitrogen deprivation experiment, yellow square node means phosphatase, blue circle node means phosphatase correlated protein; (B) Phosphatase PhosphoNetwork built from nitrate resupply experiment, yellow square node means phosphatase, blue circle node means phosphatase correlated protein.

3.2.5 Identification of Kinases Phosphorylating NRT2.1

In order to identify kinases phosphorylating NRT2.1, PhosphoNetwork from 3.1.3 was used. By combining PhosphoNetwork from deprivation and resupply experiments, 21 kinases were found correlated with NRT2.1, during them a LRR protein kinase AT5G49770 raised my further interest, since it showed similar expression pattern as NRT2.1 (Wu et al., 2016).

Four phosphosites T792, S839, S870, and S919, could be detected from phosphoproteome research. T792, S839, S870 were found located at the kinase activity domain through secondary structure prediction (Omasits et al., 2013) (Figure 19).

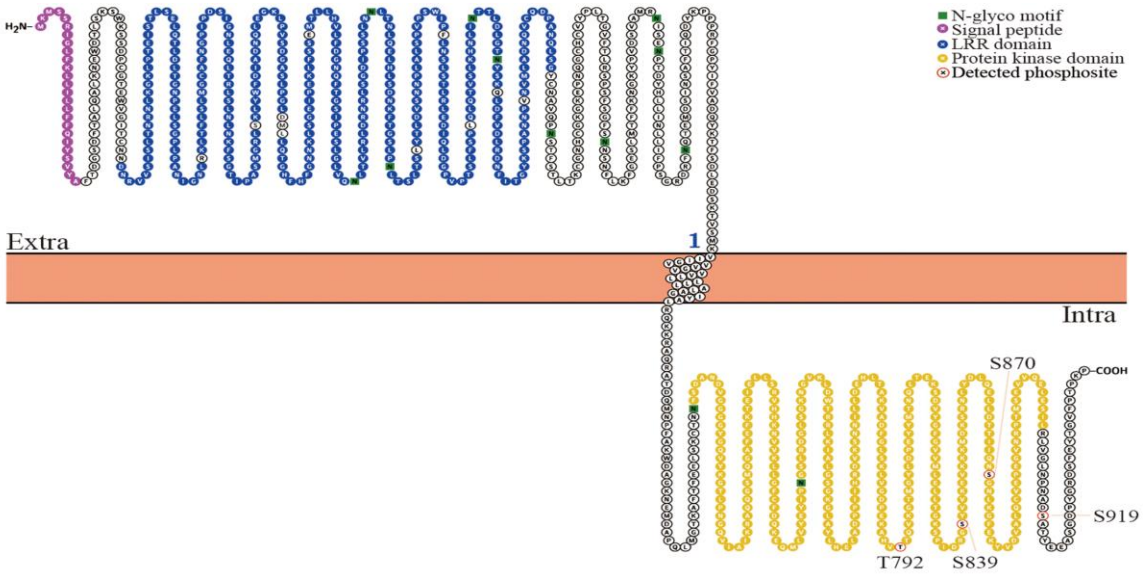

Figure 19: Predicted secondary structure of AT5G49770 and phosphosites detected from AT5G49770. Transmembrane domain were labeled with blue number; red circle means detected phosphosite; green square means N-glyco motif; purple circle means signal peptide; blue circle means LRR domain; yellow circle means protein kinase domain

3.2.5.1 Phosphopeptide Abundance of AT5G49770 at Different Time Point and Root Nitrate Influx Assay of AT5G49770 Knock-out Mutant

As shown in Figure 20A and B, non-statistical difference can be found for those detected phosphopeptides under any conditions. Besides phosphorylated S870 could be identified but not quantified in the nitrogen deprivation experiment, while in the nitrate resupply experiment, phosphorylated T792 and S870 could be identified but not quantified.

To investigate whether AT5G49770 participates in nitrate uptake or not, root nitrate influx assay was again used. AT5G49770 knock-out mutant showed a similar nitrate influx result as in WT (Figure 20C).

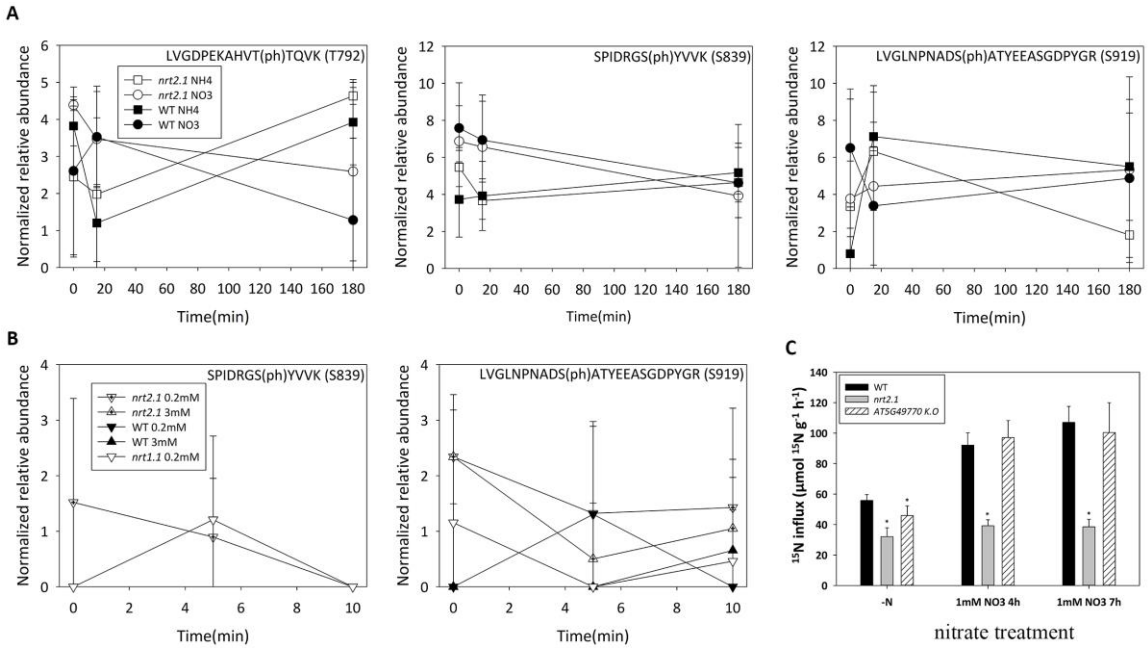

Figure 20: Phosphopeptide abundance of AT5G49770 at different time point and nitrate influx for AT5G49770 knockout mutant. (A) AT5G49770 phosphopeptides from *nrt2.1* knock-out line under ammonium deprivation (white square) and nitrate deprivation (white circle), from WT under ammonium deprivation (black square) and nitrate deprivation (black circle); (C) AT5G49770 phosphopeptides from *nrt2.1* knock-out mutant under 0.2mM nitrate resupply (doted down triangle), under 3mM nitrate resupply (doted up triangle); from WT under 0.2mM nitrate resupply (black down triangle), under 3mM nitrate resupply (black up triangle); from *nrt1.1* knock-out mutant under 0.2mM nitrate resupply (white down triangle); (D) WT, nrt2.1 knockout mutant, and AT5G49770 knockout mutant were measured after being resupplied with 1mM $^{15}NO_3^-$ at 4h and 7h. Red circle means the average of phosphodead lines, purple circle means the average of phosphomimic lines. Asterisks indicate significant differences to the wild type with p-value < 0.05, five point star indicate significant differences (p-value < 0.05) between different mutants (S-A/S-D. T-A/T-D) on the same site. Student test and Benjamini-Hochberg Procedure were chosen to calculate the p-value

3.2.5.2 Kinase AT5G49770 Interacts with NRT2.1 in Vitro and This Interaction May be Regulated through NRT2.1 Phosphorylation

rBIFC was applied to examine the direct interaction between AT5G49770 and NRT2.1. The interaction between AT5G49770 and NRT2.1 was as strong as the interaction between NAR2.1 and NRT2.1, suggesting AT5G49770 could interact with NRT2.1 (Figure 21).

I then wanted to find out if phosphosites of NRT2.1 could al affect the interaction between NRT2.1 and AT5G49770 through phosphorylation/dephosphorylation. Interestingly, both wild type NRT2.1 and phosphodead S28A mutant showed stronger interaction with AT5G49770 compare to phosphomimicking S28D (Figure 21), indicating the interaction between NRT2.1 and AT5G49770 could also be regulated through phosphorylation at S28. Mutations in other phosphorylation sites of NRT2.1 did not show such effect.

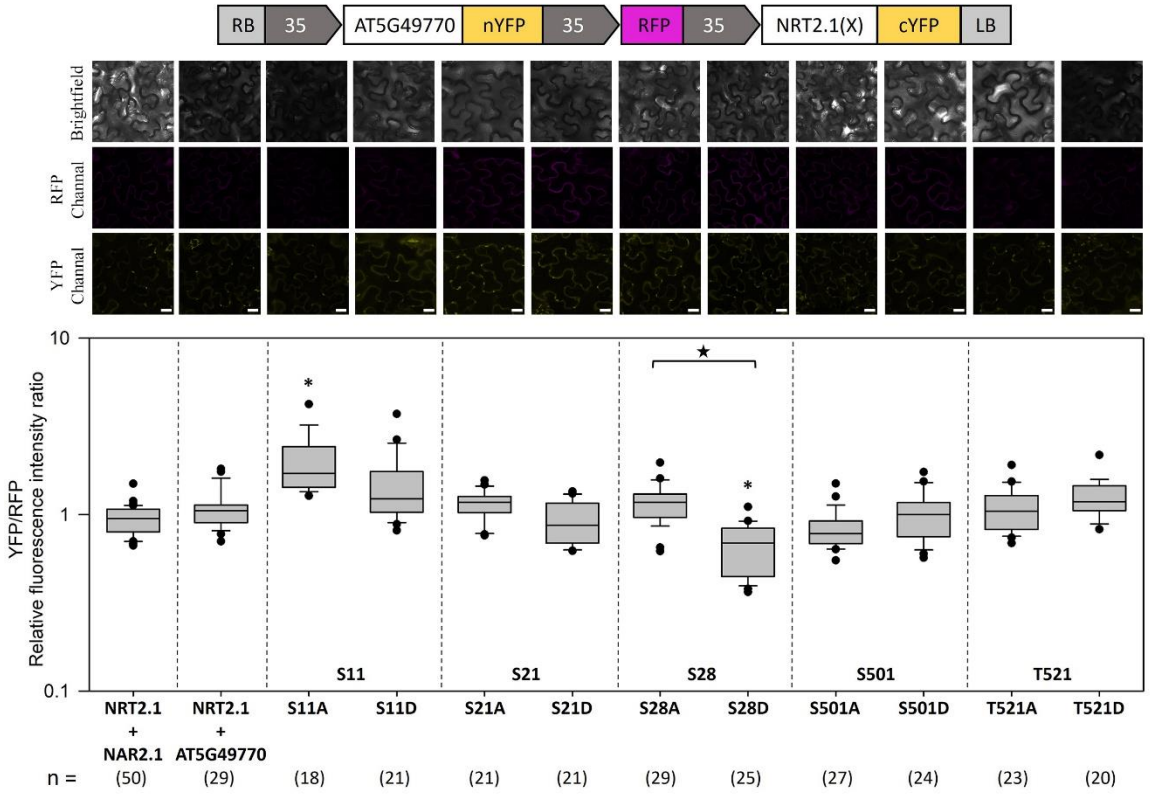

Figure 21: rBiFC results of AT5G49770 and NRT2.1 (different site mutants). The interaction of NRT2.1 and NAR2.1 was used as positive control. Numbers in the parentheses indicate the number of cells quantified. Asterisks indicate significant differences to the positive control with p-value < 0.05, five point star indicate significant differences between different mutants (S-A/S-D. T-A/T-D) on the same site (Dunn's pairwise multiple comparison was used to calculate the p-value). Representative images are shown above the boxplot graphs (scale bars: 10 μm)

3.2.5.3 AT5G49770 Kinase Could Phosphorylate NRT2.1 in Vitro and Its Kinase Activity Could be Regulated by Phosphorylation

The intracellular domain of AT5G49770 was recombinantly expressed and exposed to the substrate NRT2.1 peptides which were found phosphorylated. In those in-vitro kinase assays, phosphorylation at S21 could be detected by MS analysis (Figure 22A). These results suggest NRT2.1 could be a substrate of AT5G49770, and AT5G49770 may phosphorylate NRT2.1 at S21.

From in vitro kinase assay results, more phosphorylated S21 could be detected when incubated with phosphodead S839A recombinant protein compared to phosphomimicking S839D. But less phosphorylated S21 could be detected when incubated with phosphodead S870A mutant compare to phosphomimicking S870D (Figure 22A).

This altered activity may be caused by the change of interaction between NRT2.1 and AT5G49770 or by the change of AT5G49770 kinase activity. rBIFC and in vitro kinase activity assay were both applied to address this question. The kinase activity of phosphodead S870A mutant was significantly lower than phosphomimicking S870D mutant (Figure 22B). Phosphodead S839A mutant showed a stronger interaction with NRT2.1 compare to phosphomimicking S839D mutant, however no differential interaction could be observed from other mutated sites (Figure 23). Phosphodead or phosphomimicking at other phosphosites of AT5G49770 did not affect the interaction with NRT2.1.

These results indicate phosphorylation at S839 may affect the interaction between AT5G49770 and NRT2.1, while phosphorylation at S870 could further regulate the kinase activity of AT5G49770.

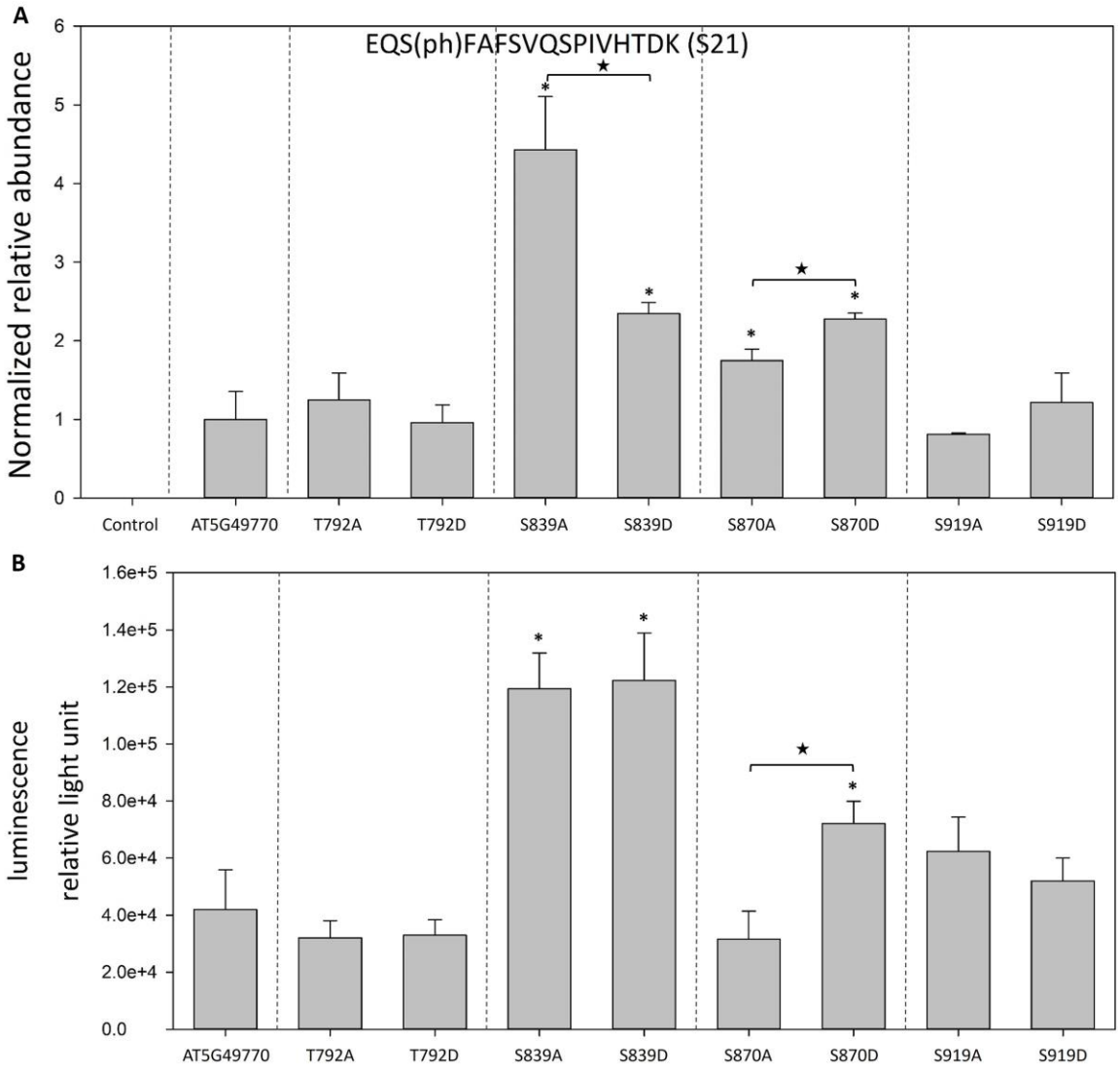

Figure 22: In vitro kinase assay and in vitro kinase activity assay. (A) In vitro kinase assay, the intracellular domain of AT5G49770 including different single site mutants were recombinant expressed and exposed to the substrate NRT2.1 peptides which were found phosphorylated. The sample without any recombinant kinase intracellular domain was used as control. Asterisks indicate significant differences to the sample incubated with the intracellular domain of AT5G49770 with p-value < 0.05, five point star indicate significant differences between different mutants (S-A/S-D. T-A/T-D) on the same site. Student test and Benjamini-Hochberg Procedure were chosen to calculate the p-value. (B) In vitro kinase activity assay, the intracellular domain of AT5G49770 including different single site mutants were recombinant expressed and exposed to the substrate myelin basic protein (MBP), the sample incubated with the intracellular domain of AT5G49770 was used as the control, higher luminescence relative light unit means stronger kinase activity. Student test and Benjamini-Hochberg Procedure were chosen to calculate the p-value.

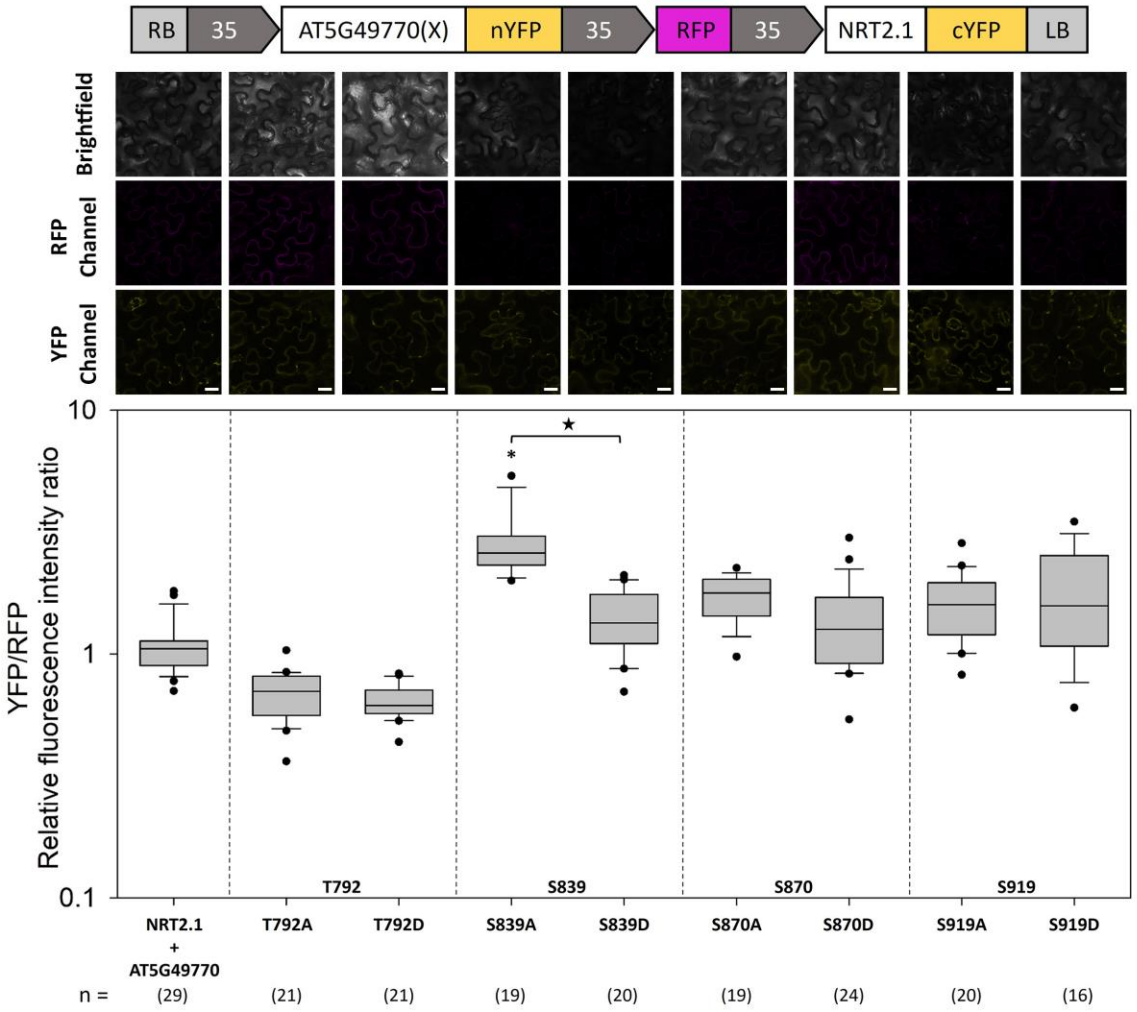

Figure 23: rBiFC results of AT5G49770 (different site mutants) and NRT2.1. The interaction of NRT2.1 and AT5G49770 was used as positive control. Numbers in the parentheses indicate the number of cells quantified. Asterisks indicate significant differences to the positive control with p-value < 0.05, five point star indicate significant differences between different mutants (S-A/S-D. T-A/T-D) on the same site (Dunn's pairwise multiple comparison was used to calculate the p-value). Representative images are shown above the boxplot graphs (scale bars: 10 μm)

3.2.5.4 Homologues of AT5G49770

There are two homologues of AT5G49770 (AT5G49760 and AT5G49780), online tool MUSCLE was used for protein sequences alignment (Madeira et al., 2019). The three homologs share over 70% similarity (Figure 24)

From further research, I was able to find out that AT5G49760 could also phosphorylate NRT2.1 at S21, while AT5G49780 could not phosphorylate NRT2.1 (Figure 25A). Interestingly, more phosphorylated S21 were detected from AT5G49760 compared to AT5G49770 (Figure 25A). Through in vitro kinase activity assay, AT5G49760 showed a higher kinase activity compare to

AT5G49770, and the kinase activity of AT5G49780 was as similar as phosphodead mutant AT5G49770S870A (Figure 25B).

The interaction between AT5G49760 and NRT2.1 is as strong as the interaction between phosphodead mutation AT5G49770S839A and NRT2.1 but stronger than AT5G49770 (Figure 25C). AT5G49780 showed a weaker interaction with NRT2.1 compare to AT5G49770 (Figure 25C).

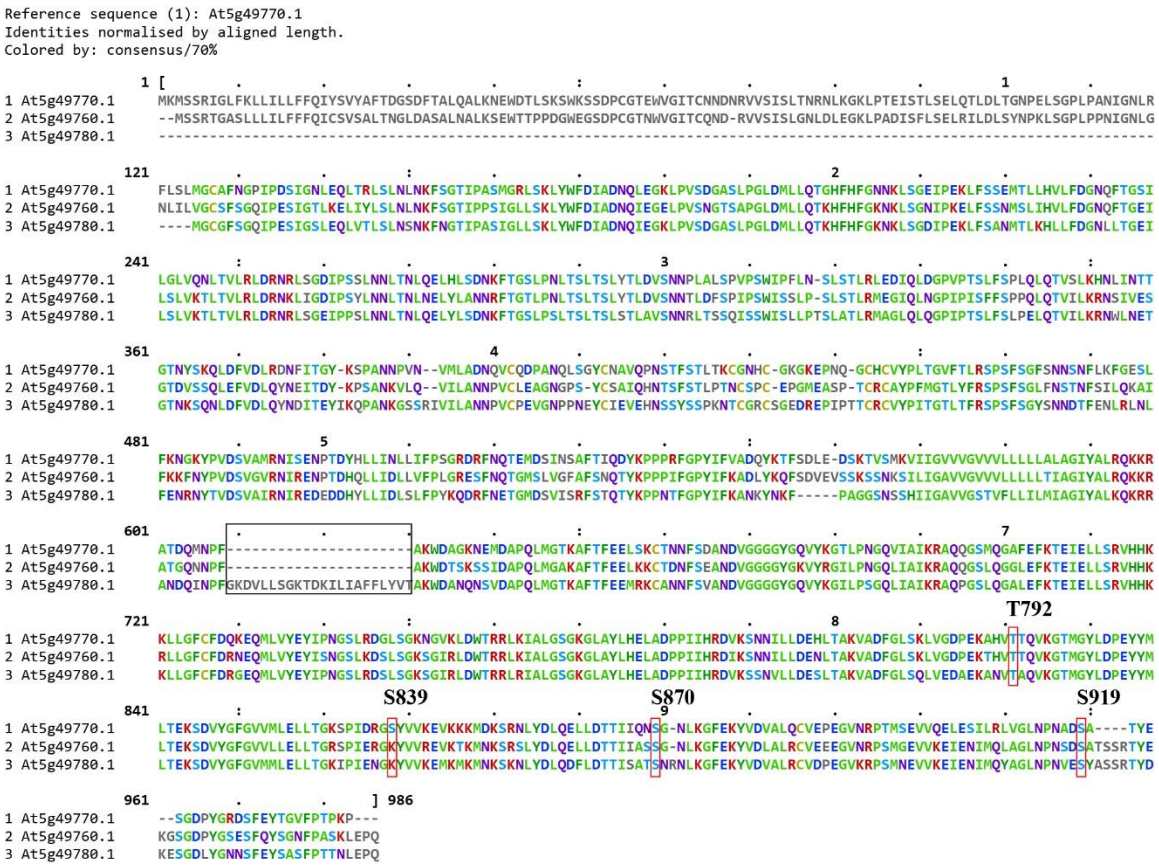

Figure 24: Protein sequence alignment of AT5G49760 AT5G49770 and AT5G49780. Black square indicates the additional sequence at amino acids 609 to 629 in AT5G49780. Red square indicates phosphosites found in AT5G49770

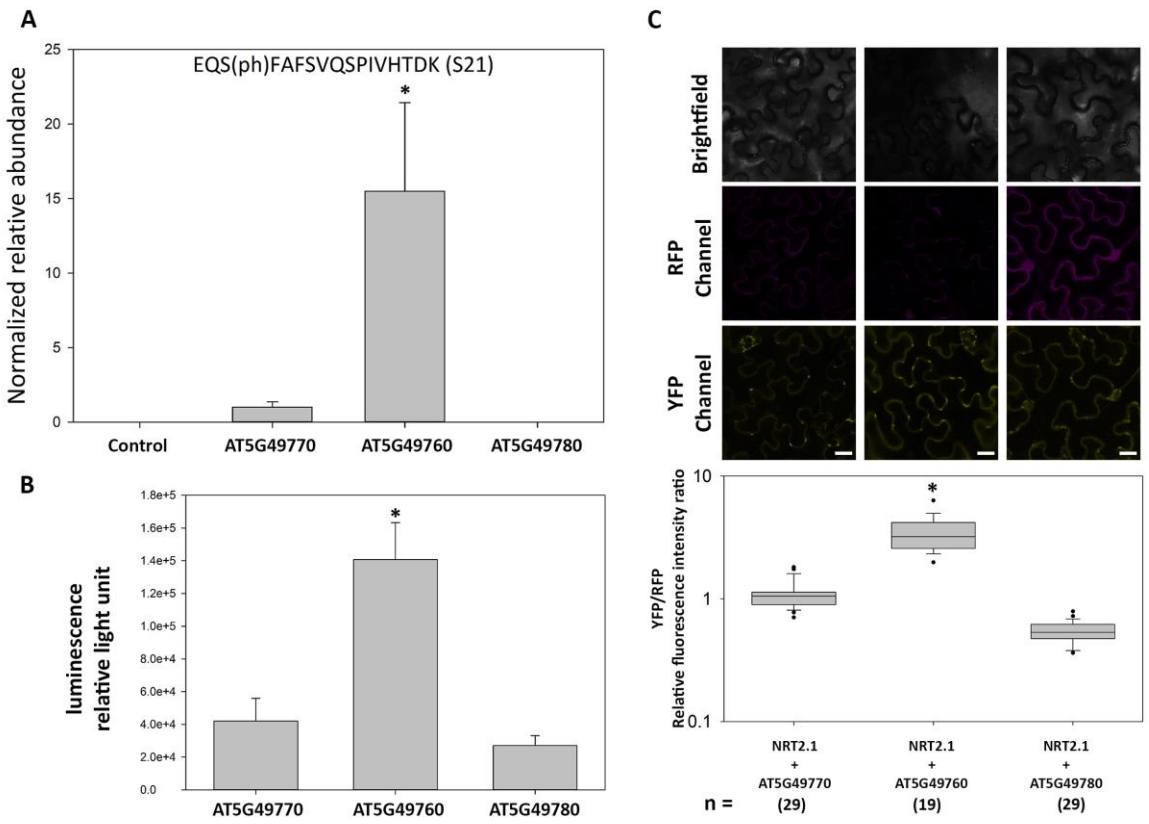

Figure 25: In vitro kinase assay and in vitro kinase activity assay. (A) In vitro kinase assay, the intracellular domain of AT5G49760, AT5G49770, and AT5G49780 were recombinant expressed and exposed to the substrate NRT2.1 peptides which were found phosphorylated. The sample without any recombinant kinase intracellular domain was used as control. Asterisks indicate significant differences to the sample incubated with the intracellular domain of AT5G49770 with p-value < 0.05. (B) In vitro kinase activity assay, the intracellular domain of AT5G49760, AT5G49770, and AT5G49780 were recombinant expressed and exposed to the substrate myelin basic protein (MBP), the sample incubated with the intracellular domain of AT5G49770 was used as the control, higher luminescence relative light unit means stronger kinase activity. Student test and Benjamini-Hochberg Procedure were chosen to calculate the p-value. (C) rBiFC results of AT5G49770, AT5G49760, AT5G49780 and NRT2.1. The interaction of NRT2.1 and AT5G49770 was used as positive control. Numbers in the parentheses indicate the number of cells quantified. Asterisks indicate significant differences to the positive control with p-value < 0.05. (Dunn's pairwise multiple comparison was used to calculate the p-value). Representative images are shown above the boxplot graphs (scale bars: 10 μm)

3.2.6 Functional Model of the S21-S28 Phospho-Switch

The interaction of NRT2.1 and NAR2.1 could be enhanced through phosphorylation at S28 of NRT2.1, while phosphorylation at S21 reduced this interaction. Possibly structural effects favor the interaction of NRT2.1 with its activator NAR2.1 only when S28 is phosphorylated, and S21 is dephosphorylated.

Phosphorylation at S28 reduced the interaction between AT5G49770 and NRT2.1 and this interaction could be further reduced by phosphorylation at S839 of AT5G49770. In contrast, phosphorylation at NRT2.1 S21 weakened the interaction with NAR2.1, but had no adverse effect on the interaction of NRT2.1 with AT5G40770. I assume that S28 – depending on the phosphorylation status – serves as a common interaction regulation site for either NAR2.1 or AT5G49770.

When NRT2.1 is active, S28 is phosphorylated, NRT2.1 interacts with NAR2.1 but not with AT5G49770, so S21 stays dephosphorylated. At the same time, S839 of AT5G49770 is phosphorylated to further reduce its interaction possibility with NRT2.1, and S870 of AT5G49770 is most likely dephosphorylated to become inactive and save energy. During the transition of NRT2.1 from active into inactive, phosphatase/phosphatases dephosphorylate NRT2.1 at S28 and AT5G49770 at S839 respectively, so both of them are ready for their interaction. When S28 is dephophorylated, AT5G49770 will replace NAR2.1 to interact with NRT2.1, and S870 of this kinase will be phosphorylated to increase its kinase activity. Under this condition, S21 will be rapidly phosphorylated, since doubly-phosphorylated peptide with S21 and S28 was very rarely detected from all my phosphoproteome data. The resulting status of NRT2.1 with phosphorylated S21 and dephosphorylated S28 then is inactive and NAR2.1 does not interact. During NRT2.1 transformation from inactive into active, a yet unknown kinase will phosphorylate NRT2.1 at S28, and S839 of AT5G49770 will become phosphorylated as well (Figure 26).

Thus, serines S21 and S28 in the N-terminus of NRT2.1 act like a phospho-switch by which the activating interaction of NAR2.1 with NRT2.1 is enabled or disabled. Activity change in nitrate transport is a final result.

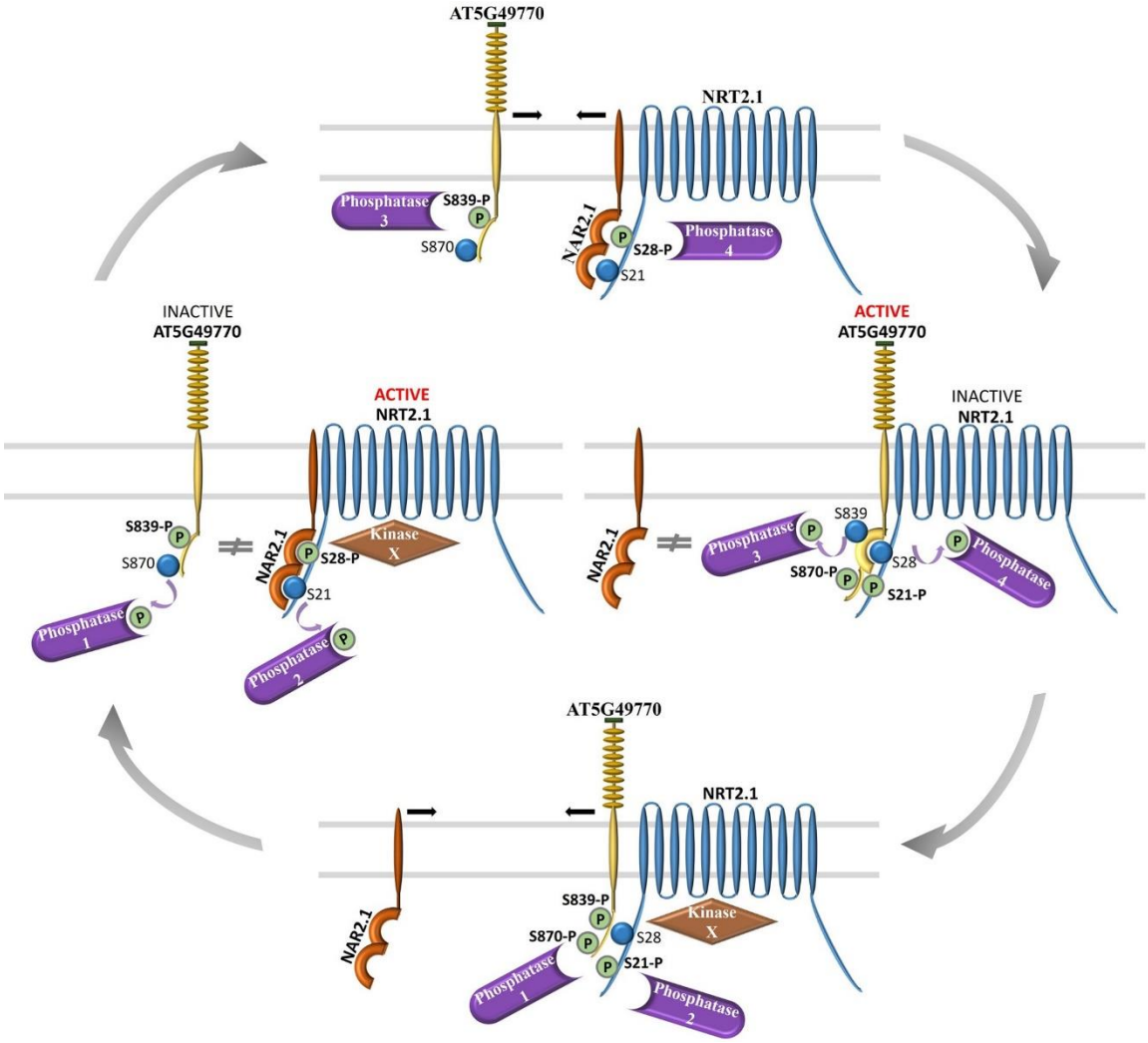

Figure 26: Functional model of the S21-S28 phospho-switch. When S28 is phosphorylated, NRT2.1 interacts with NAR2.1 but not AT5G49770, so S21 stays dephosphorylated, NRT2.1 and NAR2.1 become an active nitrate transporter system. When S28 is dephophorylated, AT5G49770 will replace NAR2.1 to interact with NRT2.1, and phosphorylation at S839 of AT5G49770 may further secure this interaction, and the kinase activity could be further enhanced through dephosphorylation at S870 under this condition, S21 will be rapidly phosphorylated, the nitrate transporter system become inactive.

4 Discussion

4.1.1 Maize Root Hair Proteome Responds to Different Nutrients

This study extends the previous known maize root hair proteome by about 82% (Nestler et al., 2011), although 366 previously identified proteins were not found in this study. These missing proteins may well be due to differences in mass spectrometer instrumentation and data analysis. However, it is also possible that these differences can be attributed to progress in gene assembly and protein model definition, which may have consolidated protein identifiers from 2011 to 2014. Furthermore, different maize genotypes have been used in the two studies (inbred B73 in the previous study vs hybrid line here). The molecular responses to the deprivation of different nutrients observed here match many known aspects that have been revealed in detail from model species. For example, we found downregulation of primary enzymes involved in nitrate and ammonium assimilation under nitrogen deprivation as well as with iron and zinc deprivations. These ions act as cofactors in several primary metabolism enzymes, whereas potassium, which also affected nitrogen assimilation, serves as the major cation counterbalancing nitrate uptake (Marschner, 2011). As expected, nitrogen deprivation stimulated amino acid synthesis, whereas amino acid degradation was prevented (Scheible et al., 2004). Magnesium deprivation was correlated with impaired phloem loading and sucrose transport from the shoots to roots, and its relation to sucrose metabolism was observed by protein abundance changes upon Mg deprivation. Furthermore, Mg^{2+} acts as a cofactor in ribosomes, potentially explaining the effects on ribosomal proteins (Marschner, 2011). Consistent with the study on Arabidopsis (Zargar et al., 2015), very few changes under Mn deprivation were identified. In general, our study identified few transporters, which is expected for total protein extracts. In addition, this low identification rate of transporters is in agreement with the fact that maize seedlings initially do not take up nutrients from the medium. Rather, nutrients are remobilized from stored reserves in the seed.

The molecular responses to iron deprivation have been studied in proteomic changes in the tomato (Li et al., 2008) or Arabidopsis (Lan et al., 2011) root proteome, especially the upregulation of the TCA cycle and the regulation of redox processes. Under Fe deprivation in Arabidopsis, the expected iron-regulated proteins for dicotyledonous strategy I plants, FRO2, IRT1, and AHA2, were found. Strategy I iron uptake relies on proton secretion into the rhizosphere (by AHA2), reduction of Fe^{3+} to Fe^{2+} (by FRO2), and subsequent Fe^{2+} uptake via IRT1. In grasses, such as maize, iron uptake strategy II is predominant, which relies on the production and secretion of phytosiderophores and uptake of Fe^{3+}-chelate complexes via the Yellow Striped 1 (YS1) transporter (Schaaf et al., 2004). Consistent with the lack of strategy I in maize, we did not detect IRT1, FRO, or the regulatory FIT transcription factor. However, we also did not detect the YS1 transporter, but this is consistent with the fact that iron uptake from the rhizosphere occurs only at later developmental stages, when sufficient carbon precursors for phytosiderophore production are available from photosynthesis (Marschner, 2011). However, we found upregulation of AHA2 under

Fe and P deprivations, as well as the expected upregulation of the phosphate transporter PHT1.4 under P deprivation and upregulation of sucrose synthesis. In soybean, some sulfate transporters and ABC transporters were exclusively identified in root hair proteomes but not in root proteomes lacking root hairs (Brechenmacher et al., 2012). Several other nutrient transporters and channels, apparently abundant in soybean root hairs and detected by MS/MS, were not detected here. Furthermore, the differential detection of an essential protein for root hair formation (RTH5), noteworthy for its higher abundance in P deprivation, may indicate that this protein is crucial for longer and denser hairs under deprivation conditions. Denser and longer root hairs, frequently observed with P deprivation in root hairs (Stetter et al., 2015), were observed only about 10 days after germination. Our main interest in studying short exposures was particularly focused on early effects and cellular adjustments without having the background of larger proteome differences due to differentiation that has already progressed.

Our findings that N deprivation induces proteins of glycolytic processes and reduces proteins involved in N assimilation (e.g., nitrate reductase) confirm results from a phosphoproteomic study on nitrogen starvation−resupply in Arabidopsis (Engelsberger and Schulze, 2012), where nitrate reductase was activated upon nitrogen resupply. The changes in the plasma membrane proteome with iron deficiency identified a large number of signaling proteins (Hopff et al., 2013). However, less is known about deprivation responses to other micronutrients, such as Mn and Zn. A recent study on Fe, Zn, and Mn deprivation has shed some light on the proteome changes in response to a lack of these elements in Arabidopsis seedlings (Zargar et al., 2015). In that study, Arabidopsis seedlings were grown on micronutrient-deprived plates for 10 days, microsomes of root tissue were prepared, and quantitation was performed by iTRAQ. The seedlings displayed visible root growth phenotypes, indicating typical deprivation symptoms. Here, we used 4 day old maize seedlings grown in aeroponics without visible deprivation symptoms or morphological adaptations. In our study, we did not expect visible deprivation symptoms, as the maize seed is rather large and can provide larger amounts of nutrients to the growing root compared to that of Arabidopsis.

4.1.2 Maize Root Hair May Sense the External Lack of Nutrients Even at Its Early Development Stage

Overall, surprisingly large nutrient-specific differential protein abundance levels were identified in our study, clearly indicating that the root hairs were either sensing the external lack of individual nutrients or experiencing cell-specific nutrient deficiencies. These two possibilities are not mutually exclusive. However, we consider the latter hypothesis to be less likely, as sufficient nutrients are stored in the seed and should be relatively mobile across short distances and rhizodermal cells (White and Veneklaas, 2012). This is particularly the case for root hairs, since they are radially symplastically connected with the inner root cylinder. A study of maize germination showed that internal P did not influence the onset or rate of uptake of exogenous P by the young root; rather, phosphate uptake was exclusively dependent on the availability of P in the nutrient solution

(Nadeem et al., 2012). Rhizodermal cells are separated from the inner tissue in maize by the exodermis, and cell walls of 4 day old plants already contain significant amounts of impermeable suberin in their cell wall (Schreiber et al., 2005). Furthermore, the normal radial directionality of transport from the outside to the inside may impose an obstacle to the nutrient support of root hairs from storage organs.

4.2.1 Global Phosphoproteome of Nitrate Responses

In this research, more phosphopeptides were detected comparing to a previous similar study done by Engelsberger and Schulze in 2012. This difference should be mainly due to the usage of new MS technology (Q-Exactive vs Orbitrap), which allowed faster and more sensitive acquisition of raw data.Also, interpretation of spectra by new algorithm (Perseus vs. MS-Quant) has led to an increase in data reliability. Due to application of the new method for phosphopeptide enrichment (Wu et al., 2017), more phosphopeptides were found in the nitrate resupply study than in the nitrogen deprivation study.

Through over-representation pathway analysis, several pathways were found over-represented under both nitrogen deprivation and nitrate resupply conditions, such as regulation of transcription, DNA synthesis, calcium signaling, and receptor kinase. My result suggests phosphorylation should be very important for the function of proteins involved in transcription, DNA synthesis, calcium signaling, and receptor kinase when plants are confront with external nitrogen stimuli. Interestingly, glycolysis were only found over-represented in WT under ammonium deprivation and cell wall precursor synthesis were only found over-represented in WT after 15 minutes nitrate deprivation or 3 hours ammonium deprivation. Pathway related to G-proteins was over-represented in *nrt1.1* knock-out mutant under both low and high nitrate resupply conditions and *nrt2.1* knock-out mutant only under high concentration nitrate resupply. These have demonstrated that different stimuli may result in altered phosphorylation events of proteins from specific pathways, sometimes in a time dependent way.

Identification of phosphorylation site sequences and studies with corresponding model peptides have demonstrated the specificity of kinases, and the amino acid sequence motif surrounding the serine/threonine/tyrosine residues of the substrate proteins is a major factor defining specificity of the kinases (Kemp and Pearson, 1990) (Amanchy et al., 2007). Through applying motif analysis, nine different motifs were detected, and some of them are found to be target motifs of MAPK, SnRK2, or CDPK, indicating these protein kinases may play vital role in plant response to nitrogen. During these motifs, [-pS-P-] were frequently reported by many other phopshoproteome-related studies. This is probably because [-pS-P-] is known as the target motif of MPKs which have been found to participate in a broad range of biological activities.

Most detected motifs could be found in both up-regulated and down-regulated groups from deprivation and resupply experiment, suggesting an inverse regulation of different kinase or phosphatase family members, and their activity can be regulated by nitrogen deprivation and nitrate

resupply. Except these motifs, [-pS-F-] was only found in down-regulated group from both experiment, and in nitrate deprivation experiment, no such motif was detected from down-regulated group. These results indicate nitrogen treatment may cause specific response of some protein kinases or phosphatases.

Comparing to WT, no specific motifs could be detected in *nrt2.1* knock-out mutant from nitrogen deprivation experiment, but motifs in *nrt2.1* knock-out mutant from nitrate resupply experiment was detected. These indicate NRT2.1 may be a nitrogen deprivation sensor by which the function of certain protein kinases or phosphatases could be regulated.

To date, no motif was found specifically in response to any particular stimuli. One possible reason may be that, most kinases people have found and studied are involved in response to more than one stimuli. For instance, MAPKs in plant respond to a range of environmental stimuli including but not limited to drought, heat, and biotic attack (Tena et al., 2001). CIPKs and CDPKs may respond to more stimuli considering the fact that calcium is a versatile intracellular messenger in plant cells (Shi et al., 2018) (Wang et al., 2018a) (Luan, 2009).

4.2.2 PhosphoNetwork

Plant development and response to environmental stimuli require the harmonious regulation of protein activity, protein localization, and protein-protein interaction which can be further regulated through phosphorylation. So there is a high possibility that these phosphorylation events could be correlated. Such correlation analyses were already successfully applied in co-expression networks (Winter et al., 2007) and allowed to derive regulatory relationships on the level of gene expression. Based on this idea and with the help of Pearson correlation analysis, I built the PhosphoNetwork using the phosphoproteome data in my research. Since the more efficient phosphopeptide enrichment method was used in the nitrate resupply experiment, more phosphopeptides were detected compare to the nitrogen deprivation experiment, which result in more correlations found under nitrate resupply condition. I only focused on two types of PhosphoNetwork in this research, one is Kinase PhosphoNetwork containing only kinases and their correlated proteins, the other is Phosphatase PhosophoNetwork containing phosphatases and their correlated proteins. Excitingly, some known kinases and their substrates from precious studies were found in the PhosphoNetwork as well, validating the approach taken here. Although those previous studies have provided sufficient results to demonstrate which kinases phosphorylate which substrates, the mechanisms and regulation of these correlations still remain big questions. Fortunately, the PhosphoNetwork may provide an opportunity to address this question. In the PhosphoNetwork, only part of correlations could be found under every conditions and plant lines I used in my study, such as well studied CTR1 and its proved substrate EIN2, FERONIA and its substrate AHA2. In 2009, Umezawa found phosphatases from group A PP2Cs could interact and inactivate SnRK2s through dephosphorylation (Umezawa et al., 2009). In my PhosphoNetwork one phosphatase AT1G22280 from PP2Cs was found to be correlated with SnRK2.2 when 3 mM nitrate was resupplied to

nitrogen starved WT, and this correlation was lost when the resupplied nitrate concentration reduced to 0.2 mM. In *nrt2.1* knock-out line, AT1G22280 was found correlated with SnRK2.2 under 3 mM nitrate resupply condition but not under 0.2 mM nitrate resupply condition (Table 2). However in *nrt1.1* knock-out line these results are just opposite that AT1G22280 was correlated with SnRK2.2 under 0.2 mM nitrate resupply not 3 mM nitrate (Table 2). These suggest that, if this PP2C AT1G22280 did correlate with SnRK2.2 the way Umezawa demonstrated for other PP2Cs and SnRK2s, then this correlation may respond to different nitrate concentration sensed by NRT1.1. As a matter of fact, similar conditional correlation has been found and studied when people investigated the BR-signaling pathway in plant. In this pathway a BR involved conditional interaction was well demonstrated. When BRs such as BL are absent, the interaction between BR receptor BRI1 and co-receptor BAK1 was inhibited. When BL is present, it binds to the receptor BRI1 triggering the formation of a BRI1-BAK1 heterodimer to initiate BR signaling (Dejonghe et al., 2014) (Nolan et al., 2017) (Clouse, 2011) (Kim and Wang, 2010). All together, these findings indicate that the PhosphoNetwork may possess the potential to explore the regulation mechanism behind condition-dependent phosphorylation events.

NIN-LIKE PROTEIN 7 (NLP7) is a transcription factor, and it participates in nitrate signaling (Konishi and Yanagisawa, 2013). In 2017, a study indicated that the CPK activity could control nuclear retention of NLP7, and the CPK activity was regulated by nitrate-coupled calcium (Liu et al., 2017). A recent research showed that in Arabidopsis, the root elongation could be modulated by BR signaling kinase BSK3, and this research also demonstrated that low N could specifically upregulate transcript levels of the BR co-receptor BAK1 to activate BR signaling and stimulate root elongation (Jia et al., 2019). Although NLP7 itself was not identified, in the kinase PhosphoNetwork established in the nitrate resupply experiment, calcium signaling module and BR module were found suggesting there may be more players involved in phosphorylation responses triggered by nitrate-coupled calcium or BR signaling.

Interestingly, not until I finished building this PhosphoNetwork, did I find a similar approach being used to reconstruct maize seed protein networks in 2013. The only difference between their approach and the one used in this study is that, in their approach, only phosphopeptides from each kinase activation loops were used for correlation analysis (Walley et al., 2013). However, in my approach, all phosphopeptides detected from kinases were chosen for correlation analysis. Walley et al did so since phosphorylation at activation loop has been proven to be one important mechanism in regulating many kinases activity (Adams, 2003) (Burza et al., 2006) (Shah et al., 2001), and through excluding non-activation loop located phosphopeptides, their approach may give a more accurate prediction than mine. However their approach may also exclude the probability to discover kinase-substrate network, in which the kinase activity was regulated through phosphorylation at non-activation loop site. This non-activation loop phosphorylation activity regulation mechanism has been reported (Johnson et al., 1996) (Nolen et al., 2004).

4.2.3 Multisite Phosphorylation Involved Phospho-switch

In this study, a multisite phosphorylation involved phospho-switch model was established. In this model, two phosphosites were supposed to regulate the activity of nitrate transporter NRT2.1. Similar regulation of transporters activity at the plasma membrane by multiple phosphorylation sites have been found and well-studied. For example, phosphorylation at Ser-280 and Ser-283 could regulate the activity of plasma membrane located water channel PIP2;1 (Prado et al., 2013).

Interestingly, the kinase AT5G49770 to phosphorylate its predicted substrate NRT2.1 was also supposed to be regulated by two phosphosites, and these sites may have distinct roles. Phosphorylation of AT5G49770 at S839 affects its interaction with NRT2.1 while phosphorylation at S870 regulates its kinase activity. It has been shown that multisite phosphorylation found in kinase can affect their activity or their interaction partners. By using an Arabidopsis suspension culture system, Thomas Nühse and his colleagues found microbial elicitors induced dual phosphorylation at Thr221 and Tyr223 of the Arabidopsis MPK 6, and the activity of MPK6 was regulated by its phosphorylation at these two sites (Nühse et al., 2000). Other studies have demonstrated that MAPKs, not only MPK6, can be activated through double phosphorylation at a conserved motif TEY (Cristina et al., 2010). Through a study on human cells, people found single phosphorylated (phosphorylation at T389) ribosomal protein S6 kinase 1 (S6K1) and triple phosphorylated (phosphorylation at T389, S424, and S429) S6K1 interacted and phosphorylated different substrates (Arif et al., 2019).

Combing the phospho-switch model established in this study with previous studies mentioned above. Multisite phosphorylation involved regulation mechanism could be a general controlling principle for many biological processes.

4.2.4 AT5G49770 and Its Homologues

Four phosphorylation sites were detected from AT5G49770, results from rBIFC, in vitro kinase assay, and in vitro kinase activity assay indicate that S839 may be involved in regulating the interaction between AT5G49770 and NRT2.1, S870 may regulate AT5G49770 kinase activity. In Arabidopsis, AT5G49770 has two orthologs AT5G49760 and AT5G49780. AT5G49760 was highly expressed in leaf tissue and anthers, and showed rather low expression values in roots. AT5G49780 showed moderate general expression also in roots, but at lower levels than kinase AT5G49770 (Winter et al., 2007). All phosphopeptides identified for AT5G49770 were proteotypic peptides clearly identifying AT5G49770. Interestingly, all four phosphorylation sites identified for AT5G49770 except S839 are highly conserved across all three orthologs. S839 is unique to AT5G49770, while in AT5G49760 and AT5G49780 a lysine is present at the respective position within the sequence (Figure 15). Surprisingly, rBIFC results showed that interaction of AT5G49760 and NRT2.1 was as strong as the interaction between phosphodead mutation AT5G49770S839A and NRT2.1 but stronger than AT5G49770. AT5G49780 showed a much weaker interaction with NRT2.1 compared to AT5G49770 even it has the same lysine like

AT5G49760 does (Figure 14). Possibly, the differences in activity are connected to the additional sequence at amino acids 609 to 629 in AT5G49780 (Figure 15). In the in vitro kinase assays, AT5G49780 was largely inactive, while AT5G49760 displayed a higher activity towards substrate peptide EQSFAFSVQSPIVHTDK than did AT5G49770. This high activity could possibly be explained by the regulatory phosphorylation site identified for AT5G49770 with S839, which is not present in AT5G49760 and therefore this kinase show stronger interaction with its substrate. It is also very interesting that even S870 can further regulate kinase activity, but interaction between kinase and substrate seems to contribute more to the final phosphorylation of NRT2.1 at S21. Since the in vitro phosphorylation assay was conducted with recombinant kinase domains of each kinase homolog, the native kinase domain of AT5G49770 is expected to be not highly phosphorylated and thus yielded lower activity than recombinant kinase domain with phosphomimicking S839D mutations.

AT5G49760 was recently named as hydrogen-peroxide-induced Ca^{2+} increases mutant1 (HPCA1) since this LRR receptor kinase could sense extracellular H_2O_2 (exH_2O_2) and then activate Ca^{2+} channels in guard cells (Wu et al., 2020). Considering the high similarity between HPCA1 and AT5G49770 (HPCA-LIKE1/HPCAL1) sequences, it is not bold to assume that HPCAL1 may sense exH_2O_2 in root cells as well. Previous studies also proved that there is a connection between external nitrogen stimuli and root H_2O_2 accumulation (Shin et al., 2005) (Kong et al., 2013) (Chaput et al., 2020). Combing these studies together with our discovery, I speculate that nitrogen-induced exH_2O_2 accumulation in root may be sensed by HPCAL1 which then regulate NRT2.1 transport activity.

MAPKs were also known as components of exH_2O_2 downstream signaling (Zipfel and Oldroyd, 2017) (Boller and Felix, 2009). In Wu's research, *hpca1* mutants showed less H_2O_2-induced phosphorylation of MAPK3 and MAPK6 compared to WT. This indicated that besides mediating H_2O_2-induced activation of Ca^{2+} channels in guard cells, HPCA1 may be a H_2O_2 sensor upstream of MAPKs which are involved in H_2O_2 signaling (Wu et al., 2020) . Interestingly, in the PhosphoNetwork showed in this research, HPCAL1 was found correlated with MAPK and calcium signaling modules (Figure 17).

To sum up, these results suggest that HPCAL1 may function as a sensor of external nitrogen-stimuli-induced exH_2O_2 in Arabidopsis root. It may sense external nitrogen-deprivation-induced exH_2O_2 and then activate NRT2.1. Simultaneously HPCAL1 may transmit this exH_2O_2 signal through regulating its downstream components such as Ca^{2+} channel and MAPKs which would help plant cells to cope with possible nitrogen starvation problem.

5 Conclusions and Perspective

We conclude that root hairs may experience deficiencies very early, as suggested by the significant and nutrient-specific responses to individual nutrient deprivations, and that these very early proteomic adjustments lay the basis for future differentiation processes and the development of typical root hair phenotypes. In summary, our work presents a global profiling of protein abundance changes under very early nutrient deficiencies, which may serve as reference for further studies on nutrient-related adaptations. And this work also proved that maize root hair can be used as a suitable material for signal cell type research.

This work has proved that development of MS technology and phosphopeptide enrichment method can greatly improve detection of phosphopeptides, which is very important for promoting progress of phosphoproteomics study. NRT1.1 and NRT2.1 may play roles in mediating phosphorylation signal transduction. PhosphoNetwork provides another solution to predict kinases and their substrate proteins, and this method can also be used in investigating phosphatases and their target proteins. This work functionally characterizes two phosphorylation sites which work together as a phopsho-switch in the N-terminus of NRT2.1. Thereby, NRT2.1 is not regulated directly, but differential phosphorylation at S28 and S21 affects the interaction with the activator protein NAR2.1, the S21/S28 phospho-switch is likely to be a regulator of nitrate uptake into root cells through NRT2.1.

However, this work just uncovered a tiny piece of the whole puzzle, there are still a lot of questions need to be answered. Such as which kinases phosphorylated the other phosphorylation sites of NRT2.1, and how their kinase activity being regulated. Moreover, the role of HPCAL1 in sensing external nitrogen stimuli-induced exH_2O_2 in Arabidopsis root still needs to be certified and the regulatory mechanism behind this still needs to be explored.

6 Supplementary Data

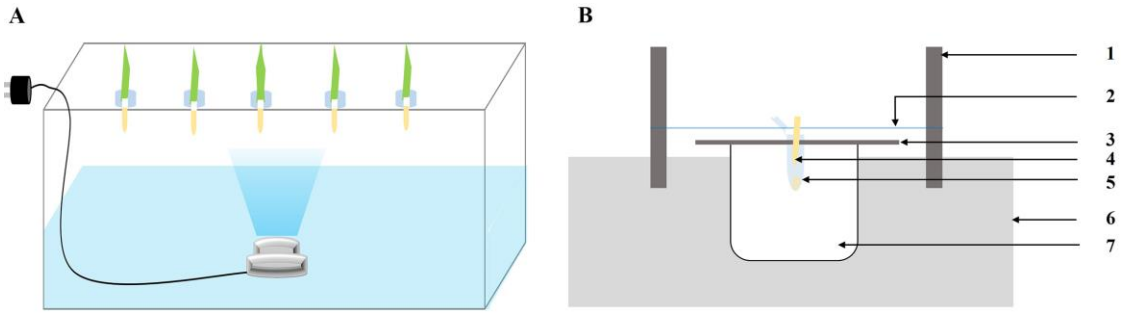

Supplementary Figure S1: Growth and harvesting of maize root hairs. (A) Schematic diagram of the aeroponic growth systems. (B) Harvesting strategy for root hairs over a nylon string directly into liquid nitrogen. 1-stand, 2-nylon line, 3-holder, 4-root, 5-tube with liquid N, 6-stand, 7-beaker.

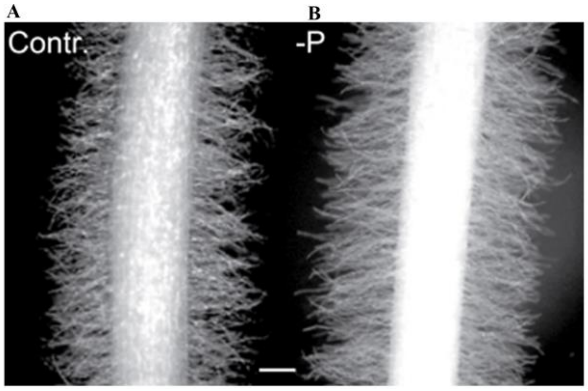

Supplementary Figure S2: Maize root hairs when grown for 5 days between wet filter paper and after 6 further days on selective agar plates. (A) Control agar with all nutrients. (B) Phosphorus depletion medium. Scaling bar 0.5 cm. Pictures of seminal roots 4 cm from the root tip.

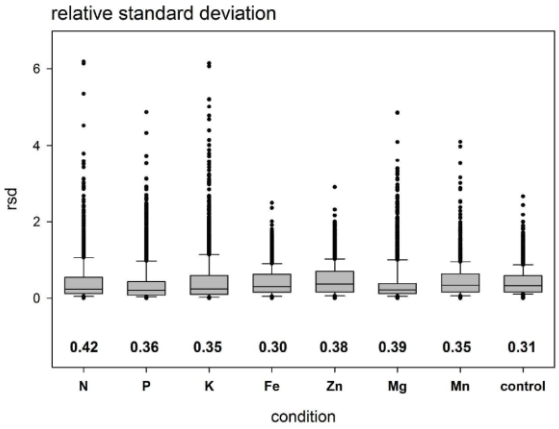

Supplementary Figure S3: Overview of the relative standard deviation within two to three biological replicates. Averages are indicated.

Supplementary Table S1: Composition of the modified ¼ Hoagland solution for full nutrition and different nutrient-deprived media.

Nutrient	Final Concentration µm	N	P	K	Fe	Zn	Mn	Mg
NH_4NO_3	1000		X	X	X	X	X	X
KH_2PO_4	1000	X		X	X	X	X	X
KCl	1000		X					X
NaH_2PO_4	1000			X				X
$CaCl_2$	1000	X	X	X	X	X	X	X
$MgSO_4 \times 7H_2O$	500	X	X	X	X	X	X	
Na_2EDTA-Fe(II)	100	X	X	X		X	X	X
$MnSO_4$	9	X	X	X	X	X		X
$ZnSO_4 \times 7H_2O$	0.765	X	X	X	X		X	X
$CuSO4 \times 5H_2O$	0.32	X	X	X	X	X	X	X
$Na_2MoO_4 \times 2H_2O$	0.016	X	X	X	X	X	X	X
H_3BO_3	0.46	X	X	X	X	X	X	X

Supplementary Table S2: Preparation of the mutant strand synthesis reaction.

Name	Amount Used
10×reaction buffer	5 µl
dsDNA template	50 ng
Oligonucleotide primer 1	125 ng
Oligonucleotide primer 2	125 ng
dNTP mix	1 µl
PfuUltra HF DNA polymerase (2.5 U/µl)	1 µl
ddH_2O	To a final volume of 50 µl

Supplementary Table S3: cycling parameters.

Segment	Cycles	Temperature	Time
1	1	95ºC	30 seconds
2	30	95ºC	30 seconds
		55ºC	1 minute
		68ºC	1 minute/kb of plasmid length
3	1	68ºC	10 minutes

Supplementary Table S4: Primers for site-direct mutagenesis.

Name	Amino Acid Site	Sequence
NRT2.1-S11A-F	Ser 11	CTCCATGCATGGCGCTCCCCGGCTC
NRT2.1-S11A-R	Ser 11	GAGCCGGGGAGCGCCATGCATGGAG
NRT2.1-S11D-F	Ser 11	GTGACTCCATGCATGTCGCTCCCCGGCTCACC
NRT2.1-S11D-R	Ser 11	GGTGAGCCGGGGAGCGACATGCATGGAGTCAC
NRT2.1-S21A-F	Ser 21	TGCACCGAGAAAGCAAAGGCTTGTTCTCTACCGGTGAC
NRT2.1-S21A-R	Ser 21	GTCACCGGTAGAGAACAAGCCTTTGCTTTCTCGGTGCA
NRT2.1-S21D-F	Ser 21	TTGCACCGAGAAAGCAAAGTCTTGTTCTCTACCGGTGACT
NRT2.1-S21D-R	Ser 21	AGTCACCGGTAGAGAACAAGACTTTGCTTTCTCGGTGCAA
NRT2.1-S28A-F	Ser 28	CGGTGCAAGCACCAATTGTG
NRT2.1-S28A-R	Ser 28	CACAATTGGTGCTTGCACCG
NRT2.1-S28D-F	Ser 28	CGGTGCAAGATCCAATTGTG
NRT2.1-S28D-R	Ser 28	CACAATTGGATCTTGCACCG
NRT2.1-S501A-F	Ser 501	GCAGAAGAACATGCATCAAGGAGCCCTCCGGTTTGC
NRT2.1-S501A-R	Ser 501	GCAAACCGGAGGGCTCCTTGATGCATGTTCTTCTGC
NRT2.1-S501D-F	Ser 501	AAGCAGAAGAACATGCATCAAGGAGACCTCCGGTTTGCC
NRT2.1-S501D-R	Ser 501	GGCAAACCGGAGGTCTCCTTGATGCATGTTCTTCTGCTT
NRT2.1-T521A-F	Thr 521	AGGCGGCGCAGCAGCAGAGCGGAC
NRT2.1-T521A-R	Thr 521	GTCCGCTCTGCTGCTGCGCCGCCT
NRT2.1-T521D-F	Thr 521	TTCTCAGGCGGATCAGCAGCAGAGCGGACGCGGCG
NRT2.1-T521D-R	Thr 521	CGCCGCGTCCGCTCTGCTGCTGATCCGCCTGAGAA
AT5G49770-T792A-F	Thr 792	GTTCCTTTCACTTGTGTTGCGACATGAGCTTTTTCAGGG
AT5G49770-T792A-R	Thr 792	CCCTGAAAAAGCTCATGTCGCAACACAAGTGAAAGGAAC
AT5G49770-T792D-F	Thr 792	CCATGGTTCCTTTCACTTGTGTATCGACATGAGCTTTTTCAGGGTCC
AT5G49770-T792D-R	Thr 792	GGACCCTGAAAAAGCTCATGTCGATACACAAGTGAAAGGAACCATGG
AT5G49770-S839A-F	Ser 839	CTTTACCTCTTTCACAACATAGGCGCCTCTATCTATCGGACTTTTA
AT5G49770-S839A-R	Ser 839	TAAAAGTCCGATAGATAGAGGCGCCTATGTTGTGAAAGAGGTAAAG
AT5G49770-S839D-F	Ser 839	TCTTTACCTCTTTCACAACATAGTCGCCTCTATCTATCGGACTTTTAC
AT5G49770-S839D-R	Ser 839	GTAAAAGTCCGATAGATAGAGGCGACTATGTTGTGAAAGAGGTAAAGA
AT5G49770-S870A-F	Ser 870	AACCCTTTCAAATTCCCGGCGTTTTGGATAATTGTCGTGTCC
AT5G49770-S870A-R	Ser 870	GGACACGACAATTATCCAAAACGCCGGGAATTTGAAAGGGTT
AT5G49770-S870D-F	Ser 870	GAACCCTTTCAAATTCCCGTCGTTTTGGATAATTGTCGTGTCCA
AT5G49770-S870D-R	Ser 870	TGGACACGACAATTATCCAAAACGACGGGAATTTGAAAGGGTTC
AT5G49770-S919A-F	Ser 919	TCCTCGTATGTTGCTGCATCGGCGTTAGGGTTTAA
AT5G49770-S919A-R	Ser 919	TTAAACCCTAACGCCGATGCAGCAACATACGAGGA
AT5G49770-S919D-F	Ser 919	GATGCTTCCTCGTATGTTGCATCATCGGCGTTAGGGTTTAATCCAA
AT5G49770-S919D-R	Ser 919	TTGGATTAAACCCTAACGCCGATGATGCAACATACGAGGAAGCATC

Supplementary Table S5: Primers for expression of recombinant kinase intracellular domain.

Name	Sequence
Intra-AT5G49760-F	CATATGGGGATTTACGCTCTTAGGC
Intra-AT5G49760-R	GTCGACTTGGGGCTCAAGCTTTG
Intra-AT5G49770-F	TTCCATATGAGACAGAAGAAGAGAG
Intra-AT5G49770-R	GTCGACGGGTTTTGGAGTTGG
Intra-AT5G49780-F	GAATTCATGCTTAAGCAAAAGAGAA
Intra-AT5G49780-R	GTCGACTTGAGGTTCGAGGTTTGTA

Supplementary Table S6: Primers for rBiFC gateway cloning.

Name	Sequence
attB1-NRT2.1-F	GGGGACAAGTTTGTACAAAAAAGCAGGCTTAATGGGTGATTCTACTGGT
attB4-NRT2.1-R	GGGGACAACTTTGTATAGAAAAGTTGGGTGAACATTGTTGGGTGTGT
attB3-NAR2.1-F	GGGGACAACTTTGTATAATAAAGTTGTAATGGCGATCCAGAAGATC
attB2-NAR2.1-R	GGGGACCACTTTGTACAAGAAAGCTGGGTTTTTGCTTTGCTCTATCTT
attB3-AT5G49770-F	GGGGACAACTTTGTATAATAAAGTTGTAATGAAGATGAGTTCAAGA
attB2-AT5G49770-R	GGGGACCACTTTGTACAAGAAAGCTGGGTTGGGTTTTGGAGTTGGGAA
attB3-AT5G49760-F	GGGGACAACTTTGTATAATAAAGTTGTAATGAGTTCAAGAACTGGA
attB2-AT5G49760-R	GGGGACCACTTTGTACAAGAAAGCTGGGTTTTGGGGCTCAAGCTTTGAAGC
attB3-AT5G49780-F	GGGGACAACTTTGTATAATAAAGTTGTAATGGGATGTGGTTTCAGT
attB2-AT5G49780-R	GGGGACCACTTTGTACAAGAAAGCTGGGTTTTGAGGTTCGAGGTTTGTAG

7 Bibliography

Adams, J.A. (2003). Activation loop phosphorylation and catalysis in protein kinases: is there functional evidence for the autoinhibitor model? Biochemistry **42,** 601-607.

Alboresi, A., Gestin, C., Leydecker, M.T., Bedu, M., Meyer, C., and Truong, H.N. (2005). Nitrate, a signal relieving seed dormancy in Arabidopsis. Plant, Cell & Environment **28,** 500-512.

Amanchy, R., Periaswamy, B., Mathivanan, S., Reddy, R., Tattikota, S.G., and Pandey, A. (2007). A curated compendium of phosphorylation motifs. Nature biotechnology **25,** 285.

Arif, A., Jia, J., Willard, B., Li, X., and Fox, P.L. (2019). Multisite phosphorylation of S6K1 directs a kinase phospho-code that determines substrate selection. Molecular cell **73,** 446-457. e446.

Bailey, T.L., Boden, M., Buske, F.A., Frith, M., Grant, C.E., Clementi, L., Ren, J., Li, W.W., and Noble, W.S. (2009). MEME SUITE: tools for motif discovery and searching. Nucleic acids research **37,** W202-W208.

Bates, T.R., and Lynch, J.P. (2001). Root hairs confer a competitive advantage under low phosphorus availability. Plant and Soil **236,** 243-250.

Benjamini, Y., and Hochberg, Y. (1995). Controlling the false discovery rate: a practical and powerful approach to multiple testing. Journal of the Royal statistical society: series B (Methodological) **57,** 289-300.

Bittsánszky, A., Pilinszky, K., Gyulai, G., and Komives, T. (2015). Overcoming ammonium toxicity. Plant Science **231,** 184-190.

Boller, T., and Felix, G. (2009). A renaissance of elicitors: perception of microbe-associated molecular patterns and danger signals by pattern-recognition receptors. Annual review of plant biology **60,** 379-406.

Bouguyon, E., Brun, F., Meynard, D., Kubeš, M., Pervent, M., Leran, S., Lacombe, B., Krouk, G., Guiderdoni, E., and Zažímalová, E. (2015). Multiple mechanisms of nitrate sensing by Arabidopsis nitrate transceptor NRT1. 1. Nature Plants **1,** 15015.

Brandt, B., Brodsky, D.E., Xue, S., Negi, J., Iba, K., Kangasjärvi, J., Ghassemian, M., Stephan, A.B., Hu, H., and Schroeder, J.I. (2012). Reconstitution of abscisic acid activation of SLAC1 anion channel by CPK6 and OST1 kinases and branched ABI1 PP2C phosphatase action. Proceedings of the National Academy of Sciences **109,** 10593-10598.

Brechenmacher, L., Nguyen, T.H.N., Hixson, K., Libault, M., Aldrich, J., Pasa‐Tolic, L., and Stacey, G. (2012). Identification of soybean proteins from a single cell type: the root hair. Proteomics **12,** 3365-3373.

Burza, A.M., Pękala, I., Sikora, J., Siedlecki, P., Malagocki, P., Bucholc, M., Koper, L., Zielenkiewicz, P., Dadlez, M., and Dobrowolska, G. (2006). Nicotiana tabacum osmotic stress-activated kinase is regulated by phosphorylation on Ser-154 and Ser-158 in the kinase activation loop. Journal of Biological Chemistry **281,** 34299-34311.

Camanes, G., Pastor, V., Cerezo, M., García-Andrade, J., Vicedo, B., García-Agustín, P., and Flors, V. (2012). A deletion in NRT2. 1 attenuates Pseudomonas syringae-induced hormonal perturbation, resulting in primed plant defenses. Plant physiology **158,** 1054-1066.

Cerezo, M., Tillard, P., Filleur, S., Muños, S., Daniel-Vedele, F., and Gojon, A. (2001). Major alterations of the regulation of root NO3− uptake are associated with the mutation of Nrt2. 1 and Nrt2. 2 genes in Arabidopsis. Plant Physiology **127,** 262-271.

Chaput, V., Martin, A., and Lejay, L. (2020). Redox metabolism: the hidden player in carbon and nitrogen signaling? Journal of experimental botany **71,** 3816-3826.

Choi, H.-i., Park, H.-J., Park, J.H., Kim, S., Im, M.-Y., Seo, H.-H., Kim, Y.-W., Hwang, I., and Kim, S.Y. (2005). Arabidopsis calcium-dependent protein kinase AtCPK32 interacts with ABF4,

a transcriptional regulator of abscisic acid-responsive gene expression, and modulates its activity. Plant Physiology **139,** 1750-1761.

Chopin, F., Wirth, J., Dorbe, M.-F., Lejay, L., Krapp, A., Gojon, A., and Daniel-Vedele, F. (2007). The Arabidopsis nitrate transporter AtNRT2. 1 is targeted to the root plasma membrane. Plant Physiology and Biochemistry **45,** 630-635.

Clouse, S.D. (2011). Brassinosteroid signal transduction: from receptor kinase activation to transcriptional networks regulating plant development. The Plant Cell **23,** 1219-1230.

Clowes, F. (2000). Pattern in root meristem development in angiosperms. The New Phytologist **146,** 83-94.

Conn, S.J., Hocking, B., Dayod, M., Xu, B., Athman, A., Henderson, S., Aukett, L., Conn, V., Shearer, M.K., and Fuentes, S. (2013). Protocol: optimising hydroponic growth systems for nutritional and physiological analysis of Arabidopsis thaliana and other plants. Plant methods **9,** 4.

Cox, J., and Mann, M. (2008). MaxQuant enables high peptide identification rates, individualized ppb-range mass accuracies and proteome-wide protein quantification. Nature biotechnology **26,** 1367.

Cox, J., Neuhauser, N., Michalski, A., Scheltema, R.A., Olsen, J.V., and Mann, M. (2011). Andromeda: a peptide search engine integrated into the MaxQuant environment. Journal of proteome research **10,** 1794-1805.

Cox, J., Hein, M.Y., Luber, C.A., Paron, I., Nagaraj, N., and Mann, M. (2014). Accurate proteome-wide label-free quantification by delayed normalization and maximal peptide ratio extraction, termed MaxLFQ. Molecular & cellular proteomics **13,** 2513-2526.

Cristina, M.S., Petersen, M., and Mundy, J. (2010). Mitogen-activated protein kinase signaling in plants. Annual review of plant biology **61,** 621-649.

Dai Vu, L., Gevaert, K., and De Smet, I. (2018). Protein language: post-translational modifications talking to each other. Trends in plant science.

Datta, S., Kim, C.M., Pernas, M., Pires, N.D., Proust, H., Tam, T., Vijayakumar, P., and Dolan, L. (2011). Root hairs: development, growth and evolution at the plant-soil interface. Plant and Soil **346,** 1-14.

De Angeli, A., Monachello, D., Ephritikhine, G., Frachisse, J., Thomine, S., Gambale, F., and Barbier-Brygoo, H. (2006). The nitrate/proton antiporter AtCLCa mediates nitrate accumulation in plant vacuoles. Nature **442,** 939.

Dejonghe, W., Mishev, K., and Russinova, E. (2014). The brassinosteroid chemical toolbox. Current opinion in plant biology **22,** 48-55.

Deng, M., Moureaux, T., and Caboche, M. (1989). Tungstate, a molybdate analog inactivating nitrate reductase, deregulates the expression of the nitrate reductase structural gene. Plant physiology **91,** 304-309.

Dóczi, R., Hatzimasoura, E., Bilooei, S.F., Ahmad, Z., Ditengou, F.A., López-Juez, E., Palme, K., and Bögre, L. (2019). The MKK7-MPK6 MAP Kinase Module Is a Regulator of Meristem Quiescence or Active Growth in Arabidopsis. Frontiers in plant science **10**.

Dodd, A.N., Kudla, J., and Sanders, D. (2010). The language of calcium signaling. Annual review of plant biology **61,** 593-620.

Engelsberger, W.R., and Schulze, W.X. (2012). Nitrate and ammonium lead to distinct global dynamic phosphorylation patterns when resupplied to nitrogen‐starved Arabidopsis seedlings. The Plant Journal **69,** 978-995.

Esteban, R., Ariz, I., Cruz, C., and Moran, J.F. (2016). Mechanisms of ammonium toxicity and the quest for tolerance. Plant Science **248,** 92-101.

Fang, X.Z., Tian, W.H., Liu, X.X., Lin, X.Y., Jin, C.W., and Zheng, S.J. (2016). Alleviation of proton toxicity by nitrate uptake specifically depends on nitrate transporter 1.1 in Arabidopsis. New Phytologist **211,** 149-158.

Feng, J., Volk, R.J., and Jackson, W.A. (1994). Inward and outward transport of ammonium in roots of maize and sorghum: contrasting effects of methionine sulphoximine. Journal of experimental botany **45,** 429-439.

Filleur, S., Dorbe, M.-F., Cerezo, M., Orsel, M., Granier, F., Gojon, A., and Daniel-Vedele, F. (2001). An Arabidopsis T‐DNA mutant affected in Nrt2 genes is impaired in nitrate uptake. FEBS letters **489,** 220-224.

Foehse, D., and Jungk, A. (1983). Influence of phosphate and nitrate supply on root hair formation of rape, spinach and tomato plants. Plant and soil **74,** 359-368.

Furihata, T., Maruyama, K., Fujita, Y., Umezawa, T., Yoshida, R., Shinozaki, K., and Yamaguchi-Shinozaki, K. (2006). Abscisic acid-dependent multisite phosphorylation regulates the activity of a transcription activator AREB1. Proceedings of the National Academy of Sciences **103,** 1988-1993.

Gahoonia, T., and Nielsen, N. (2003). Phosphorus (P) uptake and growth of a root hairless barley mutant (bald root barley, brb) and wild type in low‐and high‐P soils. Plant, Cell & Environment **26,** 1759-1766.

Geiger, D., Scherzer, S., Mumm, P., Stange, A., Marten, I., Bauer, H., Ache, P., Matschi, S., Liese, A., and Al-Rasheid, K.A. (2009). Activity of guard cell anion channel SLAC1 is controlled by drought-stress signaling kinase-phosphatase pair. Proceedings of the National Academy of Sciences **106,** 21425-21430.

Gent, L., and Forde, B.G. (2017). How do plants sense their nitrogen status? Journal of experimental botany **68,** 2531-2539.

Gifford, M.L., Dean, A., Gutierrez, R.A., Coruzzi, G.M., and Birnbaum, K.D. (2008). Cell-specific nitrogen responses mediate developmental plasticity. Proceedings of the National Academy of Sciences **105,** 803-808.

Gilroy, S., and Jones, D.L. (2000). Through form to function: root hair development and nutrient uptake. Trends in plant science **5,** 56-60.

Glickman, M.H., and Ciechanover, A. (2002). The ubiquitin-proteasome proteolytic pathway: destruction for the sake of construction. Physiological reviews **82,** 373-428.

Gojon, A., Krouk, G., Perrine-Walker, F., and Laugier, E. (2011). Nitrate transceptor (s) in plants. Journal of experimental botany **62,** 2299-2308.

Gowri, G., Kenis, J.D., Ingemarsson, B., Redinbaugh, M.G., and Campbell, W.H. (1992). Nitrate reductase transcript is expressed in the primary response of maize to environmental nitrate. Plant molecular biology **18,** 55-64.

Grallath, S., Weimar, T., Meyer, A., Gumy, C., Suter-Grotemeyer, M., Neuhaus, J.-M., and Rentsch, D. (2005). The AtProT family. Compatible solute transporters with similar substrate specificity but differential expression patterns. Plant Physiology **137,** 117-126.

Grefen, C., and Blatt, M.R. (2012). A 2in1 cloning system enables ratiometric bimolecular fluorescence complementation (rBiFC). Biotechniques **53,** 311-314.

Harmon, A.C., Gribskov, M., and Harper, J.F. (2000). CDPKs–a kinase for every Ca2+ signal? Trends in plant science **5,** 154-159.

Haruta, M., Sabat, G., Stecker, K., Minkoff, B.B., and Sussman, M.R. (2014). A peptide hormone and its receptor protein kinase regulate plant cell expansion. Science **343,** 408-411.

Hashimoto, K., Eckert, C., Anschütz, U., Scholz, M., Held, K., Waadt, R., Reyer, A., Hippler, M., Becker, D., and Kudla, J. (2012). Phosphorylation of calcineurin B-like (CBL) calcium sensor proteins by their CBL-interacting protein kinases (CIPKs) is required for full activity

of CBL-CIPK complexes toward their target proteins. Journal of Biological Chemistry **287,** 7956-7968.

Hetherington, A.M., and Brownlee, C. (2004). The generation of Ca2+ signals in plants. Annu. Rev. Plant Biol. **55,** 401-427.

Hey, S.J., Byrne, E., and Halford, N.G. (2009). The interface between metabolic and stress signalling. Annals of Botany **105,** 197-203.

Ho, C.-H., and Tsay, Y.-F. (2010). Nitrate, ammonium, and potassium sensing and signaling. Current opinion in plant biology **13,** 604-610.

Ho, C.-H., Lin, S.-H., Hu, H.-C., and Tsay, Y.-F. (2009). CHL1 functions as a nitrate sensor in plants. Cell **138,** 1184-1194.

Hochholdinger, F., Wen, T.J., Zimmermann, R., Chimot‐Marolle, P., Da Costa e Silva, O., Bruce, W., Lamkey, K.R., Wienand, U., and Schnable, P.S. (2008). The maize (Zea mays L.) roothairless3 gene encodes a putative GPI‐anchored, monocot‐specific, COBRA‐like protein that significantly affects grain yield. The Plant Journal **54,** 888-898.

Hopff, D., Wienkoop, S., and Lüthje, S. (2013). The plasma membrane proteome of maize roots grown under low and high iron conditions. Journal of proteomics **91,** 605-618.

Hu, H.C., Wang, Y.Y., and Tsay, Y.F. (2009). AtCIPK8, a CBL‐interacting protein kinase, regulates the low‐affinity phase of the primary nitrate response. The Plant Journal **57,** 264-278.

Huang, N.-C., Chiang, C.-S., Crawford, N.M., and Tsay, Y.-F. (1996). CHL1 encodes a component of the low-affinity nitrate uptake system in Arabidopsis and shows cell type-specific expression in roots. The Plant Cell **8,** 2183-2191.

Huber, J.L., Huber, S.C., Campbell, W.H., and Redinbaugh, M.G. (1992). Reversible light/dark modulation of spinach leaf nitrate reductase activity involves protein phosphorylation. Archives of Biochemistry and Biophysics **296,** 58-65.

Hwang, I., Sze, H., and Harper, J.F. (2000). A calcium-dependent protein kinase can inhibit a calmodulin-stimulated Ca2+ pump (ACA2) located in the endoplasmic reticulum of Arabidopsis. Proceedings of the National Academy of Sciences **97,** 6224-6229.

Jia, Z., Giehl, R.F., Meyer, R.C., Altmann, T., and von Wirén, N. (2019). Natural variation of BSK3 tunes brassinosteroid signaling to regulate root foraging under low nitrogen. Nature communications **10,** 2378.

Johnson, L.N., Noble, M.E., and Owen, D.J. (1996). Active and inactive protein kinases: structural basis for regulation. Cell **85,** 149-158.

Ju, C., Yoon, G.M., Shemansky, J.M., Lin, D.Y., Ying, Z.I., Chang, J., Garrett, W.M., Kessenbrock, M., Groth, G., and Tucker, M.L. (2012). CTR1 phosphorylates the central regulator EIN2 to control ethylene hormone signaling from the ER membrane to the nucleus in Arabidopsis. Proceedings of the National Academy of Sciences **109,** 19486-19491.

Kadota, Y., Liebrand, T.W., Goto, Y., Sklenar, J., Derbyshire, P., Menke, F.L., Torres, M.A., Molina, A., Zipfel, C., and Coaker, G. (2019). Quantitative phosphoproteomic analysis reveals common regulatory mechanisms between effector‐and PAMP‐triggered immunity in plants. New Phytologist **221,** 2160-2175.

Kapila, J., De Rycke, R., Van Montagu, M., and Angenon, G. (1997). An Agrobacterium-mediated transient gene expression system for intact leaves. Plant science **122,** 101-108.

Kemp, B.E., and Pearson, R.B. (1990). Protein kinase recognition sequence motifs. Trends in biochemical sciences **15,** 342-346.

Kerscher, O., Felberbaum, R., and Hochstrasser, M. (2006). Modification of proteins by ubiquitin and ubiquitin-like proteins. Annu. Rev. Cell Dev. Biol. **22,** 159-180.

Kim, T.-W., and Wang, Z.-Y. (2010). Brassinosteroid signal transduction from receptor kinases to transcription factors. Annual review of plant biology **61,** 681-704.

Kobayashi, Y., Murata, M., Minami, H., Yamamoto, S., Kagaya, Y., Hobo, T., Yamamoto, A., and Hattori, T. (2005). Abscisic acid‐activated SNRK2 protein kinases function in the gene‐regulation pathway of ABA signal transduction by phosphorylating ABA response element‐binding factors. The Plant Journal **44,** 939-949.

Kong, L., Wang, F., Si, J., Feng, B., Zhang, B., Li, S., and Wang, Z. (2013). Increasing in ROS levels and callose deposition in peduncle vascular bundles of wheat (Triticum aestivum L.) grown under nitrogen deficiency. Journal of Plant Interactions **8,** 109-116.

Konishi, M., and Yanagisawa, S. (2013). Arabidopsis NIN-like transcription factors have a central role in nitrate signalling. Nature communications **4,** 1617.

Kotur, Z., Mackenzie, N., Ramesh, S., Tyerman, S.D., Kaiser, B.N., and Glass, A.D. (2012). Nitrate transport capacity of the Arabidopsis thaliana NRT2 family members and their interactions with AtNAR2. 1. New Phytologist **194,** 724-731.

Krouk, G. (2017). Nitrate signalling: Calcium bridges the nitrate gap. Nature plants **3,** 17095.

Krouk, G., Crawford, N.M., Coruzzi, G.M., and Tsay, Y.-F. (2010a). Nitrate signaling: adaptation to fluctuating environments. Current opinion in plant biology **13,** 265-272.

Krouk, G., Lacombe, B., Bielach, A., Perrine-Walker, F., Malinska, K., Mounier, E., Hoyerova, K., Tillard, P., Leon, S., and Ljung, K. (2010b). Nitrate-regulated auxin transport by NRT1. 1 defines a mechanism for nutrient sensing in plants. Developmental cell **18,** 927-937.

Kumagai, E., Araki, T., and Ueno, O. (2011). Ammonia emission from leaves of different rice (Oryza sativa L.) cultivars. Plant Production Science **14,** 249-253.

Lam, H.-M., Coschigano, K., Oliveira, I., Melo-Oliveira, R., and Coruzzi, G. (1996). The molecular-genetics of nitrogen assimilation into amino acids in higher plants. Annual review of plant biology **47,** 569-593.

Lan, P., Li, W., Wen, T.-N., and Schmidt, W. (2012). Quantitative phosphoproteome profiling of iron-deficient Arabidopsis roots. Plant physiology **159,** 403-417.

Lan, P., Li, W., Lin, W.-D., Santi, S., and Schmidt, W. (2013). Mapping gene activity of Arabidopsis root hairs. Genome biology **14,** R67.

Lan, P., Li, W., Wen, T.-N., Shiau, J.-Y., Wu, Y.-C., Lin, W., and Schmidt, W. (2011). iTRAQ protein profile analysis of Arabidopsis roots reveals new aspects critical for iron homeostasis. Plant physiology **155,** 821-834.

Laugier, E., Bouguyon, E., Mauriès, A., Tillard, P., Gojon, A., and Lejay, L. (2012). Regulation of high-affinity nitrate uptake in roots of Arabidopsis depends predominantly on posttranscriptional control of the NRT2. 1/NAR2. 1 transport system. Plant physiology **158,** 1067-1078.

Lee, S.C., Lan, W.-Z., Kim, B.-G., Li, L., Cheong, Y.H., Pandey, G.K., Lu, G., Buchanan, B.B., and Luan, S. (2007a). A protein phosphorylation/dephosphorylation network regulates a plant potassium channel. Proceedings of the National Academy of Sciences **104,** 15959-15964.

Lee, Y.H., Foster, J., Chen, J., Voll, L.M., Weber, A.P., and Tegeder, M. (2007b). AAP1 transports uncharged amino acids into roots of Arabidopsis. The Plant Journal **50,** 305-319.

Lehmann, S., Gumy, C., Blatter, E., Boeffel, S., Fricke, W., and Rentsch, D. (2010). In planta function of compatible solute transporters of the AtProT family. Journal of experimental botany **62,** 787-796.

Lejay, L., Tillard, P., Lepetit, M., Olive, F.D., Filleur, S., Daniel‐Vedele, F., and Gojon, A. (1999). Molecular and functional regulation of two NO3‐uptake systems by N‐and C‐status of Arabidopsis plants. The Plant Journal **18,** 509-519.

Li, B., Li, G., Kronzucker, H.J., Baluška, F., and Shi, W. (2014). Ammonium stress in Arabidopsis: signaling, genetic loci, and physiological targets. Trends in Plant Science **19,** 107-114.

Li, G., Tillard, P., Gojon, A., and Maurel, C. (2016). Dual regulation of root hydraulic conductivity and plasma membrane aquaporins by plant nitrate accumulation and high-affinity nitrate transporter NRT2. 1. Plant and Cell Physiology **57,** 733-742.

Li, J., Wu, X.D., Hao, S.T., Wang, X.J., and Ling, H.Q. (2008). Proteomic response to iron deficiency in tomato root. Proteomics **8,** 2299-2311.

Li, W., Wang, Y., Okamoto, M., Crawford, N.M., Siddiqi, M.Y., and Glass, A.D. (2007). Dissection of the AtNRT2. 1: AtNRT2. 2 inducible high-affinity nitrate transporter gene cluster. Plant physiology **143,** 425-433.

Lima, J.E., Kojima, S., Takahashi, H., and von Wirén, N. (2010). Ammonium triggers lateral root branching in Arabidopsis in an AMMONIUM TRANSPORTER1; 3-dependent manner. The Plant Cell **22,** 3621-3633.

Lin, L.-L., Hsu, C.-L., Hu, C.-W., Ko, S.-Y., Hsieh, H.-L., Huang, H.-C., and Juan, H.-F. (2015). Integrating phosphoproteomics and bioinformatics to study brassinosteroid-regulated phosphorylation dynamics in Arabidopsis. BMC genomics **16,** 533.

Lin, W.-D., Liao, Y.-Y., Yang, T.J., Pan, C.-Y., Buckhout, T.J., and Schmidt, W. (2011). Coexpression-based clustering of Arabidopsis root genes predicts functional modules in early phosphate deficiency signaling. Plant physiology **155,** 1383-1402.

Lipson, D., and Näsholm, T. (2001). The unexpected versatility of plants: organic nitrogen use and availability in terrestrial ecosystems. Oecologia **128,** 305-316.

Little, D.Y., Rao, H., Oliva, S., Daniel-Vedele, F., Krapp, A., and Malamy, J.E. (2005). The putative high-affinity nitrate transporter NRT2. 1 represses lateral root initiation in response to nutritional cues. Proceedings of the National Academy of Sciences **102,** 13693-13698.

Liu, C., Lu, F., Cui, X., and Cao, X. (2010). Histone methylation in higher plants. Annual review of plant biology **61,** 395-420.

Liu, K.-H., Huang, C.-Y., and Tsay, Y.-F. (1999). CHL1 is a dual-affinity nitrate transporter of Arabidopsis involved in multiple phases of nitrate uptake. The Plant Cell **11,** 865-874.

Liu, K.-h., Niu, Y., Konishi, M., Wu, Y., Du, H., Chung, H.S., Li, L., Boudsocq, M., McCormack, M., and Maekawa, S. (2017). Discovery of nitrate–CPK–NLP signalling in central nutrient–growth networks. Nature **545,** 311.

Liu, K.H., and Tsay, Y.F. (2003). Switching between the two action modes of the dual‐affinity nitrate transporter CHL1 by phosphorylation. The EMBO journal **22,** 1005-1013.

Liu, L.-H., Ludewig, U., Frommer, W.B., and von Wirén, N. (2003a). AtDUR3 encodes a new type of high-affinity urea/H+ symporter in Arabidopsis. The Plant Cell **15,** 790-800.

Liu, L.-H., Ludewig, U., Gassert, B., Frommer, W.B., and von Wirén, N. (2003b). Urea transport by nitrogen-regulated tonoplast intrinsic proteins in Arabidopsis. Plant physiology **133,** 1220-1228.

Loqué, D., and von Wirén, N. (2004). Regulatory levels for the transport of ammonium in plant roots. Journal of experimental botany **55,** 1293-1305.

Luan, S. (2009). The CBL–CIPK network in plant calcium signaling. Trends in plant science **14,** 37-42.

Ma, Z., Bielenberg, D., Brown, K.M., and Lynch, J.P. (2001). Regulation of root hair density by phosphorus availability in Arabidopsis thaliana. Plant, Cell & Environment **24,** 459-467.

Madeira, F., Lee, J., Buso, N., Gur, T., Madhusoodanan, N., Basutkar, P., Tivey, A., Potter, S.C., Finn, R.D., and Lopez, R. (2019). The EMBL-EBI search and sequence analysis tools APIs in 2019. Nucleic acids research.

Mann, M., and Jensen, O.N. (2003). Proteomic analysis of post-translational modifications. Nature biotechnology **21,** 255.

Mao, Q.Q., Guan, M.Y., Lu, K.X., Du, S.T., Fan, S.K., Ye, Y.-Q., Lin, X.Y., and Jin, C.W. (2014). Inhibition of nitrate transporter 1.1-controlled nitrate uptake reduces cadmium uptake in Arabidopsis. Plant physiology **166,** 934-944.

Marschner, H. (2011). Marschner's mineral nutrition of higher plants. (Academic press).

Martín, Y., González, Y.V., Cabrera, E., Rodríguez, C., and Siverio, J.M. (2011). Npr1 Ser/Thr protein kinase links nitrogen source quality and carbon availability with the yeast nitrate transporter (Ynt1) levels. Journal of Biological Chemistry **286,** 27225-27235.

Masucci, J.D., Rerie, W.G., Foreman, D.R., Zhang, M., Galway, M.E., Marks, M.D., and Schiefelbein, J.W. (1996). The homeobox gene GLABRA2 is required for position-dependent cell differentiation in the root epidermis of Arabidopsis thaliana. Development **122,** 1253-1260.

Medzihradszky, M., Bindics, J., Ádám, É., Viczián, A., Klement, É., Lorrain, S., Gyula, P., Mérai, Z., Fankhauser, C., and Medzihradszky, K.F. (2013). Phosphorylation of phytochrome B inhibits light-induced signaling via accelerated dark reversion in Arabidopsis. The Plant Cell **25,** 535-544.

Menz, J., Li, Z., Schulze, W.X., and Ludewig, U. (2016). Early nitrogen‐deprivation responses in Arabidopsis roots reveal distinct differences on transcriptome and (phospho‐) proteome levels between nitrate and ammonium nutrition. The Plant Journal **88,** 717-734.

Miller, A.J., Fan, X., Shen, Q., and Smith, S.J. (2008a). Amino acids and nitrate as signals for the regulation of nitrogen acquisition. Journal of experimental botany **59,** 111-119.

Miller, M.L., Jensen, L.J., Diella, F., Jørgensen, C., Tinti, M., Li, L., Hsiung, M., Parker, S.A., Bordeaux, J., and Sicheritz-Ponten, T. (2008b). Linear motif atlas for phosphorylation-dependent signaling. Sci. Signal. **1,** ra2-ra2.

Miura, K., Jin, J.B., and Hasegawa, P.M. (2007). Sumoylation, a post-translational regulatory process in plants. Current opinion in plant biology **10,** 495-502.

Morcuende, R., Bari, R., Gibon, Y., Zheng, W., Pant, B.D., BlÄSing, O., Usadel, B., Czechowski, T., Udvardi, M.K., and Stitt, M. (2007). Genome‐wide reprogramming of metabolism and regulatory networks of Arabidopsis in response to phosphorus. Plant, Cell & Environment **30,** 85-112.

Mori, I.C., Murata, Y., Yang, Y., Munemasa, S., Wang, Y.-F., Andreoli, S., Tiriac, H., Alonso, J.M., Harper, J.F., and Ecker, J.R. (2006). CDPKs CPK6 and CPK3 function in ABA regulation of guard cell S-type anion-and Ca2+-permeable channels and stomatal closure. PLoS biology **4,** e327.

Muller, B., and TOURAINE, B. (1992). Inhibition of NO□3 Uptake by Various Phloem-Translocated Amino Acids in Soybean Seedlings. Journal of experimental botany **43,** 617-623.

Muños, S., Cazettes, C., Fizames, C., Gaymard, F., Tillard, P., Lepetit, M., Lejay, L., and Gojon, A. (2004). Transcript profiling in the chl1-5 mutant of Arabidopsis reveals a role of the nitrate transporter NRT1. 1 in the regulation of another nitrate transporter, NRT2. 1. The Plant Cell **16,** 2433-2447.

Nadeem, M., Mollier, A., Morel, C., Vives, A., Prud'homme, L., and Pellerin, S. (2011). Relative contribution of seed phosphorus reserves and exogenous phosphorus uptake to maize (Zea mays L.) nutrition during early growth stages. Plant and Soil **346,** 231-244.

Nadeem, M., Mollier, A., Morel, C., Vives, A., Prud'homme, L., and Pellerin, S. (2012). Maize (Zea mays L.) endogenous seed phosphorus remobilization is not influenced by exogenous phosphorus availability during germination and early growth stages. Plant and soil **357,** 13-24.

Negi, J., Matsuda, O., Nagasawa, T., Oba, Y., Takahashi, H., Kawai-Yamada, M., Uchimiya, H., Hashimoto, M., and Iba, K. (2008). CO 2 regulator SLAC1 and its homologues are essential for anion homeostasis in plant cells. Nature **452,** 483.

Nestler, J., Schütz, W., and Hochholdinger, F. (2011). Conserved and unique features of the maize (Zea mays L.) root hair proteome. Journal of proteome research **10,** 2525-2537.

Nestler, J., Liu, S., Wen, T.J., Paschold, A., Marcon, C., Tang, H.M., Li, D., Li, L., Meeley, R.B., and Sakai, H. (2014). Roothairless5, which functions in maize (Z ea mays L.) root hair initiation and elongation encodes a monocot‐specific NADPH oxidase. The Plant Journal **79,** 729-740.

Neuhäuser, B., Dynowski, M., and Ludewig, U. (2009). Channel-like NH3 flux by ammonium transporter AtAMT2. FEBS letters **583,** 2833-2838.

Nolan, T., Chen, J., and Yin, Y. (2017). Cross-talk of Brassinosteroid signaling in controlling growth and stress responses. Biochemical Journal **474,** 2641-2661.

Nolen, B., Taylor, S., and Ghosh, G. (2004). Regulation of protein kinases: controlling activity through activation segment conformation. Molecular cell **15,** 661-675.

Nühse, T.S., Peck, S.C., Hirt, H., and Boller, T. (2000). Microbial elicitors induce activation and dual phosphorylation of the Arabidopsis thaliana MAPK 6. Journal of Biological Chemistry **275,** 7521-7526.

Oaks, A. (1994). Primary nitrogen assimilation in higher plants and its regulation. Canadian Journal of Botany **72,** 739-750.

Ohkubo, Y., Tanaka, M., Tabata, R., Ogawa-Ohnishi, M., and Matsubayashi, Y. (2017). Shoot-to-root mobile polypeptides involved in systemic regulation of nitrogen acquisition. Nature Plants **3,** 1-6.

Okamoto, M., Kumar, A., Li, W., Wang, Y., Siddiqi, M.Y., Crawford, N.M., and Glass, A.D. (2006). High-affinity nitrate transport in roots of Arabidopsis depends on expression of the NAR2-like gene AtNRT3. 1. Plant physiology **140,** 1036-1046.

Omasits, U., Ahrens, C.H., Müller, S., and Wollscheid, B. (2013). Protter: interactive protein feature visualization and integration with experimental proteomic data. Bioinformatics **30,** 884-886.

Orsel, M., Chopin, F., Leleu, O., Smith, S.J., Krapp, A., Daniel-Vedele, F., and Miller, A.J. (2006). Characterization of a two-component high-affinity nitrate uptake system in Arabidopsis. Physiology and protein-protein interaction. Plant Physiology **142,** 1304-1317.

Osuna, D., Usadel, B., Morcuende, R., Gibon, Y., Bläsing, O.E., Höhne, M., Günter, M., Kamlage, B., Trethewey, R., and Scheible, W.R. (2007). Temporal responses of transcripts, enzyme activities and metabolites after adding sucrose to carbon‐deprived Arabidopsis seedlings. The Plant Journal **49,** 463-491.

Park, B.S., Song, J.T., and Seo, H.S. (2011). Arabidopsis nitrate reductase activity is stimulated by the E3 SUMO ligase AtSIZ1. Nature communications **2,** 400.

Pertl, H., Himly, M., Gehwolf, R., Kriechbaumer, R., Strasser, D., Michalke, W., Richter, K., Ferreira, F., and Obermeyer, G. (2001). Molecular and physiological characterisation of a 14-3-3 protein from lily pollen grains regulating the activity of the plasma membrane H+ ATPase during pollen grain germination and tube growth. Planta **213,** 132-141.

Pitts, R.J., Cernac, A., and Estelle, M. (1998). Auxin and ethylene promote root hair elongation in Arabidopsis. The Plant Journal **16,** 553-560.

Prado, K., Boursiac, Y., Tournaire-Roux, C., Monneuse, J.-M., Postaire, O., Da Ines, O., Schäffner, A.R., Hem, S., Santoni, V., and Maurel, C. (2013). Regulation of Arabidopsis leaf hydraulics involves light-dependent phosphorylation of aquaporins in veins. The Plant Cell **25,** 1029-1039.

Pratt, J.M., Simpson, D.M., Doherty, M.K., Rivers, J., Gaskell, S.J., and Beynon, R.J. (2006). Multiplexed absolute quantification for proteomics using concatenated signature peptides encoded by QconCAT genes. Nature protocols **1,** 1029.

Rappsilber, J., Ishihama, Y., and Mann, M. (2003). Stop and go extraction tips for matrix-assisted laser desorption/ionization, nanoelectrospray, and LC/MS sample pretreatment in proteomics. Analytical chemistry **75,** 663-670.

Rayapuram, N., Bigeard, J., Alhoraibi, H., Bonhomme, L., Hesse, A.-M., Vinh, J., Hirt, H., and Pflieger, D. (2018). Quantitative phosphoproteomic analysis reveals shared and specific targets of Arabidopsis mitogen-activated protein kinases (MAPKs) MPK3, MPK4, and MPK6. Molecular & Cellular Proteomics **17,** 61-80.

Rentsch, D., Schmidt, S., and Tegeder, M. (2007). Transporters for uptake and allocation of organic nitrogen compounds in plants. FEBS letters **581,** 2281-2289.

Sadanandom, A., Ádám, É., Orosa, B., Viczián, A., Klose, C., Zhang, C., Josse, E.-M., Kozma-Bognár, L., and Nagy, F. (2015). SUMOylation of phytochrome-B negatively regulates light-induced signaling in Arabidopsis thaliana. Proceedings of the National Academy of Sciences **112,** 11108-11113.

Saito, S., Hamamoto, S., Moriya, K., Matsuura, A., Sato, Y., Muto, J., Noguchi, H., Yamauchi, S., Tozawa, Y., and Ueda, M. (2018). N‐myristoylation and S‐acylation are common modifications of Ca2+‐regulated Arabidopsis kinases and are required for activation of the SLAC1 anion channel. New Phytologist **218,** 1504-1521.

Schaaf, G., Ludewig, U., Erenoglu, B.E., Mori, S., Kitahara, T., and von Wirén, N. (2004). ZmYS1 functions as a proton-coupled symporter for phytosiderophore-and nicotianamine-chelated metals. Journal of Biological Chemistry **279,** 9091-9096.

Scheible, W.-R., Gonzalez-Fontes, A., Lauerer, M., Muller-Rober, B., Caboche, M., and Stitt, M. (1997). Nitrate acts as a signal to induce organic acid metabolism and repress starch metabolism in tobacco. The Plant Cell **9,** 783-798.

Scheible, W.-R., Morcuende, R., Czechowski, T., Fritz, C., Osuna, D., Palacios-Rojas, N., Schindelasch, D., Thimm, O., Udvardi, M.K., and Stitt, M. (2004). Genome-wide reprogramming of primary and secondary metabolism, protein synthesis, cellular growth processes, and the regulatory infrastructure of Arabidopsis in response to nitrogen. Plant physiology **136,** 2483-2499.

Schiefelbein, J., Zheng, X., and Huang, L. (2014). Regulation of epidermal cell fate in Arabidopsis roots: the importance of multiple feedback loops. Frontiers in Plant Science **5,** 47.

Schimel, J.P., and Bennett, J. (2004). Nitrogen mineralization: challenges of a changing paradigm. Ecology **85,** 591-602.

Schlesier, B., Bréton, F., and Mock, H.-P. (2003). A hydroponic culture system for growingArabidopsis thaliana plantlets under sterile conditions. Plant molecular biology reporter **21,** 449-456.

Schreiber, L., Franke, R., and Lessire, R. (2005). Biochemical characterization of elongase activity in corn (Zea mays L.) roots. Phytochemistry **66,** 131-138.

Schulze, W.X., and Usadel, B. (2010). Quantitation in mass-spectrometry-based proteomics. Annual review of plant biology **61,** 491-516.

Schweighofer, A., Hirt, H., and Meskiene, I. (2004). Plant PP2C phosphatases: emerging functions in stress signaling. Trends in plant science **9,** 236-243.

Segonzac, C., Boyer, J.-C., Ipotesi, E., Szponarski, W., Tillard, P., Touraine, B., Sommerer, N., Rossignol, M., and Gibrat, R. (2007). Nitrate efflux at the root plasma membrane: identification of an Arabidopsis excretion transporter. The Plant Cell **19,** 3760-3777.

Seo, J., and Lee, K.-J. (2004). Post-translational modifications and their biological functions: proteomic analysis and systematic approaches. Journal of biochemistry and molecular biology **37,** 35-44.

Shah, K., Vervoort, J., and de Vries, S.C. (2001). Role of threonines in the Arabidopsis thaliana somatic embryogenesis receptor kinase 1 activation loop in phosphorylation. Journal of Biological Chemistry **276,** 41263-41269.

Shi, S., Li, S., Asim, M., Mao, J., Xu, D., Ullah, Z., Liu, G., Wang, Q., and Liu, H. (2018). The Arabidopsis calcium-dependent protein kinases (CDPKs) and their roles in plant growth regulation and abiotic stress responses. International journal of molecular sciences **19,** 1900.

Shin, R., Berg, R.H., and Schachtman, D.P. (2005). Reactive oxygen species and root hairs in Arabidopsis root response to nitrogen, phosphorus and potassium deficiency. Plant and Cell Physiology **46,** 1350-1357.

Sohlenkamp, C., Shelden, M., Howitt, S., and Udvardi, M. (2000). Characterization of Arabidopsis AtAMT2, a novel ammonium transporter in plants. FEBS letters **467,** 273-278.

Soto, G., Alleva, K., Mazzella, M.A., Amodeo, G., and Muschietti, J.P. (2008). AtTIP1; 3 and AtTIP5; 1, the only highly expressed Arabidopsis pollen‐specific aquaporins, transport water and urea. FEBS letters **582,** 4077-4082.

Stacey, G., Koh, S., Granger, C., and Becker, J.M. (2002). Peptide transport in plants. Trends in plant science **7,** 257-263.

Stecker, K.E., Minkoff, B.B., and Sussman, M.R. (2014). Phosphoproteomic analyses reveal early signaling events in the osmotic stress response. Plant physiology **165,** 1171-1187.

Stetter, M.G., Schmid, K., and Ludewig, U. (2015). Uncovering genes and ploidy involved in the high diversity in root hair density, length and response to local scarce phosphate in Arabidopsis thaliana. PLoS One **10,** e0120604.

Straub, T., Ludewig, U., and Neuhäuser, B. (2017). The kinase CIPK23 inhibits ammonium transport in Arabidopsis thaliana. The Plant Cell **29,** 409-422.

Sutka, M., Li, G., Boudet, J., Boursiac, Y., Doumas, P., and Maurel, C. (2011). Natural variation of root hydraulics in Arabidopsis grown in normal and salt-stressed conditions. Plant physiology **155,** 1264-1276.

Svennerstam, H., Ganeteg, U., and Näsholm, T. (2008). Root uptake of cationic amino acids by Arabidopsis depends on functional expression of amino acid permease 5. New Phytologist **180,** 620-630.

Svennerstam, H., Jämtgård, S., Ahmad, I., Huss‐Danell, K., Näsholm, T., and Ganeteg, U. (2011). Transporters in Arabidopsis roots mediating uptake of amino acids at naturally occurring concentrations. New Phytologist **191,** 459-467.

Takahashi, F., Yoshida, R., Ichimura, K., Mizoguchi, T., Seo, S., Yonezawa, M., Maruyama, K., Yamaguchi-Shinozaki, K., and Shinozaki, K. (2007). The mitogen-activated protein kinase cascade MKK3–MPK6 is an important part of the jasmonate signal transduction pathway in Arabidopsis. The Plant Cell **19,** 805-818.

Tang, W., Kim, T.-W., Oses-Prieto, J.A., Sun, Y., Deng, Z., Zhu, S., Wang, R., Burlingame, A.L., and Wang, Z.-Y. (2008). BSKs mediate signal transduction from the receptor kinase BRI1 in Arabidopsis. Science **321,** 557-560.

Tanz, S.K., Castleden, I., Hooper, C.M., Vacher, M., Small, I., and Millar, H.A. (2012). SUBA3: a database for integrating experimentation and prediction to define the SUB cellular location of proteins in A rabidopsis. Nucleic acids research **41,** D1185-D1191.

Tena, G., Asai, T., Chiu, W.-L., and Sheen, J. (2001). Plant mitogen-activated protein kinase signaling cascades. Current opinion in plant biology **4,** 392-400.

Thimm, O., Bläsing, O., Gibon, Y., Nagel, A., Meyer, S., Krüger, P., Selbig, J., Müller, L.A., Rhee, S.Y., and Stitt, M. (2004). MAPMAN: a user‐driven tool to display genomics data sets onto diagrams of metabolic pathways and other biological processes. The Plant Journal **37,** 914-939.

Tournaire-Roux, C., Sutka, M., Javot, H., Gout, E., Gerbeau, P., Luu, D.-T., Bligny, R., and Maurel, C. (2003). Cytosolic pH regulates root water transport during anoxic stress through gating of aquaporins. Nature **425,** 393.

Trueman, L.J., Richardson, A., and Forde, B.G. (1996). Molecular cloning of higher plant homologues of the high-affinity nitrate transporters of Chlamydomonas reinhardtii and Aspergillus nidulans. Gene **175,** 223-231.

Tsay, Y.-F., Schroeder, J.I., Feldmann, K.A., and Crawford, N.M. (1993). The herbicide sensitivity gene CHL1 of Arabidopsis encodes a nitrate-inducible nitrate transporter. Cell **72,** 705-713.

Umezawa, T., Sugiyama, N., Takahashi, F., Anderson, J.C., Ishihama, Y., Peck, S.C., and Shinozaki, K. (2013). Genetics and phosphoproteomics reveal a protein phosphorylation network in the abscisic acid signaling pathway in Arabidopsis thaliana. Sci. Signal. **6,** rs8-rs8.

Umezawa, T., Sugiyama, N., Mizoguchi, M., Hayashi, S., Myouga, F., Yamaguchi-Shinozaki, K., Ishihama, Y., Hirayama, T., and Shinozaki, K. (2009). Type 2C protein phosphatases directly regulate abscisic acid-activated protein kinases in Arabidopsis. Proceedings of the National Academy of sciences **106,** 17588-17593.

von der Fecht-Bartenbach, J., Bogner, M., Dynowski, M., and Ludewig, U. (2010). CLC-b-mediated NO− 3/H+ exchange across the tonoplast of Arabidopsis vacuoles. Plant and Cell Physiology **51,** 960-968.

Walch-Liu, P., Liu, L.-H., Remans, T., Tester, M., and Forde, B.G. (2006). Evidence that L-glutamate can act as an exogenous signal to modulate root growth and branching in Arabidopsis thaliana. Plant and Cell Physiology **47,** 1045-1057.

Walch‐Liu, P., Neumann, G., Bangerth, F., and Engels, C. (2000). Rapid effects of nitrogen form on leaf morphogenesis in tobacco. Journal of experimental botany **51,** 227-237.

Walley, J.W., Shen, Z., Sartor, R., Wu, K.J., Osborn, J., Smith, L.G., and Briggs, S.P. (2013). Reconstruction of protein networks from an atlas of maize seed proteotypes. Proceedings of the National Academy of Sciences **110,** E4808-E4817.

Wang, R., Liu, D., and Crawford, N.M. (1998). The Arabidopsis CHL1 protein plays a major role in high-affinity nitrate uptake. Proceedings of the national academy of sciences **95,** 15134-15139.

Wang, R., Okamoto, M., Xing, X., and Crawford, N.M. (2003). Microarray analysis of the nitrate response in Arabidopsis roots and shoots reveals over 1,000 rapidly responding genes and new linkages to glucose, trehalose-6-phosphate, iron, and sulfate metabolism. Plant physiology **132,** 556-567.

Wang, R., Tischner, R., Gutiérrez, R.A., Hoffman, M., Xing, X., Chen, M., Coruzzi, G., and Crawford, N.M. (2004). Genomic analysis of the nitrate response using a nitrate reductase-null mutant of Arabidopsis. Plant physiology **136,** 2512-2522.

Wang, X., Hao, L., Zhu, B., and Jiang, Z. (2018a). Plant calcium signaling in response to potassium deficiency. International journal of molecular sciences **19,** 3456.

Wang, Y.-Y., Hsu, P.-K., and Tsay, Y.-F. (2012). Uptake, allocation and signaling of nitrate. Trends in plant science **17,** 458-467.

Wang, Y.-Y., Cheng, Y.-H., Chen, K.-E., and Tsay, Y.-F. (2018b). Nitrate transport, signaling, and use efficiency. Annual review of plant biology **69,** 85-122.

Webb, A.A., McAinsh, M.R., Taylor, J.E., and Hetherington, A.M. (1996). Calcium ions as intracellular second messengers in higher plants. Advances in Botanical Research.

Welchman, R.L., Gordon, C., and Mayer, R.J. (2005). Ubiquitin and ubiquitin-like proteins as multifunctional signals. Nature reviews Molecular cell biology **6,** 599.

Wen, T.-J., Hochholdinger, F., Sauer, M., Bruce, W., and Schnable, P.S. (2005). The roothairless1 gene of maize encodes a homolog of sec3, which is involved in polar exocytosis. Plant physiology **138,** 1637-1643.

White, P.J., and Veneklaas, E.J. (2012). Nature and nurture: the importance of seed phosphorus content. Plant and soil **357,** 1-8.

Winter, D., Vinegar, B., Nahal, H., Ammar, R., Wilson, G.V., and Provart, N.J. (2007). An "Electronic Fluorescent Pictograph" browser for exploring and analyzing large-scale biological data sets. PloS one **2,** e718.

Wirth, J., Chopin, F., Santoni, V., Viennois, G., Tillard, P., Krapp, A., Lejay, L., Daniel-Vedele, F., and Gojon, A. (2007). Regulation of root nitrate uptake at the NRT2. 1 protein level in Arabidopsis thaliana. Journal of Biological Chemistry **282,** 23541-23552.

Witte, C.-P. (2011). Urea metabolism in plants. Plant Science **180,** 431-438.

Wolters, J.C., Abele, R., and Tampé, R. (2005). Selective and ATP-dependent translocation of peptides by the homodimeric ATP binding cassette transporter TAP-like (ABCB9). Journal of Biological Chemistry **280,** 23631-23636.

Wu, F., Chi, Y., Jiang, Z., Xu, Y., Xie, L., Huang, F., Wan, D., Ni, J., Yuan, F., and Wu, X. (2020). Hydrogen peroxide sensor HPCA1 is an LRR receptor kinase in Arabidopsis. Nature **578,** 577-581.

Wu, X., Chu, L., Xi, L., Pertl-Obermeyer, H., Li, Z., Sklodowski, K., Sanchez-Rodriguez, C., Obermeyer, G., and Schulze, W.X. (2019). Sucrose-Induced Receptor Kinase 1 is modulated by an interacting kinase with short extracellular domain. Molecular & Cellular Proteomics**,** mcp.RA119.001336.

Wu, X.N., Xi, L., Pertl-Obermeyer, H., Li, Z., Chu, L.-C., and Schulze, W.X. (2017). Highly Efficient Single-Step Enrichment of Low Abundance Phosphopeptides from Plant Membrane Preparations. Frontiers in plant science **8,** 1673.

Wu, Y., Xun, Q., Guo, Y., Zhang, J., Cheng, K., Shi, T., He, K., Hou, S., Gou, X., and Li, J. (2016). Genome-wide expression pattern analyses of the Arabidopsis leucine-rich repeat receptor-like kinases. Molecular plant **9,** 289-300.

Xiao, S.-H., and Manley, J.L. (1997). Phosphorylation of the ASF/SF2 RS domain affects both protein-protein and protein-RNA interactions and is necessary for splicing. Genes & development **11,** 334-344.

Xu, G., Fan, X., and Miller, A.J. (2012). Plant nitrogen assimilation and use efficiency. Annual review of plant biology **63,** 153-182.

Xu, J., and Zhang, S. (2015). Mitogen-activated protein kinase cascades in signaling plant growth and development. Trends in plant science **20,** 56-64.

Yong, Z., Kotur, Z., and Glass, A.D. (2010). Characterization of an intact two‐component high‐affinity nitrate transporter from Arabidopsis roots. The Plant Journal **63,** 739-748.

Yuan, L., Loqué, D., Kojima, S., Rauch, S., Ishiyama, K., Inoue, E., Takahashi, H., and von Wirén, N. (2007). The organization of high-affinity ammonium uptake in Arabidopsis roots depends on the spatial arrangement and biochemical properties of AMT1-type transporters. The Plant Cell **19,** 2636-2652.

Zargar, S.M., Fujiwara, M., Inaba, S., Kobayashi, M., Kurata, R., Ogata, Y., and Fukao, Y. (2015). Correlation analysis of proteins responsive to Zn, Mn, or Fe deficiency in Arabidopsis roots based on iTRAQ analysis. Plant cell reports **34,** 157-166.

Zauber, H., and Schulze, W.X. (2012). Proteomics wants cRacker: automated standardized data analysis of LC–MS derived proteomic data. Journal of proteome research **11,** 5548-5555.

Zhang, H., and Forde, B.G. (2000). Regulation of Arabidopsis root development by nitrate availability. Journal of experimental botany**,** 51-59.

Zhao, C., Zayed, O., Yu, Z., Jiang, W., Zhu, P., Hsu, C.-C., Zhang, L., Tao, W.A., Lozano-Durán, R., and Zhu, J.-K. (2018). Leucine-rich repeat extensin proteins regulate plant salt tolerance in Arabidopsis. Proceedings of the National Academy of Sciences **115,** 13123-13128.

Zhao, X., Bai, X., Jiang, C., and Li, Z. (2019). Phosphoproteomic Analysis of Two Contrasting Maize Inbred Lines Provides Insights into the Mechanism of Salt-Stress Tolerance. International journal of molecular sciences **20,** 1886.

Zheng, X., He, K., Kleist, T., Chen, F., and Luan, S. (2015). Anion channel SLAH 3 functions in nitrate‐dependent alleviation of ammonium toxicity in A rabidopsis. Plant, cell & environment **38,** 474-486.

Zhu, S.-Y., Yu, X.-C., Wang, X.-J., Zhao, R., Li, Y., Fan, R.-C., Shang, Y., Du, S.-Y., Wang, X.-F., and Wu, F.-Q. (2007). Two calcium-dependent protein kinases, CPK4 and CPK11, regulate abscisic acid signal transduction in Arabidopsis. The Plant Cell **19,** 3019-3036.

Zipfel, C., and Oldroyd, G.E. (2017). Plant signalling in symbiosis and immunity. Nature **543,** 328-336.

8 Acknowledgements

Firstly and foremost I would like to express my deepest appreciation to my supervisor Prof. Dr. Waltraud Schulze who is an excellent teacher and an even valuable friend. She has provided me innumerable good suggestions during my study. I did not only get benefit from her professional knowledge and experience, but also from her open mind and patience. She is always happy to discuss with me about my experiment design or my new ideals regarding to the project. And she will take my advice and encourage me to follow my ideals as soon as she accept them. These qualities of her have helped me a lot during my research. In the days I wrote my thesis, she also helped me with offering countless guidance and infinite patience which greatly supported me to complete my writing. From her I know what characteristics a qualified scientist should have: positive attitude, hard-working and an open mind.

Secondly I would like to extend my sincere thanks to postdocs in our group: Dr. Heidi Obermeyer Dr. Lin Xi and Dr. Xuna Wu. Heidi taught me how to perform expression of recombinant proteins, Lin shared her experience about MS-based proteomics sample preparation. Xuna guided me when I did phosphoproteome-related work which contained several different experiments. Other members in the group also helped me a lot in the work. Lingcui Chu shared her experimental experience with me. Jiahui Wang, Max Gilbert, Susanne Liner, and Denise Llanos were always there to offer help when I needed. Zhaoxia Zhang not only helped me with writing several R language scripts when I needed some for my work, but also with solving problems in my daily life. Our secretary Melina Effner was always busy with dealing with different documents for me. It is a pleasure for me to work in the team.

I am also grateful to Dr. Andreas Schaller, Dr. Annick Stintzi, and their fellow members from department of plant physiology and biotechnology (190c), Dr. Uwe Ludewig, Dr. Benjamin Neuhäuser as well as their fellow members from department of nutritional physiology of crops (340h), from these amazing teams I could always get the help I needed. I would like to thank Dr. Christopher Grefen from ZMBP who helped us with establishment of rBiFC system.

Finally I am extremely grateful to my family in China, they have sacrificed a lot to support my study and given me endless encouragement.

9 Declaration in lieu of an oath on independent work

According to Sec. 18(3) sentence 5 of the University of Hohenheim's Doctoral Regulations for the Faculties of Agricultural Sciences, Natural Sciences, and Business, Economics and Social Sciences

1. The dissertation submitted on the topic

External Nutrition Stimuli Induced Proteome and Phosphoproteome Responses of Maize Root Hairs and Arabidopsis Root Microsomal Fraction

is work done independently by me.

2. I only used the sources and aids listed and did not make use of any impermissible assistance from third parties. In particular, I marked all content taken word-for-word or paraphrased from other works.

3. I did not use the assistance of a commercial doctoral placement or advising agency.

4. I am aware of the importance of the declaration in lieu of oath and the criminal consequences of false or incomplete declarations in lieu of oath.

I confirm that the declaration above is correct. I declare in lieu of oath that I have declared only the truth to the best of my knowledge and have not omitted anything.

Stuttgart, 16th December 2020

Place, Date

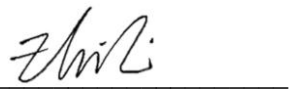

Signature

10 Curriculum Vitae

Personal Information:

Name: Zhi Li

Date of Birth: 31-Oct-1985

Place of birth: Hubei Province, China

Address: Department of Plant Systems Biology (190D), U290, Garbenstraße 30, University of Hohenheim, 70599 Stuttgart, Germany

Phone: +49 (0)711 459 24772

E-mail: li.zhi@uni-hohenheim.de; zhili.bw@gmail.com

Education and Professional Experience:

2004-2008 Bachelor in Bioengineering (Huazhong University of Science and Technology, China)

2009-2012 Master in Biochemistry and Molecular Biology (South-Central University for Nationalities, China)

2012-2014 Research-assistant working with Prof. Dr. Laihua Liu in College of Resources and Environmental Sciences (China Agricultural University, China)

2014-now Ph.D Candidate of Plant Systems Biology (University Hohenheim, Germany. Supervisor: Prof. Dr. Waltraud Schulze)

Academic Conferences:

10-12 July 2017 3rd Summer Academy in Plant Molecular Biology (poster), Heiligkreuztal, Germany

22-26 August 2016 EMBO Conference: The nitrogen nutrition of plants (poster), Montpeellier, France

29 June- 03 July 2015 The 7th Maxquant Summer School (Poster), Martinsried, Germany

25-27 June 2015 Plant Growth, Nutrition& Environment Interaction (Talk), Vienna, Austria

07-09 May 2014 2nd International Meeting Plant Primary Metabolism: Synthesis, Storage and Degradation Processes, Heidelberg, Germany

Publication List:

Zhi Li, Daniel Phillip, Benjamin Neuhauser, Waltraud X. Schulze and Uwe Ludewig (2015) Protein Dynamics in Young Maize Root Hairs in Response to Macroand Micronutrient Deprivation. (Journal of proteome research)

Jochen Menz, **Zhi Li**, Waltraud X. Schulze and Uwe Ludewig (2016) Early nitrogen-deprivation responses in Arabidopsis roots reveal distinct differences on transcriptome and (phospho-)proteome levels between nitrate and ammonium nutrition. (the Plant Journal)

Carlos M. Figueroa, Regina Feil, Hirofumi Ishihara, Mutsumi Watanabe, Katharina Kolling, Ursula Krause, Melanie Hohne, Beatrice Encke, William C. Plaxton, Samuel C. Zeeman, **Zhi Li**, Waltraud X. Schulze, Rainer Hoefgen, Mark Stitt and John E. Lunn (2016) Trehalose 6–phosphate coordinates organic and amino acid metabolism with carbon availability. (the Plant Journal)

Aurore Jacquot, **Zhi Li**, Alain Gojon, Waltraud Schulze and Laurence Lejay (2017) Post-translational regulation of nitrogen transporters in plants and microorganisms. (Journal of Experimental Botany)

Wu XN, Xi L, Obermeyer H, **Li Z**, Chu LC, and Schulze WX (2017) Highly efficient single-step enrichment of low abundance phosphopeptides from plant membrane preparations. (Frontiers in Plant Science)

Xuna Wu, Liangcui Chu, Lin Xi, Heidi Pertl-Obermeyer, **Zhi Li**, Kamil Sklodowski, Clara Sanchez-Rodriguez, Gerhard Obermeyer and Waltraud X Schulze (2019) Sucrose-Induced Receptor Kinase 1 is modulated by an interacting kinase with short extracellular domain. (Molecular & Cellular Proteomics)

Aurore Jacquot, Valentin Chaput, Adeline Mauries, **Zhi Li**, Pascal Tillard, Cécile Fizames, Pauline Bonillo, Fanny Bellegarde, Edith LAUGIER, Véronique Santoni, Sonia Hem, Antoine Martin, Alain Gojon, Waltraud Schulze, and Laurence Lejay (2020) NRT2.1 phosphorylation prevents root high affinity nitrate uptake activity in Arabidopsis thaliana. (New Phytologist) submitted

Zhi Li, Xu Na Wu, Aurore Jaquot, Larence Lejay , and Waltraud X Schulze (2020) A phospho-switch in the N-terminus of NRT2.1 affects nitrate uptake by controlling the interaction of NRT2.1 with NAR2.1. (Biorxiv)

Stuttgart, 16th December 2020 _____ Zhi Li _____

Place, Date Signature